THÈSE DE DOCTORAT DE

L'UNIVERSITE DE RENNES 1

ECOLE DOCTORALE N° 601
Mathématiques et Sciences et Technologies de l'Information et de la Communication

Spécialité : Mathématiques

Par

Anna GORDENKO

Dynamique aléatoire dans des tableaux de Young et sur la droite réelle

Random dynamics in Young diagrams and on the real line

Thèse présentée et soutenue à l'Université de Rennes 1, le 15 décembre 2020
Unité de recherche : Institut de Recherche Mathématique de Rennes

Rapporteurs avant soutenance :

Sara Brofferio	Professeur, Université Paris-Est Créteil
Igor Pak	Full Professor, University of California, Los Angeles

Composition du Jury :

Président :	Julio Rebelo	Professeur, Université Paul Sabatier, Toulouse
Examinateurs :	Sara Brofferio	Professeur, Université Paris-Est Créteil, Créteil
	Cédric Boutillier	Maître de conférences, Sorbonne Université, Paris
	Igor Pak	Full Professor, University of California, Los Angeles
	Julio Rebelo	Professeur, Université Paul Sabatier, Toulouse
Dir. de thèse :	Christophe Dupont	Professeur, Université Rennes 1, Rennes
Co-dir. de thèse :	Victor Kleptsyn	Chargé de recherche, CNRS, Université Rennes 1, Rennes

Random dynamics in Young diagrams and on the real line.

A. Gordenko [1]

[1]Univ Rennes, CNRS, IRMAR - UMR 6625, F-35000 Rennes, France.

Je remercie Sara Brofferio et Igor Pak pour le temps et les efforts qu'ils ont consacré à la lecture scrupuleuse de ce texte et pour leur retour qui m'a énormément aidé.

Je remercie vivement Cédric Boutillier et Julio Rebelo d'avoir accepté de faire partie de mon jury de thèse, j'en suis très honorée.

Le laboratoire d'IRMAR m'a toujours chaleureusement accueilli et soutenu, surtout en ces temps difficiles, et je voudrais remercier tous les collègues et surtout le personnel administratif.

Finalement, je voudrais remercier mes deux directeurs de thèse, Christophe Dupont et Victor Kleptsyn, sans lesquels ce travail n'aurait jamais été écrit.

Contents

Chapter 1

Introduction

Ma thèse est dédiée à deux questions différentes, toutes les deux liées aux problèmes des systèmes dynamiques aléatoires.

Dans le Chapitre 2 j'étudie le comportement des grands tableaux de Young gauches. Particulièrement, la description de leur comportement local se révèle être liée à une chaîne de Markov topologique, à savoir le processus TASEP modifié sur le cercle, et sa mesure d'entropie maximale.

Chapitre 3 est dédié à l'étude des mesures stationnaires pour des systèmes dynamiques aléatoires non-symétriques sur la droite réelle et aux propriétés asymptotiques de la dynamique inversée dans le temps.

Les deux prochaines sections sont dédiées à la description detaillée du contexte historique de ces domaines et aux résultats obtenus.

Je voudrais remercier Vadim Gorin, Alexey Bufetov, Leonid Petrov, Greta Panova, Alejandro Morales, Igor Pak, Sara Brofferio and Grigory Merzon pour leur interêt et les discussions fructueuses.

1.1 Les formes limites des grands tableaux de Young gauches et une modification du TASEP

1.1.1 Aperçu du problème

Les diagrammes de Young (YD) et certaines notions reliées étaient étudiées depuis longtemps (par exemple, voir les travaux de Feit, Carlitz-Riordan,

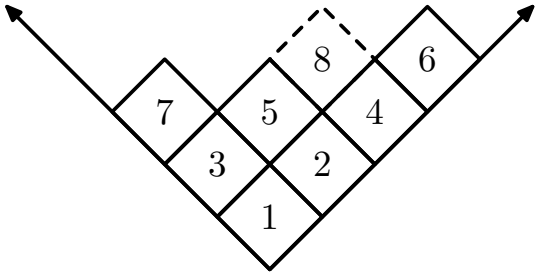

Figure 1.1: Standard Young Tableau

De Concini, Edelman et Berele-Regev [18, 11, 12, 17, 4]). Ces études ont été motivées par des raisons combinatoires (YD de taille n correspond aux partitions du nombre n) ainsi que par la théorie des représentations (YD de taille n dénombre les représentations irreductibles du groupe symétrique S_n). On note $\mathbb{Y}_n$ l'ensemble de tous de YD de taille n.

Le *graphe de Young* est un graphe orienté dont des sommets sont les diagrammes de Young et dont les arêtes vont d'un YD à tous les YD qu'on obtient en ajoutant une cellule au diagramme initial. En langue de la théorie des représentations, $\lambda \in \mathbb{Y}_n$ est jointe à tous $\mu \in \mathbb{Y}_{n+1}$ contenus dans la représentation induit de S_{n+1}, ou, ce qui est le même, si la représentation ρ_λ est contenue dans la restriction de la représentation correspondante ρ_μ à S_n. Ceci avec le fait que la multiplicité d'une telle inclusion n'excède pas 1 implique que la dimension $\dim \lambda$ d'une représentation irréductible ρ_λ, associée à l'YD λ, est égale au nombre de chemins dans le graphe de Young qui joignent le diagramme vide (ou unicellulaire) à λ.

Un chemin dans le graphe de Young, commençant au diagramme vide, peut être encodé en écrivant dans chaque cellule le numéro du pas auquel elle a été ajoutée, donc la correspondence bijective avec un *tableau de Young standard* est réalisée. Cette correspondence, par définition, est une façon de mettre les nombres $\{1, \ldots, n\}$ dans les cellules d'YD du taille n de telle manière que les nombres croissent dans chaque rangée et dans chaque colonne, et chaque nombre ne se retrouve qu'une seule fois. (La construction similaire avec un chemin commençant d'une YD *non-vide* conduit à la notion de *tableau de Young gauche*.)

La théorie des représentations motive l'étude de la mesure de Plancherel; cette dernière est une mesure μ_n de probabilité sur l'ensemble Y_n des tableaux

de Young de taille fixée n, définie par

$$\mu_n(\{\lambda\}) = \frac{\dim^2 \lambda}{n!}.$$

Le fait que cette mesure soit de probabilité provient de la relation classique

$$\sum_{\lambda \in \mathbb{Y}_n} \dim^2 \lambda = n!$$

Cette mesure donne lieu à une mesure centrale $\bar{\mu}$ sur les chemins du graphe de Young. La notion d'une *mesure centrale* en général est définie de la manière suivante. Soit un graphe G avec un ensemble gradué de sommets $V = \bigsqcup_n V_n$, dont les arêtes joignent les sommets de V_n aux sommets de V_{n+1}. Par définition, la mesure de probabilité sur l'ensemble de chemins $\omega = \{\omega_n\}_{n=0}^{\infty}$, $\omega_n \in V_n$, est *centrale* si pour chaque n et chaque $v \in V_n$ la partie initiale $\omega_0, \omega_1, \ldots, \omega_{n-1}, \omega_n$ du chemin conditionnée à $\omega_n = v$ est distribuée uniformément sur tous les chemins qui arrivent à v au n-ième pas.

Il est facile de voir qu'une mesure centrale est nécessairement Markovienne (le futur est indépendant du passé). Aussi, des mesures marginales μ_n qui donnent la loi de ω_n sont *en accord* l'une à l'autre: pour tout $m < n$, la loi μ_m de ω_m est obtenue si on prend la loi du m-ième élément ω_m d'un chemin allant vers un $v \in V_n$, et on moyennise ces distributions par rapport à la loi μ_n pour v. Inversement, une suite des mesures μ_n définit une mesure centrale, dès qu'ils sont en accord. L'un des exemples basiques de mesures centrales est celui des mesures de Bernoulli: un chemin aléatoire (x_n, y_n), où x_n et y_n sont respectivement le nombre du piles et faces après avoir lancé une pièce de Bernoulli n fois. En effet, conditionnés au nombre $k = x_n$ des réussites après n lancerts d'une pièce, tous les $\binom{n}{k}$ placements possibles de ces réussites sont équiprobables — quelque soit la probabilité p de réussite.

Comme nous l'avons mentionné, il est connu (mais pas évident) que les mesures de Plancherel μ_n sur les ensembles $\mathbb{Y}_n$ sont en accord l'une avec l'autre, et donc donnent lieu à la mesure centrale sur l'ensemble des chemins dans le graphe de Young. Cette mesure a la probabilité de transition de $\lambda \in \mathbb{Y}_{n-1}$ à $\lambda' \in \mathbb{Y}_n$

$$p_{\lambda \nearrow \lambda'} = \frac{\dim \lambda'}{n \dim \lambda}.$$

Il est facile de vérifier que ces probabilités définissent une chaîne de Markov avec les loi marginales μ_n en temps n, donc donnent la probabilité de tran-

sition à l'envers

$$\mathbb{P}(\omega_{n-1} = \lambda \mid \omega_n = \lambda') = \frac{\dim \lambda}{\dim \lambda'} \tag{1.1}$$

(où $\omega_0 = \emptyset, \omega_1, \omega_2, \ldots$ est un chemin choisi au hasard par rapport à cette mesure) et donc satisfont la définition de la mesure centrale (la relation (1.1) implique que la distribution sur les segments initiaux des chemins allant vers $\lambda \in \mathbb{Y}_n$ est uniforme).

Le paradigme général des combinatoires asymptotiques est qu'un objet combinatoire large satisfait souvent une "loi des grands nombres" : si on le rééchelonne proprement, il ressemble a une "forme" déterminée. Il y a plusieurs exemples de tels résultats (pour exemple voir [41, 45, 3]). Parmi ceux liés aux YD, le premier que nous voudrions mentionner est le théorème de forme limite, découvert indépendamment en 1970's par Versik et Kerov en USSR et par Logan et Shepp aux États-Unis. À savoir: soit $\lambda \in \mathbb{Y}_n$ une YD aléatoire (en notation française), on le comprime $\frac{1}{\sqrt{n}}$ fois, et on le tourne de 45° dans le sens anti-horaire. Cela donne une figure aléatoire F_n d'aire unitaire, place entre les rayons $y = |x|$. On considère sa bordure externe, prolonge par $y = |x|$ en dehors le diagramme, comme une graphique d'une fonction 1-Lipshitz f_λ.

Théorème 1.1.1 (Vershik, Kerov [46], Logan, Shepp [31]). *f_λ converge en probabilité dans la C^0-topologie vers la fonction limite $\Omega(x)$, définie par*

$$\Omega(x) = \begin{cases} \frac{2}{\pi}(\sqrt{2-x^2} + x \arcsin \frac{x}{\sqrt{2}}), & |x| \le \sqrt{2}, \\ |x|, & |x| \ge \sqrt{2}. \end{cases}$$

Ainsi, le chemin dans le graphe de Young $\omega_0 \nearrow \omega_1 \nearrow \cdots \nearrow \omega_n$ peut être transformé: en le comprimant $1/\sqrt{n}$ fois, on obtient une famille croissante de figures d'aire $\alpha = 0, \frac{1}{n}, \ldots, 1$; en tournant ces figures de 45°, on considére leurs bordures externes (prolonges) comme les graphiques des fonctions 1-Lipschitz $F_\alpha(x)$. Cela, avec la définition de la mesure centrale, motive les deux questions suivantes:

Question 1.1.1. *Que on peut dire d'un chemin typique entre $\emptyset$ et un* **grand** *diagramme de Young donné λ?*

Question 1.1.2. *Que on peut dire d'un chemin choisi au hasard entre un grand diagramme de Young donné λ_1 et un autre grand diagramme de Young donnée $\lambda_2 \supset \lambda_1$?*

Dans ces deux cas, on peut aussi s'intéresser à l'asymptotique du *nombre* de ces chemins, l'estimation de type "grandes déviations" pour le nombre de chemins non typique inclus.

La première question a déjà obtenu sa réponse par les méthodes de la théorie des représentations ([42]). La seconde a été étudie avec les méthodes du principe variationnel par plusieurs auteurs: Morales, Pak et Panova [36] via des *diagrammes excites* et la formule de Naruse, et par Sun [43] via les pavages de dominos et le modèle de perles. Toutefois, il est intéressant d'approcher ces questions avec l'utilisation les autres méthodes, et c'est le point de départ du Chapitre 2.

Avant cela, nous voudrions mentionner des cas, où la Question 1.1.1 peut être attaquée par des méthodes simples combinatoires. On a déjà constaté que la mesure $\bar{\mu}$ est centrale. Cela implique que si on choisit d'abord un diagramme $\lambda \in \mathbb{Y}_n$ par rapport à la mesure de Plancherel et après un chemin $\emptyset = \omega_0, \omega_1, \ldots, \omega_N = \lambda$ dans le graphe de Young uniformément au hasard, alors le diagramme ω_j qu'on obtient à chaque pas j sera distribué par rapport à la mesure μ_j correspondante. Donc, l'application du théorème de Vershik-Kerov-Logan-Shepp donne que le chemin $F_\alpha(x)$ correspondant converge en probabilité vers celui obtenu par rééchelonnement de la forme Ω,

$$h_\alpha(x) = \sqrt{\alpha}\,\Omega(\frac{x}{\sqrt{\alpha}}).$$

Donc, le chemin aléatoire vers un diagramme de Young Plancherel-aléatoire (et donc presque de formeΩ) est donn par le rééchellement d'Ω.

Puis, un chemin entre un diagramme vide et un diagramme de forme carré ou réctangulaire λ peut être décrit par les mêmes méthodes que dans la théorème de Vershik-Kerov-Logan-Shepp, ce qu'ont fait Pittel et Romik dans [39]. À préciser : le nombre de chemins qui traverse un diagramme λ' de taille j est un produit du nombre de chemins entre $\emptyset$ et λ' et du nombre de chemins entre λ' et λ. Le premier peut être calculé via la formule de crochets, et après une transformation logarithmique en une fonctionnelle de type "entropy" évalué sur λ'. L'argument de Pittel et Romik dit qu'on peut calculer le dérnier de la même manière, car le diagramme de Young gauche λ/λ' (qui est la différence $\lambda \setminus \lambda'$), tournée 180°, devient un diagramme de Young simple. Donc, on peut estimer le nombre de chemins traversant λ', et en maximisant la fonctionnelle d'entropie correspondant on trouve la forme limite désirée du chemin; voyez Fig. 1.1.1.

Ces arguments conduisent aussi à la question de nombre de chemins entre

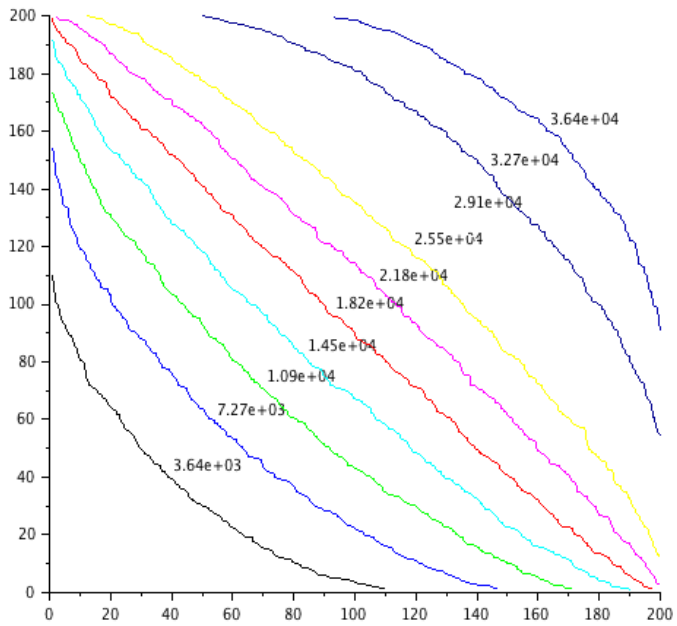

Figure 1.2: YT aléatoire, correspondant à l'YD carré 100×100.

un diagramme de Young et l'autre, ou, ce qui revient au même, à la question du nombre de *Tableaux de Young standard gauches* de la forme λ/λ' indiquée (qui est la façon d'énumérer des cellules de $\lambda \setminus \lambda'$ en ordre d'apparence au long du chemin : décroissant dans chaque rangée et chaque colonne).

Elle est étudiée dans les travaux récents de Morales, Pak, Panova et Tassy [32, 33, 34, 35, 36], en utilisant la formule de Naruse (la formule des crochets modifiée [37]) et la notion d'YD excitée. Ces auteurs ont conjecturé ([35, Conjecture 1]) et ils ont prouvé ([36]) que si les grands diagrammes λ_N et λ'_N ont les formes asymptotiques L_λ et $L_{\lambda'}$ respectivement (c'est à dire, les diagrammes comprimés convergent), le nombre de chemins f^{λ_N/λ'_N} de λ'_N à λ_N a une asymtotique de la forme

$$\log F^{\lambda_N/\lambda'_N} = \frac{1}{2} n_N \log n_N + n_N \cdot c(L_{\lambda'}, L_\lambda) + o(n_N),$$

où $n_N = |\lambda_N/\lambda'_N|$ et c est une fonctionnelle. (Aussi, pour λ' beaucoup plus petite que λ cette question est étudiée dans [16], avec des méthodes de théorie des représentations.)

1.1.2 Des formules explicites

Dans le Chapitre 2 nous présentons les arguments qui nous permettent de deviner la formule explicite de cette fonctionnelle.

Définition 1.1.1. À un grand YT gauche de forme λ/λ' de taille n (le nombre des cellules) nous mettons en correspondance une fonction $g(t,x)$: $[0,1] \times \mathbb{R} \to \mathbb{R}_+$, définie de la manière suivante. Pour $j = 0, 1, \ldots, n$, soit $g(\frac{j}{n}, x)$ une fonction dont le graphe est le borde externe du diagramme composé des premières j cellules de YT, tourné par 45 dégrés et contracté $\sqrt{n}$ fois. Cette fonction-là est prolongée sur chaque intervalle $t \in [\frac{j}{n}, \frac{j+1}{n}]$ en manière affine.

Définition 1.1.2. Soit λ_N/λ'_N une famille des YD gauches de tailles n_N, tels que 45°-tournés $\frac{1}{\sqrt{n_N}}$-rééchelonnés, ces YDs sont uniformément délimité et convergent vers une forme asymptotique L/L'. On dit que la fonction $g(t,x)$ définit la forme asymptotique du YT correspondant à cette série si les fonctions $g_N(t,x)$ correspondantes aux YTs gauches aléatoires des formes λ_N/λ'_N convergent en probabilité vers $g(t,x)$.

Conjecture 1.1.1. • *La fonction $g(t,x)$ qui définit la forme asymptotique d'un YT gauche de la forme L/L', maximise la fonctionnelle*

$$\mathcal{L}[g] = \int_0^1 \int_{\mathbb{R}} g'_t(-\log g'_t + \log\cos\frac{\pi g'_x}{2})\,dx\,dt - \log\frac{\pi}{\sqrt{2}}. \tag{1.2}$$

avec les valeurs limites $g(0,x)$ et $g(1,x)$ données par les formes de L et L' respectivement. La constante additive n'est pas nécessaire pour le problème de maximisation, mais elle est importante pour les autres conclusions.

- *Le nombre F^{λ_N/λ'_N} de tels tableaux se comporte comme*

$$\log F^{\lambda_N/\lambda'_N} = \frac{1}{2}n_N\log n_N + n_N\mathcal{L}[g] + o(n_N), \tag{1.3}$$

où $n_N = |\lambda_N/\lambda'_N|$ est le nombre de cellules (on rappelle que g est choisi d'avoir l'aire unitaire).

En plus, soit $g_0(t,x)$ une autre fonction continue et presque partout lisse, satisfaisant les mêmes conditions limites et les restrictions d'aire

$$\forall t \in [0,1] \quad \int_{\mathbb{R}} (g_0(t,x) - g_0(0,x))\,dx = t.$$

Pour chaque N on peut considérer le nombre $F^{\lambda_N/\lambda'_N}_{\varepsilon,g_0}$ de tels YT que la fonction g correspondante est ε-proche (en C^0-topoligie) à la fonction g_0. En fait, la fonctionnelle $\mathcal{L}$ devrait décrire l'asymptotique du nombre de ces chemins pour chaque g_0, et c'est la raison elle apparaît dans la conjecture précedente.

Conjecture 1.1.2. *Le nombre $F^{\lambda_N/\lambda'_N}_{\varepsilon,g_0}$ d'YT de la forme λ_N/λ'_N et ε-proche de la forme g_0 se comporte asymptotiquement comme*

$$\log F^{\lambda_N/\lambda'_N}_{\varepsilon,g_0} = \frac{1}{2}n_N\log n_N + n_N\cdot\mathcal{L}[g_0] + o(n_N)$$

quand $n_N \to \infty$ et $\varepsilon \to 0$. On a plus précisément :

$$\lim_{\varepsilon\to 0}\limsup_{N\to\infty}\frac{1}{n_N}\left(\log F^{\lambda_N/\lambda'_N}_{\varepsilon,g_0} - \frac{1}{2}n_N\log n_N + n_N\cdot\mathcal{L}[g_0]\right) = 0.$$

Remarque 1.1.1. Avec une notion de proximité entre les YDs gauches et leurs formes limites un peu plus forte (le bord de forme limite doit être dans const fois la taille d'une cellule), ces conjectures découlent de ce que Sun a prouvé dans sa prépublication : voir Définition 5.4, Théorèmes 7.1, 7.15 et 9.1 dans [43]. Mais nous croyons qu'on peut affaiblir ces hypothèses ; aussi, on peut trouver intéressant qu'on peut obtenir ces prédictions avec une approche directe et pas compliquée.

Remarque 1.1.2. Il est à noter qu'on peut choisir une autre échelle pour la renormalisation de la fonction g. Supposons que l'on ait choisi la normalisation d'aire égale à 2; formellement, on considère $\tilde{g}(t,x) = \sqrt{2}\, g(t, \frac{x}{\sqrt{2}})$. Cette normalisation vient de considération des diagrammes de maya, voyez Remarque 2.1.1. Ici, la fonctionnelle $\mathcal{L}$ se réécrit sous la forme :

$$\mathcal{L}[g] = \widetilde{\mathcal{L}}[\tilde{g}] := \frac{1}{2}\int_0^1 \int_{\mathbb{R}} (-\log \frac{\pi \tilde{g}'_t}{2} + \log\cos\frac{\pi \tilde{g}'_x}{2})\, \tilde{g}'_t \, dx\, dt. \tag{1.4}$$

Le facteur $\frac{1}{2}$ provient du changement d'aire, et la constante $\log \frac{\pi}{\sqrt{2}}$ disparaît grace au remplacement de $\log g'_t$ par $\log \frac{\pi \tilde{g}'_t}{2} = \log \frac{\pi g'_t}{\sqrt{2}}$.

C'est intéressant de noter que dans (1.4) les dérivées dans les deux directions de $\tilde{g}$ sont multipliées par $\frac{\pi}{2}$, suggérant, peut être, que $\frac{\pi \tilde{g}}{2}$ soit un objet plus "naturel" dans un sens à préciser.

Remarque 1.1.3. Un autre rééchelonnement par le facteur n, mène à $\tilde{G}(t,x) := \sqrt{n}\, \tilde{g}(\frac{t}{n}, \frac{x}{\sqrt{n}})$, donne la figure d'aire $2n$. Ainsi, la partie droite de (1.3) (sauf le terme-erreur) peut être écrit comme

$$\hat{\mathcal{L}}[\tilde{G}] = \frac{1}{2}\int_{\mathbb{R}} \int_0^n (-\log \frac{\pi \tilde{G}'_t}{2} + \log\cos\frac{\pi \tilde{G}'_x}{2})\, \tilde{G}'_t \, dx\, dt. \tag{1.5}$$

1.1.3 La modification de TASEP et le calcul de son entropie

On note qu'on peut regarder les diagrammes de Young gauches standards (ou, ce qui revient au même, les chemins dans le graphe de Young) comme une sorte spéciale de pavages de dominos sur une partie spéciale du réseau hexagonal. En plus, en passant à la limite dans cette construction, on peut éliminer les conditions sur les dominos, car ceux qui ne les satisfont pas ont une mesure asymptotique nulle. C'est fait dans la Section 2.1.

Ce point de vue, même s'il est simple, donne les conclusions intéressantes. On obtient une forte évidence pour la loi des grandes nombres pour le chemin entre deux grands diagrammes : il devrait y avoir une forme asymptotique du chemin, car il y en a une pour les pavages de dominos. Cela nous permet de prédire la fonctionnelle d'entropie que ce chemin maximise, et donc motive l'introduction de la modification du TASEP suivante.

On considère un cercle muni d'emplacements (trous) et les pierres placées dans certains d'entre eux. À chaque pas une des pierres se déplace dans le trou placé à droite. Dans le modèle TASEP classique, toutes les pierres qui peuvent se déplacer, le font équiprobablement. Dans notre cas, au contraire, les probabilités correspondantes sont différentes et elles dépendent de "degré de liberté" du mouvement de la pierre. C'est à dire, on choisit les probabilités de sauts de sorte que l'entropie du processus soit maximale. L'explication profonde se trouve dans Section 2.3, avec le

Théorème 1.1.2. *Pour le cercle de longueur L (c'est à dire, le nombre des trous) et avec N pierres, l'entropie de la chaîne de Markov correspondante est égal à* $\log \frac{\sin \frac{\pi N}{L}}{\sin \frac{\pi}{L}}$. *Les probabilités des états pour la mesure d'entropie maximale sont données par la mesure déterminantale dont le noyau de corrélation est décrit par la projection sur N harmoniques consécutives de Fourier (parmi L).*

Ce processus se trouve être intéressant pour lui-même : sa mesure stationnaire est déterminantale, et en passant à la limite elle donne une intuition pour le processus sinus qui apparaît sur le bord de grands YD aléatoires (Remarque 2.3.1) et pour la formule précise de la fonctionnelle dans le théorème de Morales-Pak-Panova-Tassy (Conjecture 1.1.1).

En fait, on peut aussi deviner la fonctionnelle avec un argument très simple en utilisant les équations differentielles (Section 2.2.2), qui conduit, naturellement, vers la même réponse, cristallisée dans les Conjectures 1.1.1 et 1.1.2.

1.1.4 Les relations aux modèles dimère et perles

On encode l'évolution du TASEP modifié dans un certain modèle dimère sur le graphe planaire correspondant (plutôt hexagonal). En introduisant un "impôt" sur les arêtes d'une des directions on "gèle" le modèle ; en combinant cela à un rééchellement du temps, on trouve un processus limite "diagonal" non-trivial.

D'une part, un tel processus peut être décrit explicitement à l'aide de la chaîne de Markov m-TASEP originale:

Théorème (Théorème 2.3.1)**.** *Ce processus limite est obtenu par couplage de la mesure d'entropie maximale pour la chaîne de Markov topologique inversible et d'un processus de Poisson sur* $\mathbb{R}$ *d'intensité constante, fournissant les temps des sauts. L'intensité du processus Poisson est égale à* e^h*, où* h *est l'entropie de la chaîne de Markov (donnée par Théorème 1.1.2).*

D'autre part, en utilisant la théorie de Kasteleyn [28, 29], on voit qu'on peut le décrire par une formule de type déterminantal, et obtenir une description explicite pour son noyau de corrélation:

Théorème (Théorème 2.3.2)**.** *Pour le processus limite dans le Théorème 2.3.1, la probabilité que les* pierres *soient présentes aux positions* $k_1, \ldots, k_n$ *aux moments* $t_1, \ldots, t_n$ *est égale au déterminant*

$$\det(\tilde{K}(t_a - t_b, k_a - k_b)_{a,b=1,\ldots,n}),$$

ou le noyau $\tilde{K}$ *est donné par* (2.29), (2.30).

Cela propose une preuve alternative au Théorème 1.1.2 (voyez le corollaire 2.3.2). Nous obtenons aussi la description similaire pour le processus de saut :

Théorème (Théorème 2.3.3)**.** *Pour le processus limite dans le Théorème 2.3.1, la* densité *commune de la probabilité pour les sauts en* $(k_1, t_1), \ldots, (k_n, t_n)$ *est égale au déterminant*

$$\det(\tilde{K}(t_a - t_b, k_a - k_b - 1)_{a,b=1,\ldots,n}) \tag{1.6}$$

pour N *impair*

$$\det(\omega\tilde{K}(t_a - t_b, k_a - k_b - 1)_{a,b=1,\ldots,n}) \tag{1.7}$$

pour N *pair.*

Et c'est une point de vu alternatif sur le modèle des perles consideré par Boutillier [7] et Sun [43], surtout pour son noyau de corrélation.

Finalement, les relations entre les sauts de pierres et le modèle dimère offrent une explication immédiate sur le fait que la "poissonisation" de la mesure de Plancherel est déterminantale. À préciser, cette Poissonisation peut être vu aussi via des pavages de dominos sur le réseau hexagonal (en passant à la limite), et ces derniers sont connus pour être déterminantaux. C'est fait dans Section 2.4.

1.2 Systèms dynamiques aléatoires sur la droite réelle

1.2.1 Aperçu du problème

Chapitre 3 est dédié à l'étude des systèmes dynamiques aléatoires (SDA) sur la droite réelle. C'est à dire, soit $f_1, \ldots, f_k \in \mathrm{Homeo}_+(\mathbb{R})$ un ensemble fini d'homéomorphismes qui conservent l'orientation avec les probabilités $p_1, \ldots, p_n$ de leur application, $p_1 + \cdots + p_k = 1$. À chaque pas on applique une de ces applications, choisies de manière indépendantes, selons les probabilités $p_1, \ldots, p_n$; le lecteur trouvera les précisions dans Section 3.1 à dessous.

Ce travail est motivé par l'article de Deroin et al. [15], où les auteurs ont consideré le cas de dynamiques **symétriques**, c'est à dire, on applique chaque application et son inverse avec la même probabilité. Ils ont démontré que dans le cas symétrique, sauf dans des situations dégénérées, il n'y a pas de mesure stationnaire de probabilité, mais il en existe de masse infinie. En même temps, la dynamique symétrique est toujours récurrente : il existe un intervalle compact tel que toute orbite aléatoire, commençant n'importe où, visite cet intervalle presque certainement une infinité de fois. Néanmoins, la symétrie était utilisée dans [15] de manière indispensable, et donc il était particulièrement intéressant d'étidier tous les types de comportement possibles quand on supprime cette hypothèse.

Il est à noter qu'un changement des coordonnées transforme $\mathbb{R}$ dans l'intervalle $(0, 1)$. La dynamique sur l'intervalle a été étudie par plusieurs auteurs, y compris Guivarc'h, Le Page [23], Deroin, Navas, Parwani [15], Ghaeraei, Homburg [20], Brofferio, Buraczewski, Damek, Szarek, Zdunik, Czudek, Czernous, [10, 9, 44, 13], Alsedà, Misiurewich [2], Kan [27], Bonifant, Milnor [5], Ilyashenko, Kleptsyn, Saltykov [24], et autres.

Les auteurs ont souvent étudié SDA sur $(0, 1)$ avec des hypothèses de lissage (et de minimalité) additionnelles : par exemple, dans [20, 27, 24] on suppose que la dynamique est lisse partout, dans [44, 14] — aux points d'extrémité. Cette hypothèse de lissage permet l'utilisation de la technique des exposants de Lyapunov pour décrire le comportement aux points d'extrémité.

Notamment, il est naturel d'attendre — et les auteurs mentionnés au-dessus, l'ont prouvé — que les exposants de Lyapunov aléatoires positifs aux points d'extrémité implique la "répulsion aléatoire" et donc la mesure stationnaire de probabilité a son support à l'intérieur de l'intervalle. D'autre

part, des exposants de Lyapunov negatifs impliquent que les trajectoires tendent vers les points d'extrémité presque certainement. Finalement, le cas des exposants *nuls* est proche du cas "positif" : une orbite aléatoire part presque certainement d'un voisinage d'une d'extrémité, mais cela prend un temps infini.

Les deux premiers types de comportements sont duaux l'un de l'autre de la manière suivante. Soit μ la mesure discrète de probabilité sur $\mathrm{Homeo}_+(\mathbb{R})$ qui définit la dynamique (c'est à dire $\mu(\{f_i\}) = p_i$), et soit $\hat{\mu}$ son image quand toutes les applications sont replacés par leur inverse, donc $\hat{\mu}(f) = \mu(f^{-1})$. Nous appelons la première *la dynamique avant*, la dernière *inverse*. Si pour la dynamique avant les exposants de Lyapunov sont positifs, pour l'inverse ils sont negatifs. De plus, un exposant nul pour la dynamique avant implique la même proprieté pour la dynamique inverse (et vice-versa). Cela nous permet de classer les comportements possibles pour les dynamiques avant et inverse en un petit nombre de cas.

1.2.2 Résultats principaux

Dans le Chapitre 3 on montre que les conclusions comme au-dessus (et la dualité entre les dynamiques avant et inverse) peuvent être établies sans tous hypothèse de lissage, par l'application directe de méthodes purement *topologiques*. Le premier resultat, Théorème 1.2.1 ci-dessous indique que pour une SDA sur $\mathbb{R}$ les comportements des dynamiques avant et inverse sont de quatre types différents.

Théorème 1.2.1. *Soit une SDA sur $\mathbb{R}$, définie par une mesure avec un support fini μ sur $\mathrm{Homeo}_+(\mathbb{R})$ est telle que*

$$\forall x \in \mathbb{R} \quad \exists f, g \in \operatorname{supp} \mu : \quad g(x) < x < f(x).$$

Puis, quitte à changer μ en $\hat{\mu}$ et quitte à renverser par $x \mapsto (-x)$, l'action est de précisément l'un des types suivants:

1. *en dynamique avant tous les points vont vers $+\infty$ presque certainement, en dynamique inverse tous les points vont vers $-\infty$ presque certainement;*

2. *en dynamique avant tous les points vont vers $+\infty$ presque certainement, la dynamique inverse est récurrente (tous les points presque certainement reviennent dans un intervalle compact une infinité de fois);*

3. *les deux dynamiques (avant et inverse) sont récurrentes;*

4. *en dynamique avant tous les points tendent avec une probabilité non nulle vers chaque infini, la dynamique inverse est récurrente.*

Actuellement, l'hypothèse de "support fini" peut être affaiblie par celle de "déplacements compacts" (voir Définition 3.1.2). En plus, une partie des conclusions subsiste si on l'omet complétement (Théorème 3.1.1). Mais la dynamique dans le cas infini peut se comporter beaucoup plus méchamment. À préciser, dans Section 3.4 on construit un "exemple monstre" qui illustre une dynamique non-récurrente, mais qui ne tend individuellement ni vers $+\infty$, ni vers $-\infty$.

Notre deuxième résultat est dédié à la description des mesures stationnaires (Radon) dans les parties récurrentes de ces cas. La preuve de leur existence suit essentiellement de la construction de [15], mais ici ces mesures peuvent être finies, infinies ou semi-infinies selon le comportement des dynamiques. Aussi, il est à noter que sous une hypothèse additionnelle de *proximité* de l'action (c'est à dire, un intervalle de longeur arbitraire peut être contracté dans un intervalle donné), un résultat récent de Brofferio, Buraczewski et Szarek [10, Théorème 1.1] implique que la mesure stationnaire de Radon est unique.

Théorème 1.2.2. *Soit μ une mesure de probabilité avec un support fini sur* $\mathrm{Homeo}_+(\mathbb{R})$*, satisfaisant les hypothèse de Théorème 1.2.1. Selon l'appartenance à l'une des quatre classes décrites dans Théorème 1.2.1 le SDA satisfait les propriétés suivantes:*

1. *Les dynamiques avant et inverse sont non-récurrentes.*

2. *La dynamique avant est non-récurrente. La dynamique inverse est récurrente et elle admet une mesure stationnaire* semi-infinie *de Radon : la mesure en $+\infty$ est finie, mais la mesure en $-\infty$ ne l'est pas. Cette mesure peut être construite en utilisant les probabilités à frapper pour la dynamique avant.*

3. *Les dynamiques avant et inverse sont récurrentes et admettent une mesure stationnaire infinie de Radon, mais pas de probabilité, ni semi-infinie (c'est la même conclusion que dans le cas symétrique) ;*

4. *La dynamique avant est non-récurrente ; il y a une mesure stationnaire de probabilité pour la dynamique inverse, sa fonction de distribution est la probabilité d'aller vers $+\infty$ pour un point.*

En regroupant les conclusions des Théorèmes 1.2.1 et 1.2.2, on obtient le Tableau 1.1.

no.	Dynamique avant	Dynamique inverse
1	Tout tend vers $+\infty$	Tout tend vers $-\infty$
2	Tout tend vers $+\infty$	La dynamique est récurrente et admet une mesure stationnaire semi-infinie
3	La dynamique est récurrente et admet une mesure stationnaire infinie	La dynamique est récurrente et admet une mesure stationnaire infinie
4	Chaque point tend vers $+\infty$ ou $-\infty$ avec des probabilités positives	La dynamique est récurrente et admet une mesure stationnaire de probabilité

Table 1.1: Les cas possibles pour les dynamiques

1.2.3 Plan du Chapitre 3

Nous introduisons les notations et rappelons les définitions dans Section 3.1. Après, dans la Section 3.2, on étudie les proprietés des fonctions ϕ_+ et ϕ_-, donnant les probabilités que l'orbite d'un point initial x converge vers $+\infty$ et $-\infty$ respectivement. Dans la Section 3.3 on utilise ces fonctions pour étudier les comportements possibles simultanés pour les dynamiques duaux. La Section 3.4 est consacrée à construction d'exemple monstre avec les points s'échappant vers infinie, mais oscillant entre plus et moins l'infini. Finalement, la Section 3.5 est consacrée aux constructions et à l'étude des mesures stationnaires.

Chapter 1

Introduction

My thesis is devoted to the study of two different questions, both of which are related to the problems of random dynamics.

In the Chapter 2 I study the behaviour of large random (skew) Young tableaux. The description of their local behaviour, in particular, turns out to be related with a specific topological Markov chain, the modified TASEP process on the circle, and with its measure of maximal entropy.

The Chapter 3 is devoted to the study of stationary measures for the non-symmetric random dynamical systems on the real line, and their relation to the asymptotic properties of the time-reversed dynamics.

The next two sections are devoted to the detailed description of the general background of these domains and the results obtained.

The author would like to thank Vadim Gorin, Alexey Bufetov, Leonid Petrov, Greta Panova, Alejandro Morales, Igor Pak, Sara Brofferio and Grigory Merzon for their interest to the work and helpful discussions.

1.1 Limit shapes of large skew Young tableaux and a modification of the TASEP process

1.1.1 General background and overview of the problem

The Young diagrams (YD for short) and notions, related to them, have been studied for a long time (for instance, see works of Feit, Carlitz-Riordan, De Concini, Edelman and Berele-Regev [18, 11, 12, 17, 4]). This study was

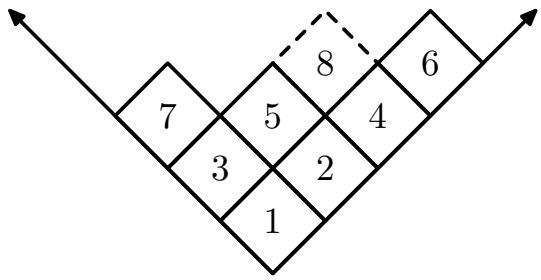

Figure 1.1: Standard Young Tableau

motivated both by the combinatorial reasons (YD of size n correspond to partitions of number n) and by the representation theory (YD of size n enumerate irreducible representations of the symmetric group S_n). We denote the set of all Young diagrams of size n by $\mathbb{Y}_n$.

The *Young graph* is an oriented graph that has Young diagrams as its vertices, and whose edges go from each YD to all YD's that can be obtained by adding a cell to the initial diagram. On the language of the representation theory, $\lambda \in \mathbb{Y}_n$ is joined to all $\mu \in \mathbb{Y}_{n+1}$ that are contained in the induced representation of S_{n+1}, or equivalently, if the representation ρ_λ is contained in the restriction of the corresponding representation ρ_μ to S_n. The latter (together with the fact that the multiplicity of such an inclusion never exceeds one) implies that the dimension $\dim \lambda$ of the irreducible representation ρ_λ, associated to the YD λ, is equal to the number of paths in the Young graph that join the empty (or one-cell) diagram with λ.

A path in the Young graph, starting at the empty diagram, can be encoded by writing in each cell the number of step at which it is added, thus putting it into a bijective correspondence with a *standard Young tableau*. The latter, by definition, is a way of putting numbers $\{1, \ldots, n\}$ in cells of the YD of size n in such a way that the numbers are increasing in each row and column, and that each number is used exactly once. (Similar construction with path going from some *non-empty* YD to another leads to the notion of a *skew Young tableau*.)

The representation theory then motivates the study of the Plancherel measure: one has

$$\sum_{\lambda \in \mathbb{Y}_n} \dim^2 \lambda = n!,$$

and hence the measure μ_n on $\mathbb{Y}_n$, defined by $\mu_n(\{\lambda\}) = \frac{\dim^2 \lambda}{n!}$, is a probability one.

This measure gives rise to a central measure $\bar{\mu}$ on the paths on the Young graph. The *central measures* in general are defined in the following way. Assume that one is given a graph G with the graded set of vertices $V = \bigsqcup_n V_n$, with edges joining vertices from V_n to the vertices from V_{n+1}. By definition, a probability measure on the paths $\omega = \{\omega_n\}_{n=0}^{\infty}$, $\omega_n \in V_n$, is *central* if for any n and any $v \in V_n$ conditional to $\omega_n = v$ the initial part $\omega_0, \omega_1, \dots, \omega_{n-1}, \omega_n$ of the path is distributed uniformly on all the paths that end at v at the moment n.

It is easy to see that a central measure is necessarily Markovian (the future is independent from the past). Also, its marginal measures μ_n defining the law of ω_n should *agree* with each other: for any $m < n$, considering the law of ω_m in a uniformly chosen path leading to vV_n and averaging with v distributed w.r.t. μ_n, we are getting μ_m. Vice versa, a sequence of measures μ_n defines a central measure (for which they serve as marginals), provided that they agree. One of the basic examples of such measures are Bernoulli ones: a random path (x_n, y_n), where x_n and y_n are respectively the number of heads and tails after tossing of a Bernoulli coin n times. Indeed, given the number $k = x_n$ of successes after tossing a coin n times, all the $\binom{n}{k}$ possible placements of these successes are equiprobable — whichever was the probability p of a success.

As we have mentioned, it is known (though not evident) that Plancherel measures μ_n on sets $\mathbb{Y}_n$ agree with each other and hence give rise to a central measure on the set of paths in the Young graph. This measure has forward transition probability from $\lambda \in \mathbb{Y}_{n-1}$ to $\lambda' \in \mathbb{Y}_n$

$$p_{\lambda \nearrow \lambda'} = \frac{\dim \lambda'}{n \dim \lambda}.$$

It is easy to check that these probabilities define a Markov chain with marginal laws μ_n at time n, giving the backward transition probability

$$\mathbb{P}(\omega_{n-1} = \lambda \mid \omega_n = \lambda') = \frac{\dim \lambda}{\dim \lambda'} \tag{1.1}$$

(where $\omega_0 = \emptyset, \omega_1, \omega_2, \dots$ is a path randomly chosen w.r.t. this measure) and hence satisfying a definition of a central measure (the relation (1.1) easily implies that the distribution on the starting segments of paths coming to $\lambda \in \mathbb{Y}_n$ is uniform).

A general paradigm of asymptotic combinatorics is that a large random combinatorial object often satisfies some kind of the "law of large numbers": if properly rescaled, it looks like a deterministic one. There are many examples of such results (for example see [41, 45, 3]). Of the ones related to YD, the first that we would like to mention here is the limit shape theorem, independently discovered in late 1970's by Versik and Kerov in the USSR and Logan and Shepp in the United States. Namely: take a random diagram $\lambda \in \mathbb{Y}_n$ (in French notation), contract it $\frac{1}{\sqrt{n}}$ times, and rotate it 45° counterclockwise. This gives a random figure F_n of unit area, placed between the rays $y = |x|$. Consider its outer boundary, extended by $y = |x|$ outside the diagram, as a graph of some 1-Lipshitz function f_λ.

Theorem 1.1.1 (Vershik, Kerov [46], Logan, Shepp [31])**.** *f_λ converges in probability in C^0-topology to the limit function $\Omega(x)$, defined by*

$$\Omega(x) = \begin{cases} \frac{2}{\pi}(\sqrt{2-x^2} + x \arcsin \frac{x}{\sqrt{2}}), & |x| \le \sqrt{2}, \\ |x|, & |x| \ge \sqrt{2}. \end{cases}$$

Now, a path in the Young graph $\omega_0 \nearrow \omega_1 \nearrow \cdots \nearrow \omega_n$ can be also transformed in this way: rescaling it $1/\sqrt{n}$ times, we get an increasing family of figures of area $\alpha = 0, \frac{1}{n}, \ldots, 1$; again, rotating these figures by 45°, we can consider their (extended) outer boundaries as graphs of 1-Lipschitz functions $F_\alpha(x)$. This, together with the definition of the central measure, motivates the following two questions:

Question 1.1.1. *What can be said about a typical path from $\emptyset$ to a given* **large** *Young diagram λ?*

Question 1.1.2. *What can be said on a random path from a given large Young diagram λ_1 to a given large Young diagram $\lambda_2 \supset \lambda_1$?*

To both these questions one can add the question of the asymptotics of the *number* of such paths, as well as the one of establishing large deviations-type estimate for the number of paths of a "non-typical" shape.

The first question is already answered by the representation theory methods (see [42]). The second one was attacked (with variational principle methods) by several authors: by Morales, Pak and Panova [36] via the *excited diagrams* and Naruse's formula, and by Sun [43] via the dimer covers and bead models. However, it is interesting to approach these questions with

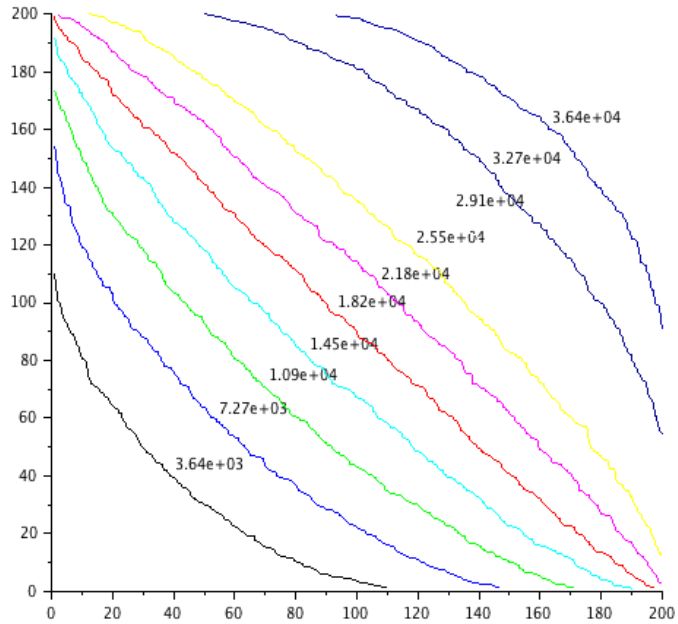

Figure 1.2: Random YT, corresponding to the 100×100 square YD.

yet another methods, and this is the starting point for our considerations in Chapter 2.

Before proceeding, we would like to mention a few cases in which the Question 1.1.1 can be attacked by simple combinatorial methods. As we have already mentioned, the measure $\bar{\mu}$ is central. This implies that if we first choose a diagram $\lambda \in \mathbb{Y}_n$ w.r.t. the Plancherel measure and then pick a path $\emptyset = \omega_0, \omega_1, \ldots, \omega_N = \lambda$ in the Young graph uniformly at random, then at each step j (with α_j equal to the area of corresponding ω_j) the diagram ω_j will be distributed w.r.t. the corresponding measure μ_j. An application of the Vershik-Kerov-Logan-Shepp theorem then gives that the corresponding path $F_\alpha(x)$ converges in probability to the one given by rescaling of the shape Ω,

$$h_\alpha(x) = \sqrt{\alpha}\,\Omega(\frac{x}{\sqrt{\alpha}}).$$

Thus, a random path to a Plancherel-random (and hence almost Ω-shaped) Young diagram is given by rescaling of Ω.

Next, a path, going towards a square- or rectangular-shaped Young di-

agram λ, can be described via the same methods as Vershik-Kerov-Logan-Shepp theorem, and it was done by Pittel and Romik in [39]. Namely: the number of paths that pass through some diagram λ' of size j is a product of number of paths from $\emptyset$ to λ' and of number of paths from λ' to λ. The former can be calculated via the hook formula, and then its logarithm transformed (approximatively) into an entropy-type functional evaluated on λ'. And the argument of Pittel and Romik says that the latter can also be calculated in this way, as the skew Young diagram λ/λ' (that is, the set-theoretical difference $\lambda \setminus \lambda'$), rotated 180°, becomes again simply a Young diagram. Thus, one can estimate the number of paths that go through λ', and maximizing the corresponding entropy functional, one finds the desired limit shape of the path; see Fig. 1.1.1.

The above arguments also lead to the question of study of the number of paths from one Young diagram to the other, or, which is the same, the number of *standard skew Young tableaux* of a given shape λ/λ' (that is, ways of enumerating cells of $\lambda \setminus \lambda'$ in order as they appear in the path: enumeration that is increasing in each row and in each column).

It was studied in recent works by Morales, Pak, Panova and Tassy [32, 33, 34, 35, 36], using Naruse's modified hook-length formula ([37]) and the notion of exited YD. They have conjectured (see [35, Conjecture 1]) and proved ([36]) that if the large diagrams λ_N and λ'_N have asymptotic shapes L_λ and $L_{\lambda'}$ respectively (that is, the rescaled diagrams converge), then the number of paths f^{λ_N/λ'_N} from λ'_N to λ_N has the asymptotics of the form

$$\log F^{\lambda_N/\lambda'_N} = \frac{1}{2} n_N \log n_N + n_N \cdot c(L_{\lambda'}, L_\lambda) + o(n_N),$$

where $n_N = |\lambda_N/\lambda'_N|$ and c is some functional. (Also, for λ' much smaller than λ this question was studied in [16], again, by the methods of the representation theory.)

1.1.2 Explicit formulae

In Chapter 2 we present arguments that allow to guess the explicit form of this functional. To state this question formally, let us give the following

Definition 1.1.1. To a given large skew YT of the shape λ/λ' and consisting of some number n of cells, put in correspondence the function $g(t,x) : [0,1] \times \mathbb{R} \to \mathbb{R}_+$, defined in the following way. For $j = 0, 1, \ldots, n$, let $g(\frac{j}{n}, x)$ be the

function such that its graph is the outer boundary of the first j cells of the YT, rotated by 45 degrees and contracted by the factor $\sqrt{n}$, and let us extend this function on each of the intervals $t \in [\frac{j}{n}, \frac{j+1}{n}]$ in an affine way.

Definition 1.1.2. Consider a sequence of skew YD λ_N/λ'_N of sizes n_N, such that the 45°-rotated $\frac{1}{\sqrt{n_N}}$-rescaled images of these skew YD are uniformly bounded and converge to some asymptotic shape L/L'. Say that the function $g(t,x)$ defines an asymptotic shape of the YT corresponding to this sequence if the functions $g_N(t,x)$ corresponding to random skew YT of the shapes λ_N/λ'_N converge in probability to $g(t,x)$.

Conjecture 1.1.1.

- *The function $g(t,x)$, defining the asymptotic shape of a skew YT of a shape L/L', maximizes the functional*

$$\mathcal{L}[g] = \int_0^1 \int_{\mathbb{R}} g'_t(-\log g'_t + \log\cos\frac{\pi g'_x}{2})\,dx\,dt - \log\frac{\pi}{\sqrt{2}}. \tag{1.2}$$

  with the boundary values $g(0,x)$ and $g(1,x)$ given by the shapes L and L' respectively. The additive constant here is surely irrelevant for the purposes of the maximization problem, but it is important for the other conclusions.

- *The number F^{λ_N/λ'_N} of such tableaux behaves as*

$$\log F^{\lambda_N/\lambda'_N} = \frac{1}{2} n_N \log n_N + n_N \mathcal{L}[g] + o(n_N), \tag{1.3}$$

  where $n_N = |\lambda_N/\lambda'_N|$ is the number of cells (recall that g is chosen to be scaled to the area 1).

Moreover, take any other continuous and almost everywhere smooth function $g_0(t,x)$, satisfying the same boundary conditions, as well as the area restrictions

$$\forall t \in [0,1] \qquad \int_{\mathbb{R}} (g_0(t,x) - g_0(0,x))\,dx = t.$$

Then for any N one can consider the number $F^{\lambda_N/\lambda'_N}_{\varepsilon,g_0}$ of the YT such that the corresponding function g is ε-close (in the C^0-topology) to the function g_0. And actually, the functional $\mathcal{L}$ should describe the asymptotics of number such paths for any g_0, and this is the reason why it appears in the previous conjecture:

Conjecture 1.1.2. *The number $F_{\varepsilon,g_0}^{\lambda_N/\lambda'_N}$ of YT of the shape λ_N/λ'_N and ε-close to the form g_0 has the asymptotic behaviour*

$$\log F_{\varepsilon,g_0}^{\lambda_N/\lambda'_N} = \frac{1}{2} n_N \log n_N + n_N \cdot \mathcal{L}[g_0] + o(n_N)$$

as $n_N \to \infty$ and as $\varepsilon \to 0$, in the sense that the double limit for the error term vanishes:

$$\lim_{\varepsilon\to 0} \limsup_{N\to\infty} \frac{1}{n_N} \left(\log F_{\varepsilon,g_0}^{\lambda_N/\lambda'_N} - \frac{1}{2} n_N \log n_N + n_N \cdot \mathcal{L}[g_0] \right) = 0.$$

Remark 1.1.1. With a slightly stronger notion of closeness for the skew Young diagrams to their limit forms (the limit shape boundary should be within const times the size of a cell), these statements follow from what is established in Sun's preprint [43]: see Definition 5.4, Theorems 7.1, 7.15 and 9.1 therein. However, we believe that these assumptions can be weakened; it seems also interesting to us that these predictions can be found by a straightforward and not too technically complicated approach.

Remark 1.1.2. Note that we can choose another scaling normalization for the function g, not necessarily choosing it to be spanned area 1. Let us pass to the total area 2 normalization; formally speaking, we consider $\tilde{g}(t,x) = \sqrt{2}\, g(t, \frac{x}{\sqrt{2}})$. This normalization comes out of maya diagram consideration, see Remark 2.1.1. In this normalization, the functional $\mathcal{L}$ can be rewritten as

$$\mathcal{L}[g] = \widetilde{\mathcal{L}}[\tilde{g}] := \frac{1}{2} \int_0^1 \int_{\mathbb{R}} (-\log \frac{\pi \tilde{g}'_t}{2} + \log\cos \frac{\pi \tilde{g}'_x}{2})\, \tilde{g}'_t \, dx\, dt. \tag{1.4}$$

The factor $\frac{1}{2}$ here is due to the area change, while the constant $\log \frac{\pi}{\sqrt{2}}$ disappears due to the replacement of $\log g'_t$ by $\log \frac{\pi \tilde{g}'_t}{2} = \log \frac{\pi g'_t}{\sqrt{2}}$.

It is interesting to note that in (1.4) the derivatives in both directions of $\tilde{g}$ are multiplied by $\frac{\pi}{2}$, possibly suggesting that $\frac{\pi \tilde{g}}{2}$ might be in some sense a more "natural" object.

Remark 1.1.3. A further rescaling by a factor of n, that is, consideration of $\tilde{G}(t,x) := \sqrt{n}\, \tilde{g}(\frac{t}{n}, \frac{x}{\sqrt{n}})$, gives a figure of area $2n$, spanned during the time n. In these terms, the right hand side of (1.3) (except for the error term) can be written as

$$\hat{\mathcal{L}}[\tilde{G}] = \frac{1}{2} \int_{\mathbb{R}} \int_0^n (-\log \frac{\pi \tilde{G}'_t}{2} + \log\cos \frac{\pi \tilde{G}'_x}{2})\, \tilde{G}'_t \, dx\, dt. \tag{1.5}$$

1.1.3 Modification of TASEP and computation of its entropy

We note that the standard skew Young diagrams (or, what is the same, paths on the Young graph) can be seen as a special kind of domino tiling on the (special part of a) hexagonal lattice. Moreover, adding a limit to this construction, one can remove the conditioning on the tiles (those not satisfying the condition have asymptotic measure zero). This is done in Section 2.1.

This point of view, though simple, leads to interesting conclusions. It gives a strong evidence for the law of large numbers for the path between two large diagrams: there should be an asymptotic shape of a path, because there is one for the domino tilings. It allows to predict the entropy functional maximized by this path, and for that motivates an introduction of the following modified version of TASEP.

Consider a circle with holes on it and stones placed in some of them. Every step one of the stones moves into the next hole to its right. In the classical TASEP model, all the stones which can move, do so with equal probabilities. In our case, however, the corresponding probabilities are different and depend on how freely a stone can move. Namely, we choose the probabilities of jumps in order for the entropy of the process to be maximal. We explain this in Section 2.3, and prove the following result

Theorem 1.1.2. *For a circle of length L with N stones on it, the entropy of the corresponding topological Markov chain is equal to* $\log \frac{\sin \frac{\pi N}{L}}{\sin \frac{\pi}{L}}$. *The probabilities of states for the measure of maximal entropy are given by a determinantal measure whose correlation kernel is given by the projection on (any) N consecutive Fourier harmonics (out of L).*

This process turns out to be interesting in its own: its stationary measure is determinantal, and passing to the limit it gives a handwaving explanation for the sine-process appearing on the boundary of the random large Young diagram (see Remark 2.3.1) and finding the precise formula for the functional, appearing in Morales-Pak-Panova-Tassy theorem (see Conjecture 1.1.1).

In fact, we note that such a functional can also be guessed by a very simple differential equations argument (see Section 2.2.2), naturally (and quite encouragingly), leading to the same answer, yielding Conjectures 1.1.1 and 1.1.2.

1.1.4 Relation to the dimer and beads models

We encode the evolution of the modified TASEP process into a certain dimer model on the corresponding planar (mostly hexagonal) graph. Introducing a "tax" on edges of one of the directions "freezes" the model; joining it with the time rescaling, we find a nontrivial "diagonal" limit process.

On one hand, such process can be explicitly described in terms of the original m-TASEP Markov chain:

Theorem (Theorem 2.3.1)**.** *This limit process is given by coupling a maximal entropy measure for the two-sided topological Markov chain and of a Poisson process on $\mathbb{R}$ of constant intensity, providing the jump moments. The intensity of the Poisson process is equal to e^h, where h is the entropy of the Markov chain (given by Theorem 1.1.2).*

On the other, using Kasteleyn theory [28, 29], we see that it can be described by a determinantal-type formula, and get an explicit description for its correlation kernel:

Theorem (Theorem 2.3.2)**.** *For the limit process in Theorem 2.3.1, the probability that the* stones *are present at positions $k_1, \dots, k_n$ at times $t_1, \dots, t_n$ is equal to the determinant*

$$\det(\tilde{K}(t_a - t_b, k_a - k_b)_{a,b=1,\dots,n}),$$

where the kernel $\tilde{K}$ is given by (2.29), (2.30).

This proposes an alternate way of establishing Theorem 1.1.2 (see Corollary 2.3.2). We also get a similar description for the jumping process:

Theorem (Theorem 2.3.3)**.** *For the limit process in Theorem 2.3.1, the common* density *of the probability for the jumps at $(k_1, t_1), \dots, (k_n, t_n)$ is equal to the determinant*

$$\det(\tilde{K}(t_a - t_b, k_a - k_b - 1)_{a,b=1,\dots,n}) \tag{1.6}$$

for odd N and to the determinant

$$\det(\omega\tilde{K}(t_a - t_b, k_a - k_b - 1)_{a,b=1,\dots,n}) \tag{1.7}$$

for even N.

This provides with an alternate viewpoint on the beads model considered by Boutillier [7] and Sun [43], and especially on its correlation kernel.

Finally, the relations between the jumping of stones and the dimer model also allows to provide an immediate (non-computational) explanation, why the Poissonization of the Plancherel measure is a determinantal one. Namely, this Poissonization can also be seen via the (passage to the limit in the) domino tilings on the hexagonal lattice, and the latter are known to be determinantal. This is done in Section 2.4.

1.2 Random dynamical systems on the real line

1.2.1 General background

Chapter 3 is devoted to the study of random dynamic systems (RDS) on the real line. That is, we are given a finite number of orientation-preserving homeomorphisms $f_1, \dots, f_k \in \mathrm{Homeo}_+(\mathbb{R})$ together with the probabilities $p_1, \dots, p_n$ of their application, $p_1 + \dots + p_k = 1$. On each step we apply one of these maps, chosen independently in accordance to these probabilities; the reader will find precise details in Section 3.1 below.

This work was motivated by the paper of Deroin et al. [15], where the authors have considered the case of **symmetric** dynamics, that is, applying any map with the same probability as its inverse. They have shown that in the symmetric case, except for some degenerate situations, there is no *probability* stationary measure (we recall the definition below), though there is an infinite Radon one. At the same time, the symmetric dynamics is always recurrent: there exists a compact interval such that a random orbit, starting from any point, almost surely visits this interval infinitely many times. However, the symmetry in [15] was used in an essential way and it is interesting to study all the possible types of behavior when this assumption is omitted.

Note, that a change of coordinates transforms $\mathbb{R}$ into the interval $(0, 1)$. The dynamics on the interval and on the real line was studied by many authors, including Guivarc'h, Le Page [23], Deroin, Navas, Parwani [15], Ghaeraei, Homburg [20], Brofferio, Buraczewski, Damek, Szarek, Zdunik, Czudek, Czernous, [10, 9, 44, 13], Alsedà, Misiurewich [2], Kan [27], Bonifant, Milnor [5], Ilyashenko, Kleptsyn, Saltykov [24], and many others.

In many of these works, their authors have studied RDS on $(0,1)$ under additional smoothness (and minimality) assumptions: e.g. in [20, 27, 24] it is assumed that dynamics is smooth everywhere, in [44, 14] — at the endpoints. This smoothness assumption has allowed to invoke the technique of the Lyapunov exponent to describe the behaviour at the endpoints.

Namely, it is quite natural to expect — and the authors, mentionned above, have shown it – that positive random Lyapunov exponents at the endpoints imply the "random repulsion" and thus a probability stationary measure, supported inside the interval. On the other hand, negative Lyapunov exponents imply that the trajectories almost surely tend to endpoints. Finally, *zero* Lyapunov exponents are somewhat close the the positive ones: a random orbit almost surely leaves the neighborhood such an endpoint, but the expectation of time to do so is infinite.

The first two types of behaviour are dual to each other in the following sense. Let us denote by μ the discrete probability measure on $\mathrm{Homeo}_+(\mathbb{R})$ defining the dynamics (that is $\mu(\{f_i\}) = p_i$), and by $\hat{\mu}$ its image when all the maps are replaced by their inverses, so $\hat{\mu}(f) = \mu(f^{-1})$. We call the former *forward dynamics*, the latter *inverse*. If for the forward dynamics the Lyapunov exponents are positive, then for the inverse one they are negative. Also, the inverse dynamics to the one with zero Lyapunov exponent also has zero Lyapunov exponent at that endpoint. This allows to describe possible behaviours for the forward and backward dynamics, grouping these in quite a few classes.

1.2.2 Main results

In this Chapter, we show that that such conclusions (and a duality between forward and backward dynamics) can be established with no smoothness assumptions at all, by direct application of purely *topological* methods. In the first result, Theorem 1.2.1 below, we show that for a random dynamical system on $\mathbb{R}$ the behaviours of forward and inverse dynamics fall into one of four "dual" classes.

Theorem 1.2.1. *Assume that RDS on $\mathbb{R}$, defined by a finitely supported measure μ on $\mathrm{Homeo}_+(\mathbb{R})$ is such that*

$$\forall x \in \mathbb{R} \quad \exists f, g \in \operatorname{supp} \mu : \quad g(x) < x < f(x).$$

Then, possibly upon interchanging μ and $\hat{\mu}$ and (or) reversing the orientation

by a space symmetry $x \mapsto (-x)$, the action falls in exactly one of the following classes:

1. *in forward dynamics all the points almost surely tend to $+\infty$, in inverse dynamics all the points almost surely tend to $-\infty$;*
2. *in forward dynamics all the points almost surely tend to $+\infty$, the inverse dynamics is recurrent (all the points almost surely return to some compact infinitely many times);*
3. *both forward and inverse dynamics are recurrent;*
4. *in forward dynamics all the points tend with positive probability to each of $+\infty$ or $-\infty$, the inverse dynamics is recurrent.*

Actually, the "finitely supported" assumption can be weakened to the "compact displacements" one (see Definition 3.1.2). Moreover, part of the conclusions survive if we drop it completely (see Theorem 3.1.1). However, the dynamics in the infinitely supported case can behave much nastier. Namely, in Section 3.4 we construct a monster, illustrating non-recurring dynamics, that does not tend individually neither to $+\infty$, nor to $-\infty$.

Our second result is devoted to the description of (Radon) stationary measures in the recurrent parts of these cases. The existence part essentially follows the construction in [15], however the interesting part is that these measures might be finite, infinite or semi-infinite — as well as their relation to the dynamics. Also, note that under an addition assumption of *proximality* of the action (that is, an arbitrary large interval can be contracted inside a given one), a recent result of Brofferio, Buraczewski and Szarek [10, Theorem 1.1] implies that the Radon stationary measure is unique.

Theorem 1.2.2. *Let μ be a finitely supported probability measure on* $\mathrm{Homeo}_+(\mathbb{R})$*, satisfying the assumptions of Theorem 1.2.1. Depending on into which of the four classes, described in Theorem 1.2.1 does it fall, we have one of the following corresponding conclusions:*

1. *Both forward and backward dynamics are non-recurrent.*
2. *The forward dynamics is non-recurrent. The backward dynamics is recurrent and admits a* semi-infinite *Radon stationary measure: the measure of half-rays to $+\infty$ is finite measure, of half-rays to $-\infty$ is not. This measure can be constructed using hitting probability for the forward dynamics.*

3. *Both forward and backward dynamics are recurrent and admit an infinite Radon stationary measure and do not admit neither a probability, nor a semi-infinite one (the same conclusion as in the symmetric case);*

4. *The forward dynamics is non-recurrent; there is a probability stationary measure for the backward dynamics, its distribution function is the probability for a point to tend to $+\infty$.*

Grouping the conclusions of Theorems 1.2.1 and 1.2.2, we get Table 1.1.

no.	Forward dynamics	Backward dynamics
1	Everything tends to $+\infty$	Everything tends to $-\infty$
2	Everything tends to $+\infty$	The dynamics is recurrent and admits a semi-infinite stationary measure
3	The dynamics is recurrent and admits an infinite stationary measure	The dynamics is recurrent and admits an infinite stationary measure
4	Every point tends to $+\infty$ or to $-\infty$, to both with positive probabilities	The dynamics is recurrent and admits a probability stationary measure

Table 1.1: Possible cases for the dynamics

1.2.3 Plan of Chapter 3

We introduce the notations and recall the definitions in Section 3.1. Then, in Section 3.2, we study the property of the functions ϕ_+ and ϕ_-, giving the probability for the images of the initial point x to tend to $+\infty$ and $-\infty$ respectively. We then apply it in Section 3.3 to study the possible behaviours for forward and backward dynamics simultaneously. Section 3.4 is devoted to the construction of the monster example with points evading to infinity while oscillating between plus and minus infinities. Finally, Section 3.5 is devoted to the constructions and study of stationary measures.

Chapter 2

Limit shapes of large skew Young tableaux and a modification of the TASEP process

2.1 Points of view: maya diagrams, dominos, beads

In this section we present different models, equivalent to a path in Young graph.

We start with recalling the classical **maya diagram.** Consider the real line with the holes at the points of $\mathbb{Z} + \frac{1}{2}$. In these holes (pictured here as white circles) black stones can be placed, each hole containing no more than one stone.

Then one can encode the outer boundary of a YD (drawn in the Russian notation) in the following way: if the edge goes down (reading it from left to right), one places a black stone in the corresponding hole, leaving the hole empty otherwise. See Fig. 2.1.

One can easily see that the "addition of a cell (provided that it can be added)" operation in terms of YD corresponds to "moving the stone to the next hole on its right (provided that it is empty)" in maya diagrams' evolution. Indeed, under the addition (or removal) of a cell, the adjacent 'up' and 'down' edges on the YD border are interchanging, thus moving the

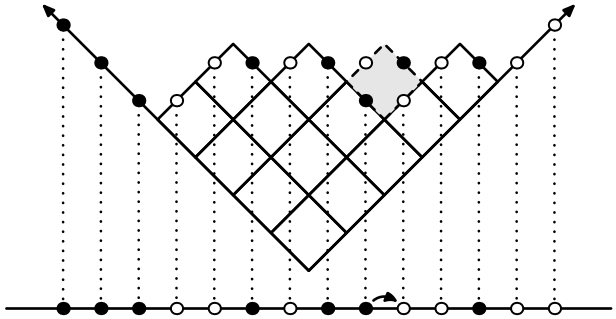

Figure 2.1: Transforming a Young diagram into a maya one; an addition of a new cell (filled square) corresponds to a jump of one of the stones (shown by an arrow).

corresponding stone into the empty hole next to it on the right. (See Fig. 2.1 and Fig. 2.2, bottom left.)

Remark 2.1.1. Note that the YD here naturally has cells of area 2, instead of 1 (so that their edges project to length 1 intervals on the x axis), and the YD itself has area equal to $2n$. This explains why the formulae (1.4) and especially (1.5) become nicer in the corresponding normalizations.

Another classical object is stacked Young diagrams. Given a path in the Young graph, one can stack the complements to the corresponding YDs, putting each of them on the top of the previous one, and considering them to be made of unit cubes instead of unit squares. This provides a 3D object, whose 3D projection gives a **lozenge tiling** by lozenges corresponding to the three possible faces of the cubes; see Fig. 2.2, top right. Lozenge tilings have also appeared in the works of Morales, Pak, Panova and Tassy [32, 33, 34, 35, 36], as they used an approach based on the **excited diagrams**, but as this is not the one we are going to use, we will not go into further details.

Still classically, a lozenge tiling can also be seen as a **dimer configuration** on the corresponding bipartite graph (a subset of the hexagonal lattice), and thus such tilings can be counted with help of the Kasteleyn theorem via the corresponding determinant. However, this approach for counting YTs has two disadvantages: first, not all the lozenge tilings correspond to the paths (one can add none or many cells on the same level), and its upper and lower boundaries depend on the shape of the skew YD that is studied (that is somewhat inconvenient).

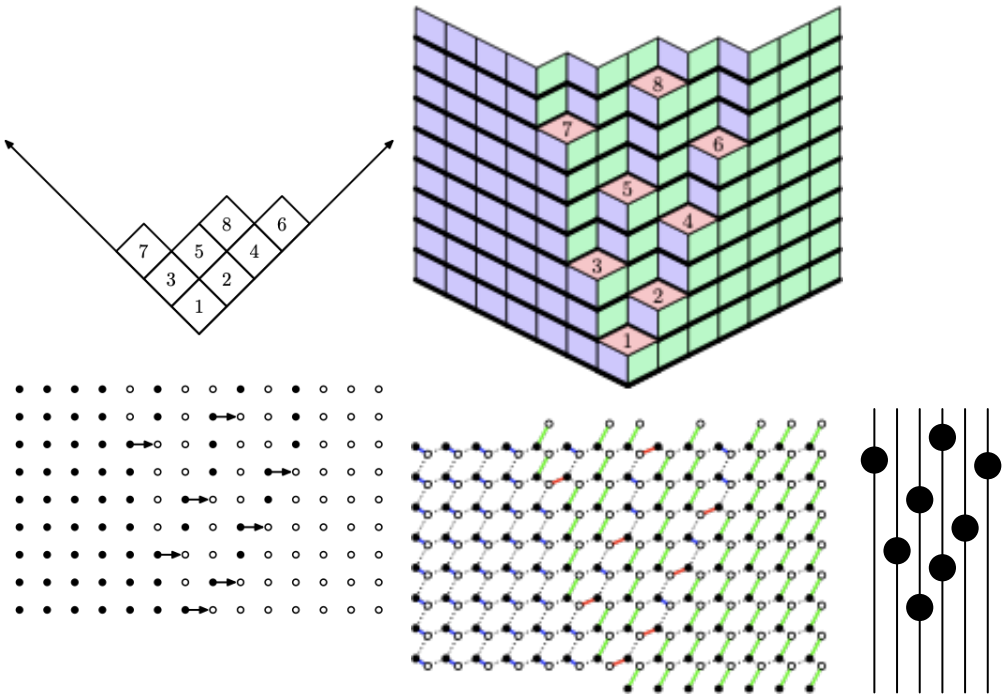

Figure 2.2: A Young Tableau (top left) and its encodings: maya diagram evolution (bottom left), stacked YD and lozenge tiling (top right), dimer configuration (bottom middle), beads model (bottom right).

To address the second issue, we thus will return back to the evolution of maya diagrams. We note that each such evolution can be encoded (in a different way!) by dimer configuration on a graph on a hexagonal lattice. Namely, the evolution of a maya diagram happens on a square lattice with the space and time coordinates x and t respectively. Consider all these points as black vertices, and inside each square let us add a white one. We will connect the white vertex in the square $\{n, n+1\} \times \{t, t+1\}$ to the vertices (n, t), $(n, t+1)$ and $(n+1, t+1)$; see Fig. 2.3.

In terms of the encoding, using the first of these edges means that there is no stone at (n, t), the second one is that a stone is present and stays at this moment where it was, and the last one that the stone that was present at (n, t) has jumped at this moment to the next hole. This process is illustrated on the bottom middle of Fig. 2.2 (red color corresponds to the edges where a stone jumps, and thus a cell is added, green edges encode empty holes, blue ones the non-jumping stones).

Note that this encoding is actually different from the one that corresponds to the stacked YDs. Indeed, though some dimer configuration via a "backward translation" correspond to none or many stones jumping at ones, we see that a stone here cannot jump farther than to the next hole (a possibility that appear in stacked YDs lozenge encoding), and the upper and lower bound are almost horizontal, with only hanging (green) edges describing the boundary conditions (namely, the placement of empty holes at the initial and final maya diagrams).

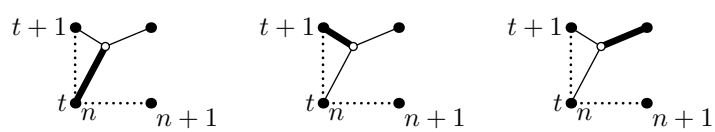

Figure 2.3: Encoding: at the moment t in the hole n there is: no stone (left), stone that stays in the hole (center), stone that jumps to the next hole (right).

A way of addressing the first aforementioned issue, the possibility of having two or zero jumps on the same level, is by increasing the number of levels. Namely, instead of the number of levels equal to the number of jumps n, take it equal to $M \gg n$. Then, to any YT corresponds to exactly $\binom{M}{n}$ different configurations with at most one jump per level. On the other hand, the num-

ber of the configurations where at least two jumps happen on the same level is easily upper bounded by const $\cdot \binom{M}{n-1}$, where the constant does not depend on M. Hence, such configurations' fraction among all the configurations tends to 0 as $M \to \infty$.

Contracting the picture const $\cdot M$ times vertically and passing to the limit as $M \to \infty$, we get a continuous-time model. On one hand, the above arguments easily describe it in the initial terms: it can be obtained from independent pair of a uniform choice of a uniformly distributed YT (describing the places of the jumps) and a n-point independent choice on the time interval (describing the [rescaled] moments when these jumps occur).

On the other hand, what we thus get is a [local version of] so-called the **beads model** (see Fig. 2.2, bottom right). It was studied in, for instance [43, 7]; its object is a discrete subset of $\mathbb{R} \times \mathbb{Z}$, with the property that between (in the $\mathbb{R}$-direction) any its two consecutive points ("beads") on the line $\mathbb{R} \times \{n\}$ there are points on both lines $\mathbb{R} \times \{n-1\}$ and $\mathbb{R} \times \{n+1\}$. This is exactly what we get for the placements of the jump sites: between any two jumps at the same place there should be the jumps in both neighboring sites; plus, for the local part of the model, the beads should satisfy the "boundary conditions". We will postpone the discussion on this dimer model till its use in Sec. 2.3.

2.2 Guessing the answer

2.2.1 Cutting the diagram

This section is devoted to a *non-rigorous* deduction of a general form of the functional that appears in Conjectures 1.1.1 and 1.1.2.

"Horizontal" cut

The first step is a "horisontal cut" of the diagram. Namely, let YDs $\lambda' \subset \lambda$ be given. Choose a number k and a sequence of "intermediable sizes" $n_0 < n_1 < \ldots < n_k$, where $|\lambda'| = n_0$, $|\lambda| = n_k$. Then the total number of paths in the Young graph from λ' to λ can be counted by splitting their set depending on the YDs passed at these sizes:

$$F^{\lambda/\lambda'} = \sum_{(\lambda_0,\ldots,\lambda_k)\in\mathcal{A}^{\lambda/\lambda'}_{n_1,\ldots,n_{k-1}}} F^{\lambda_k/\lambda_{k-1}} \cdot \ldots \cdot F^{\lambda_1/\lambda_0}, \tag{2.1}$$

where

$$\mathcal{A}^{\lambda/\lambda'}_{n_1,\ldots,n_{k-1}} = \{(\lambda_0,\ldots,\lambda_k) \mid \lambda' = \lambda_0 \subset \lambda_1 \subset \lambda_2 \subset \ldots \subset \lambda_k = \lambda, \\ \forall i = 1,\ldots,k-1 : |\lambda_i| = n_i\}.$$

Now, the sum (2.1) is comparable with its maximum summand as it differs from the latter by the factor at most the number of summands. This number, in its turn, can be estimated as

$$|\mathcal{A}^{\lambda/\lambda'}_{n_1,\ldots,n_{k-1}}| \le \prod |\mathbb{Y}_{n_i}| \le \exp\Big(\sum_{i=1}^{k-1} \pi\sqrt{\frac{2n_i}{3}}\Big),$$

where the latter inequality is due to Hardy-Ramanujan formula, $|\mathbb{Y}_n| \sim \frac{1}{4n\sqrt{3}} \exp\big(\pi\sqrt{\frac{2n}{3}}\big)$.

Thus, we get

$$\log F^{\lambda/\lambda'} - \log \max_{(\lambda_0,\ldots,\lambda_k)\in\mathcal{A}^{\lambda/\lambda'}_{n_1,\ldots,n_{k-1}}} F^{\lambda_k/\lambda_{k-1}} \cdot \ldots \cdot F^{\lambda_1/\lambda_0} \in [0; k\sqrt{n}_k].$$

Choose k much smaller than $\sqrt{n}_k = \sqrt{|\lambda|}$ and the sizes $n_1,\ldots,n_{k-1}$ to be "equally spaced" on $[n_0, n_k]$ (that is, let $n_i = n_0 + [\frac{i}{k}\cdot(n_k - n_0)]$).

It is natural to expect that for a generic skew YD of the form λ/λ', its level curves at these moments slice the (rotated $\pi/4$) diagram into long and thin slices. After rescaling they should be close to the corresponding graphs $y = g(t_i, x)$, where $t_i = \frac{n_i - n_0}{n_k - n_0} \approx \frac{i}{k}$. The (total) contribution of the paths that are "non-optimal" will be neglectable.

We get an approximation (up to $o(n)$) for $\log F^{\lambda/\lambda'}$ as

$$\sum_{i=1}^{k} \log F^{\bar\lambda_i/\bar\lambda_{i-1}},$$

where $(\bar\lambda_0, \bar\lambda_1, \ldots, \bar\lambda_k)$ is the index corresponding to the maximizing summand.

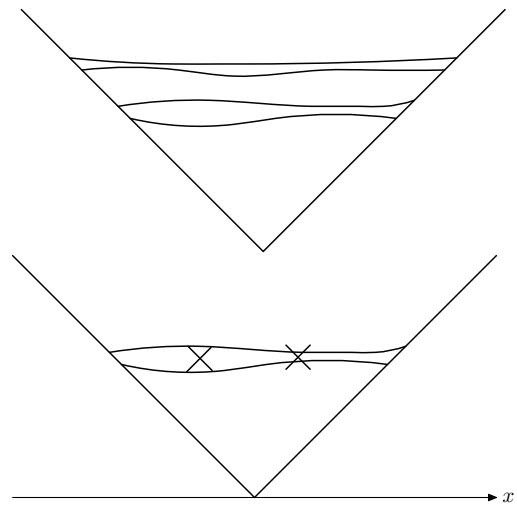

Figure 2.4: Left: "horizontal" cut, shapes λ_i at the corresponding intermediate moments t_i.
Right: "vertical" cut of a horizontal "slice" λ_i/λ_{i-1}.

The same applies to the setting of Conjecture 1.1.2: given a function g_0, we get an approximation for $\log F_{\varepsilon,g}^{\lambda_N/\lambda'_N}$ as

$$\sum_{i=1}^{k} \log F^{\bar{\lambda}_i/\bar{\lambda}_{i-1}},$$

where maximum is now taken over the set of λ_i with the additional assumption of the (rescaled) outer boundary of λ_i belonging to the ε-neighborhood of $g(t_i)$.

"Vertical" cut

Now, let us cut each "thin" diagram $\bar{\lambda}_i/\bar{\lambda}_{i-1} = D_i$ "vertically", choosing some points $p_{i,1}, \ldots, p_{i,m-1}$ inside D_i. Let $R^-_{i,j}$ be the set of cells of D_i to the lower left of $p_{i,j}$, $R^+_{i,j}$ to the upper right, and $D_{i,0}, \ldots, D_{i,m}$ the connected components of

$$D_i \setminus \bigcup_{j=1}^{m} (R^-_{i,j} \cup R^+_{i,j}) =: \tilde{D}_i.$$

One can also see $\tilde{D}_i$ as a skew YD:

$$\tilde{D}_i = \lambda_i^- / \lambda_{i-1}^+, \text{ where } \lambda_i^+ = \bar{\lambda}_i \cup \bigcup_j R_{i,j}^-, \quad \lambda_{i-1}^- = \bar{\lambda}_i \setminus \bigcup_j R_{i,j}^+.$$

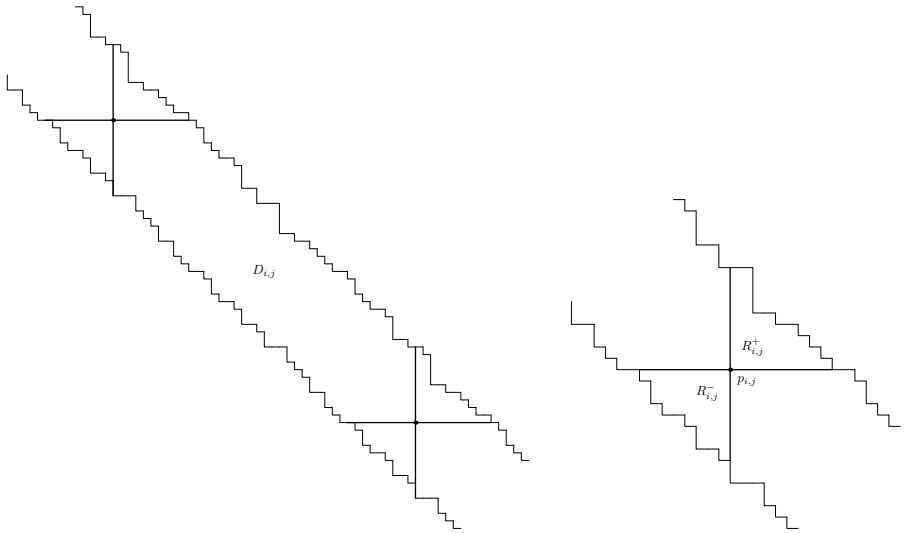

Figure 2.5: "Vertical" cut in French notation: the domains $D_{i,j}$ (left), points $p_{i,j}$ and removed corners $R_{i,j}^{\pm}$ (right).

Consider then the map from the set of skew YT of the form D_i to those of the form $\tilde{D}_i$: the cells are added in the same order with the parts $\bigcup_{j=1}^m (R_{i,j}^- \cup R_{i,j}^+)$ ignored. This map is surjective: any order for $\tilde{D}_i$ can be completed by first adding all the cells from all $R_{i,j}^-$, then $\tilde{D}_i$ itself, then all $R_{i,j}^+$. On the other hand, the maximum number of preimages does not exceed $n^{\sum_j |R_{i,j}^- \cup R_{i,j}^+|}$, as we are loosing $\sum_j |R_{i,j}^- \cup R_{i,j}^+|$ numbers that do not exceed $n = n_k - n_0$. Hence, one has

$$\log F^{D_i} - \log F^{\tilde{D}_i} \in [0, \sum_j |R_{i,j}^- \cup R_{i,j}^+| \cdot \log n],$$

and thus,

$$\sum_i \log F^{D_i} - \sum_i \log F^{\tilde{D}_i} \in [0, \log n \cdot \sum_i \sum_j |R_{i,j}^- \cup R_{i,j}^+|]. \tag{2.2}$$

For a large k sliced domains D_i can be expected to be of width $O(\sqrt{n}/k)$, and thus the cutting regions $R^{\pm}_{i,j}$ of area $O((\sqrt{n}/k)^2) = O(n/k^2)$. Taking m such regions per slice, we get a total effect of $O(\frac{n}{k^2} \cdot k \cdot m \cdot \log n)$ in the right side of (2.2), and after choosing $m = o(\frac{k}{\log n})$ this error does not exceed $o(n)$.

Note now that the orderings on different components $D_{i,j}$ of $\tilde{D}_i$ are completely independent. That is, let YT^D stay for the (skew) standard YT of the shape D. Consider the map

$$P_i : YT^{\tilde{D}_i} \to \prod_j YT^{D_{i,j}},$$

defined by restricting order of appearance of cells in $\tilde{D}_i$ on each subdiagram $D_{i,j}$. It is easy to see that this map is exactly R_i-to-one, where R_i is the multinomial coefficient

$$R_i = \binom{|\tilde{D}_i|}{|D_{i,1}|, \ldots, |D_{i,m}|} = \frac{|\tilde{D}_i|!}{|D_{i,1}|! \ldots |D_{i,m}|!}.$$

Hence,

$$\log F^{\tilde{D}_i} = \sum_j \log F^{D_{i,j}} + \log \frac{|\tilde{D}_i|!}{|D_{i,1}|! \ldots |D_{i,m}|!}.$$

Meanwhile, from Stirling's formula we have

$$\log \binom{|\tilde{D}_i|}{|D_{i,1}|, \ldots, |D_{i,m}|} = \sum_{j=1}^{m} |D_{i,j}| \cdot \left(-\log \frac{|D_{i,j}|}{|\tilde{D}_i|} \right) + o(|D_i|),$$

(as the sizes of $|D_{i,j}|$ tend to infinity at least as $\log n$); we thus get an approximation

$$\log F^{\lambda/\lambda'} = \sum_i \sum_j \left[\log F^{D_{i,j}} + |D_{i,j}| \cdot (-\log \frac{|D_{i,j}|}{|\tilde{D}_i|}) \right] + o(n). \tag{2.3}$$

Again, instead of all the paths we can consider only the paths that "resemble" a graph of a function g. For such a path $\bar{\lambda}_1, \ldots, \bar{\lambda}_{k-1}$, the skew YDs $D_{i,j}$ look like parallelograms of horizontal length $\sqrt{n} \cdot (x_{i,j} - x_{i,j-1})$ (where the vertical point $p_{i,j}$ has x-coordinate $x_{i,j}$) and of width $\sqrt{n} \cdot g'_t(t_i, x_{i,j})$ and with the slope $\tan \alpha = g'_x(t_i, x_{i,j})$.

Hence, to transform the formula (2.3) to the desired integral form, we have to estimate the logarithmic number $Z(\alpha, h, l) = \log F^{\Pi_{\alpha,h,l}}$ of skew YT in a parallelogram of length l, height h, where $1 \ll h \log h \ll l$, going under a slope $\tan \alpha$.

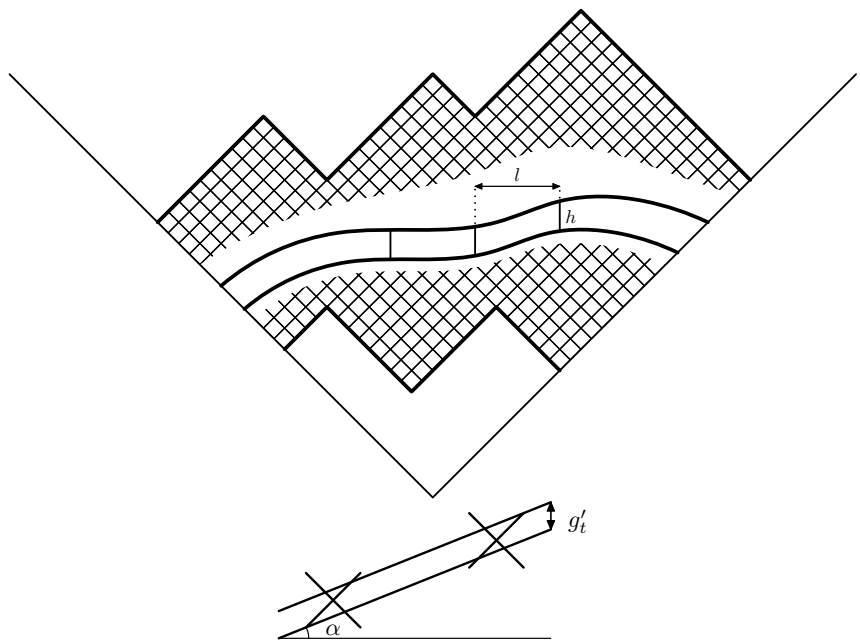

Figure 2.6: "Vertical" cuts

Parallelograms approximation

The same arguments as before imply the following two conclusions should for large $l \gg h \log h \gg 1$:

- $Z(\alpha, h_1 + h_2, l) \approx Z(\alpha, h_1, l) + Z(\alpha, h_2, l)$ — from adding an additional "intermediate moment", cutting the parallelogram "horizontally";
- $Z(\alpha, h, l_1 + l_2) \approx Z(\alpha, h, l_1) + Z(\alpha, h, l_2) + \log \binom{h(l_1+l_2)}{hl_1,\ hl_2}$ — from adding an additional midpoint, "vertically cutting in independent domains".

The latter approximation can be further rewritten as

$$Z(\alpha, h, l_1+l_2) \approx Z(\alpha, h, l_1)+Z(\alpha, h, l_2)+h(l_1+l_2)\log(l_1+l_2)-hl_1 \log l_1-hl_2 \log l_2.$$

Considering the difference $\tilde{Z}(\alpha, h, l) := Z(\alpha, h, l) - hl \log l$, we see that it is thus (approximately) additive in both h and l. Hence, it is natural to expect it to behave like

$$\tilde{Z}(\alpha, h, l) = A(\tan \alpha)hl + o(hl),$$

where $A(\tan\alpha)$ is a constant, depending only on the slope $\tan\alpha$. Thus, we get a prediction

$$Z(\alpha, h, l) = hl\log l + A(\tan\alpha)hl + o(hl). \tag{2.4}$$

As a concluding remark, note that due to the vertical symmetry (in the Russian notation) the function $A(\cdot)$ should be even.

Integral formula

Plugging (2.4) back to (2.3), we get an asymptotic expression for the number of g-shaped skew SYT:

$$\log F_{\varepsilon,g}^{\lambda/\lambda'} = \sum_{i,j} |D_{i,j}| \cdot \left[\log l_{i,j} + A(\tan\alpha_{i,j}) + \log\frac{|D_i|}{|D_{i,j}|}\right] + o(n), . \tag{2.5}$$

Here $o(n)$ is understood in the sense of a double limit as $\lim_{\varepsilon\to 0}\limsup_{n\to\infty}$, we denote by $l_{i,j}$ is the (horizontal) length of the "parallelogram" $D_{i,j}$ and by $\tan\alpha_{i,j} = g'_x(t_i, x_{i,j})$ its slope. The height $h_{i,j}$ of $D_{i,j}$ after rescaling by $\sqrt{n}$ can be approximated as

$$\frac{h_{i,j}}{\sqrt{n}} \approx g'_t(t_i, x_{i,j}) \cdot (t_i - t_{i-1});$$

as $t_i - t_{i-1} = \frac{n_i - n_{i-1}}{n}$, we get

$$h_{i,j} \approx g'_t(t_i, x_{i,j}) \cdot \frac{n_i - n_{i-1}}{\sqrt{n}}.$$

As $|D_{i,j}| \approx l_{i,j}h_{i,j}$, $|D_i| = n_i - n_{i-1}$, we can write the expression in the right hand side of (2.5) as

$$\begin{aligned}
&\log l_{i,j} + A(\alpha_{i,j}) + \log\frac{|D_i|}{|D_{i,j}|} \approx \\
&\approx \log l_{i,j} + \log(n_i - n_{i-1}) - \log\left(l_{i,j}\frac{n_i - n_{i-1}}{\sqrt{n}} g'_t(t_i, x_{i,j})\right) + A(g'_x(t_i, x_{i,j})) \approx \\
&\approx \frac{1}{2}\log n - \log g'_t(t_i, x_{i,j}) + A(g'_x(t_i, x_{i,j})).
\end{aligned} \tag{2.6}$$

Multiplying by $|D_{i,j}| \approx (t_i - t_{i-1})(x_{i,j} - x_{i,j-1}) \cdot g'_t(t_i, x_{i,j}) \cdot n$, and adding up, we finally get the desired

$$\log F_{\varepsilon,g}^{\lambda/\lambda'} = \sum_{i,j} |D_{i,j}| \cdot \left[\frac{1}{2}\log n - \log g'_t(t_i, x_{i,j}) + A(g'_x(t_i, x_{i,j}))\right] =$$
$$= \frac{1}{2} n \log n + n \left[\iint (-\log g'_t + A(g'_x)) \cdot g'_t \, dx \, dt + o(1)\right]. \quad (2.7)$$

This is exactly the statement of Conjecture 1.1.2. Taking the maximum over the possible shapes g of the skew SYT and referring to the variational principle then implies Conjecture 1.1.1. Indeed, if g_0 is the maximizing function for the functional $\mathcal{L}$ (it is easy to see that it is concave, so g_0 is unique), any other g will correspond to the exponentially smaller number of paths.

We conclude this paragraph by reminding that all the arguments therein are non-rigorous, serving as a good motivation for these conjectures, but not as a rigorous proof.

2.2.2 Differential equation

The discussion on the previous section implies that the number of g-shaped skew YT of area n should be asymptotically diven by the formula

$$\log F_{\varepsilon,g}^{\lambda/\lambda'} = \frac{1}{2} n \log n + n \cdot \mathcal{L}[g] + o(n),$$

where

$$\mathcal{L}[g] = \int_0^1 \int_{\mathbb{R}} (-g'_t \log g'_t + g'_t A(g'_x)) \, dx \, dt, \quad (2.8)$$

and the function $A(\cdot)$ is yet to be determined. Also, the limit shape of a skew YT of a given large form should be an extremal of this functional.

Remark 2.2.1. This is not an immediate conclusion, as we have used that the parameter t corresponds to the part of area filled, and hence the allowed functions g are only those satisfying $\forall t \in [0;1] : \int (g(t,x) - g(0,x)) \, dx = t$, or, equivalently, for sufficiently smooth functions,

$$\forall t \in [0;1] : \int g'_t(t,x), dx = 1. \quad (2.9)$$

Thus g is immediately an extremum of $\mathcal{L}$ only on the space of functions, given by (2.9). However, for any (increasing in t) function $g(t,x)$ we can consider its time reparametrization $\tau = \phi(t)$:

$$\phi(t) = \int \mathbb{R}(g(t,x) - g(0,x))\,dx,$$

and the corresponding function $\tilde{g}(\tau, x) = g(\phi^{-1}(t), x)$.

It is easy to see that the A-part of the functional $\mathcal{L}$, that is, $\iint A(g'_x)g'_t\,dx\,dt$ stays unchanged by such a reparametrization. Meanwhile,

$$\iint -\tilde{g}'_t \log \tilde{g}'_t\,dx\,dt = \iint -g'_t \log g'_t\,dx\,dt - \int \phi' \log \phi'\,dt,$$

and as $-\int \phi' \log \phi'\,dt \geq 0$, and strictly > 0 for all non-identity ϕ (as $\phi(0) = 0, \phi(1) = 1$ and Jensen inequality), the maximum of $\mathcal{L}$ is attained on a function g with uniform growth.

It turns out that these observations suffice to reconstruct $A(\cdot)$.

Namely, as we have mentioned in the introduction, a skew YT of a shape following from Vershik-Kerov-Logan-Shepp asymptotics is given by a family of its rescalings:

$$\Omega(t,x) = \sqrt{t} \cdot \Omega\left(\frac{x}{\sqrt{t}}\right). \tag{2.10}$$

This is an extremal of a functional $\mathcal{L}$, and thus it should satisfy the Euler-Lagrange equations:

$$\frac{\partial}{\partial t} L'_{g'_t}(g'_t, g'_x) + \frac{\partial}{\partial x} L'_{g'_x}(g'_t, g'_x) = 0, \tag{2.11}$$

where

$$L(p_t, p_x) = -p_t \log p_t + A(p_x) \cdot p_t. \tag{2.12}$$

As $\Omega(t,x)$ given by (2.10) is an explicit function, we can plug it in (2.11) and interpret it as a differential equation for unknown $A(\cdot)$.

Proposition 2.2.1. *Let $A : [-1,1] \to \mathbb{R}$ be an even function, C^2-smooth on $(-1,1)$. Then $\Omega(t,x)$ satisfies the Euler-Lagrange equation for the functional $\mathcal{L}[\cdot]$ if and only if*

$$A(p_x) = \log \cos \frac{\pi p_x}{2} + C,$$

where C is a constant.

Proof. Let us first rewrite the Euler-Lagrange equation (2.11) using the explicit form of the Lagrangian (2.12):

$$L'_{p_t} = -\log p_t - 1 + A(p_x),$$
$$L'_{p_x} = p_t \cdot A'(p_x),$$

and thus (2.11) becomes

$$\frac{\partial}{\partial t}(A(g'_x) - \log g'_t - 1) + \frac{\partial}{\partial x}(g'_t A'(g'_x)) = 0,$$

and hence

$$A''(g'_x)g''_{xx}(g'_t)^2 + 2A'(g'_x)g''_{xt}g'_t - g''_{tt} = 0. \tag{2.13}$$

Now, for $g(t,x) = \Omega(t,x)$ we have

$$\Omega'_x(t,x) = \frac{2}{\pi}\arcsin\frac{x}{\sqrt{t}}, \quad \Omega'_t(t,x) = \frac{\sqrt{t-x^2}}{\pi t}.$$

Thus $\frac{x}{\sqrt{t}} = \sin\frac{\pi\Omega_x}{2}$; substituting this into (2.13), we get

$$4A''(\Omega_x)(1-\sin^2\frac{\pi\Omega_x}{2}) - 4\pi A'(\Omega_x)\sin\frac{\pi\Omega_x}{2}\cos\frac{\pi\Omega_x}{2} - \pi^2(2\sin^2\frac{\pi\Omega_x}{2} - 1) = 0.$$

Finally, making a change of variable $\xi = \Omega_x$, we get a linear inhomogeneous differential equation

$$G'(\xi)\cdot 4\cos^2\frac{\pi\xi}{2} - 2\pi G\xi\cdot\sin(\pi\xi) + \pi^2\cos(\pi\xi) = 0,$$

for the derivative $G(\xi) = A'(\xi)$ (that should be odd as $A(\cdot)$ is even). A straightforward computation then shows that it admits a unique odd solution

$$G'(\xi) = -\frac{\pi}{2}\tan\frac{\pi\xi}{2},$$

and integrating it, we get the desired form for an even solution $A(\cdot)$:

$$A(\xi) = \log\cos\frac{\pi\xi}{2} + C.$$

We denote the "constant-free" part by $A_0(\xi) := \log\cos\frac{\pi\xi}{2}$.

□

2.2.3 Determining the constant

Note that replacing A_0 by $A_0 + C$ in (2.12) changes the total value of the functional $\mathcal{L}$ by

$$\int_0^1 \int_{\mathbb{R}} C \cdot g'_t \, dx \, dt = C \cdot \int_{\mathbb{R}} (g(1,x) - g(0,x)) \, dx = C,$$

as we choose the normalisation of g to give the figure of total area 1. This explains why the constant C is irrelevant to the problem of asymptotic shape: replacing $\mathcal{L}$ by $\mathcal{L} + C$ doesn't change its extremals. However, the value of C is important for the "total number of paths" asymptotics of Conjecture 1.1.1, and it can be found again with help of VKLS shape $\Omega(t,x)$.

Namely, one has $\sum_{\lambda \in \mathbb{Y}_n} \dim^2 \lambda = n!$. At the same time, the number of summands grows subexponentially, $|\mathbb{Y}_n| \le \exp(c \cdot \sqrt{n})$. Hence for most YD λ in the sense of the Plancherel measure, $\dim \lambda$ is close to $\sqrt{n!}$ on the logarithmic scale:

$$\forall r \quad \mu_n \left(\left\{ \lambda : \dim \lambda \le \sqrt{\frac{n!}{r|\mathbb{Y}_n|}} \right\} \right) \le \frac{1}{r},$$

hence for YDs with probability at least $1 - \frac{1}{r}$

$$\sqrt{n!} \ge F^{\lambda/\varnothing} = \dim \lambda \ge \frac{\sqrt{n!}}{\sqrt{n|\mathbb{Y}_n|}}.$$

The asymptotic shape of such diagrams is given by $\Omega(x)$, and of the corresponding YT by $\Omega(t,x)$. As

$$\log n! = \frac{1}{2} n \log n - \frac{1}{2} n + o(n)$$

and

$$\log F^{\lambda/\lambda'} = \frac{1}{2} n \log n + n \cdot \mathcal{L}[g] + o(n),$$

we have

$$\mathcal{L}[\Omega(t,x)] = -\frac{1}{2}.$$

Calculating the corresponding double integral explicitly (we omit the straightforward calculations here), one finally gets the value

$$C = -\log \frac{\pi}{\sqrt{2}}.$$

2.3 Modified TASEP and the discrete sine-process

In this section we introduce the "local" maya model, briefly described in §1.1.3, and use it to re-obtain the functional of Conjecture 1.1.1 from a different angle of approach.

2.3.1 Markov chain and the discrete sine-process

Namely, consider an analog of maya diagram on the circle instead of a real line, formed of some number L of holes. The rule "stone jumps to its right" is then rewritten as "stones jump in the positive direction"; see Fig. 2.7. As the total number of stones is preserved by a jump, this total number (that we denote N) is invariant under such a dynamics. Thus, for any L and N we get a topological Markov chain.

It is quite similar to the TASEP (**t**otally **a**symmetric **p**rocess), however, for the classical TASEP model all the stones that can jump do so equiprobably. We are concerned with the *topological* entropy of this chain (as we are interested in counting all the possible trajectories for the YTs). Thus, we are interested in the *measure of maximal entropy* for this chain (and the corresponding Markov shift as a dynamical system), thus modifying the jumping probabilities accordingly. An immediate observation is that the stones are more likely to jump if this jump does not reduce the number of degrees of freedom, creating a tightly packed group of stones, as this is likely to reduce the number of options on the next steps. In particular, the probabilities of such "crumpled" states will be reduced (contrary to the classical TASEP, where all the possible states are equiprobable).

Our main (formal) result, Theorem 1.1.2, describes the topological entropy and the maximal entropy measure for this topological Markov chain:

Theorem. *For any L, N, the entropy of the topological Markov chain defined above is equal to*

$$h = \log \frac{\sin \frac{\pi N}{L}}{\sin \frac{\pi}{L}}.$$

The corresponding measure of maximal entropy is a determinantal one; the correlation kernel, giving the distribution of possible states, is given by the projection on (any) N consecutive Fourier harmonics on the length L discrete circle.

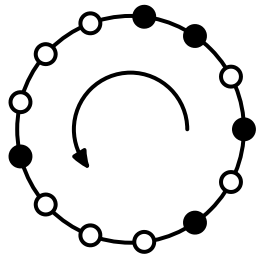

Figure 2.7: TASEP: black stones are allowed to move only in the positive direction.

Postponing its proof till §2.3.2, let us discuss the relation of this process to our main theme. Namely, we use it to describe a possible local evolution over a (large) part of it, that we consider to be winded to the circle, in the same way as parts of (hexagonal or square) lattices are winded to a torus (see, e.g. [41]). Thus, for a large YD and the corresponding maya diagram evolution, a local part of it can be modelled by taking a large circle and filling it with the same proportion of stones that are observed at this point of space and time.

Now, the corresponding height function increases by 1 at the stone and decreases by 1 at each empty hole. Hence, while going around the circle it increases by $N-(L-N)=2N-L$ (so, formally speaking, this is a multi-valued function with a logarithmic monodromy). This corresponds to the slope of $\frac{2N-L}{L}$, that has a meaning of g'_x (if this circle is but a small part of a large YT). Denoting $p := \frac{N}{L}$ the density of the stones, we see that $p = \frac{g'_x+1}{2}$, thus $\frac{\pi N}{L} = \pi p = \frac{\pi}{2}(1+g'_x)$ and hence that this ("local") entropy can be rewritten as

$$\log \frac{\sin \frac{\pi N}{L}}{\sin \frac{\pi}{L}} = \log \cos \frac{\pi g'_x}{2} - \log \sin \frac{\pi}{L}.$$

On the other hand, for large L we have $\sin \frac{\pi}{L} \approx \frac{\pi}{L}$, while $\frac{2}{L}$ is a speed at which the height function increases in average per one iteration of the process (a jump increases it in two cites, see Figure 2.1). Hence $\sin \frac{\pi}{L} \approx \frac{\pi g'_t}{2}$. Gluing independent local "circled" pieces together (in the same way as we did it in Section 2.2.1), we see that the global number of [g-shaped] paths will be given by an integral of

$$\log \cos \frac{\pi g'_x}{2} - \log \frac{\pi g'_t}{2}.$$

That is exactly what is suggested by Conjecture 1.1.2 in the form of (1.5) in Remark 1.1.3; the coefficient $\frac{1}{2}$ comes from the fact that cells are of area 2, see Remark 2.1.1).

A concluding — and still informal — remark in this paragraph is that the consideration of this process leads to a handwaving explanation of the sine process appearing as the local shape of a (Plancherel)-random Young diagram (see [6, Theorem 3]). Indeed, it is quite natural to expect that the local behaviour can be approximated by the corresponding maximal entropy measure. And there is the following

Remark 2.3.1. As we consider longer and longer circles, filled with a given limit density of stones $\frac{N_j}{L_j} \to a \in (0,1)$, the corresponding maximal entropy measures converge to the sine process. Indeed, their correlation kernels are projections on consecutive N_j harmonics out of L_j, and this kernel converges to the kernel of projection of the Fourier transform to the arc that takes a-th part of the circle (Fourier-dual to $\mathbb{Z}$). That kernel is exactly the one of the sine process,

$$K(k,l;a) = K(k-l,a) = \begin{cases} \frac{\sin \pi a(k-l)}{\pi(k-l)}, & k \neq l \\ a, & k = l. \end{cases}$$

2.3.2 Proof of Theorem 1.1.2

Let L, N be fixed, and consider the set of states of the topological Markov chain. Recall that the topological entropy is the logarithm of the spectral radius of the transition matrix T, and the corresponding eigenvalue is real and positive. Moreover, if v and u are the corresponding non-negative left and right eigenvectors, the probabilities of states for a maximal entropy measure ("Parry measure", see [40, 38]) are given by the normalization of the vector with the coordinates $u_s v_s$.

Consider first the case of N odd (this case is slightly simpler). The states of the Markov chain are enumerated by $\binom{L}{N}$ possible arrangements of the stones. Take a space $V = \mathbb{R}^L$; for any state of the chain, let $k_1 < \cdots < k_N$ be the numbers of stone-filled holes on the circle, and put in correspondence to it the element $v_{k_1,\ldots,k_N} := e_{k_1} \wedge \cdots \wedge e_{k_N} \in \Lambda^N V$.

The transition matrix T then acts on $\Lambda^N V$ in the following way. Let C be operator that cyclically permutes the base of V, that is, $C(e_k) := e_{k+1 \bmod L}$.

Then

$$T(e_{i_1}\wedge\cdots\wedge e_{i_N}) = C(e_{i_1})\wedge e_{i_2}\wedge\cdots\wedge e_{i_N}+e_{i_1}\wedge C(e_{i_2})\wedge\cdots\wedge e_{i_N}+\cdots+e_{i_1}\wedge\cdots\wedge e_{i_{N-1}}\wedge C(e_{i_N}). \tag{2.14}$$

Indeed, application of C to e_{i_k} corresponds to a possible jump of this stone; if the next hole, i_k+1-th, is filled, the jump is forbidden, that corresponds to the vanishing of the corresponding wedge product in the right hand side. Finally, as N is odd, even if $i_N = L$ and thus the jump of this stone to the position 1 leads to the cyclic re-enumeration, this doesn't affect the final result, as

$$e_{i_1}\wedge e_{i_2}\wedge\cdots\wedge e_{i_N} = e_{i_2}\wedge\cdots\wedge e_{i_N}\wedge e_{i_1}.$$

The right hand side of (2.14) is simply the operator $C\wedge E\wedge\cdots\wedge E$, where E is the identity operator on V. Hence, its eigenvalues are sums of any N different eigenvalues of C, and the eigenvectors are the wedge products of the corresponding eigenvectors of C. The eigenvalues of C are L-th power roots of unity $\lambda_k = \exp(2\pi ik/L)$, and the corresponding eigenvectors are discrete Fourier harmonics $v_k = \sum_j \exp(-2\pi ikj/L)e_j$.

Among the sums of $N = 2m+1$ different λ_k's, the maximal in absolute value are the ones corresponding to the consecutive (on the circle $\mod L$) eigenvalues; in particular, the positive and maximal one is

$$r = \lambda_{-m}+\cdots+\lambda_m = \frac{e^{2\pi i\cdot(m+\frac{1}{2})/L} - e^{-2\pi i\cdot(m+\frac{1}{2})/L}}{e^{\pi i/L} - e^{-\pi i/L}} = \frac{\sin\frac{\pi N}{L}}{\sin\frac{\pi}{L}}.$$

The topological entropy h is equal to its logarithm, thus proving the entropy part of the theorem.

Now, consider the corresponding eigenvector. It is given by the product $v_{-m}\wedge\cdots\wedge v_m \in \Lambda^N V$. Moreover, the right eigenvector u has the same coordinates (replacing of C by $C^* = C^{-1}$ leads to the same answer), though we prefer to conjugate its elements:

$$u = \overline{v_{-m}}\wedge\ldots\overline{v_m}.$$

Then, the probabilities of every state $k_1<\cdots<k_N$ are proportional to

$$\det((v_i)_{k_j})_{\substack{i=-m,\ldots,m\\ j=1,\ldots,N}}\cdot\det((\overline{v_{i'}})_{k_j})_{\substack{i'=-m,\ldots,m\\ j=1,\ldots,N}} = \det((K)_{k_j,k_{j'}})_{j,j'=1,\ldots,N}, \tag{2.15}$$

where $K = \sum_{i=-m}^{m} v_i\cdot(v_i)^*$ is the projection operator on the subspace $\langle v_{-m},\ldots,v_m\rangle\subset V$. As K is the rank N orthogonal projector, (2.15) implies

the desired description for the distribution of probabilities for the stationary measure. (In particular, (2.15) already describes a probability measure, with no need of normalization.)

Now, for the case of an even N, the only part that changes is that the length N cycle is now odd. To handle it, we take an L-th power root of minus unity, $\omega = \exp(\pi i/L)$, and instead of C consider the operator ωC, and instead of the base e_k of V we consider $\omega^k e_k$ and hence the base

$$\tilde{v}_{k_1,\dots,k_N} := \omega^{k_1+\dots+k_N} e_{k_1} \wedge \dots \wedge e_{k_N}.$$

Then again, the action of $\omega C \wedge E \wedge \dots \wedge E$ in this base becomes the action of the transition matrix T; note that now for the jump from $k_N = L$ to 1 one gets two changes of sign, one from the length N cycle, and another from $w^L = -1$:

$$\omega^{k_1+\dots+k_{N-1}+L} e_{k_1} \wedge \dots \wedge (\omega C \cdot e_L) = \omega^{1+k_1+\dots+k_{N-1}} e_1 \wedge e_{k_1} \wedge \dots \wedge e_{k_{N-1}}.$$

Now, the eigenvalues of ωC are $\omega\lambda_j$, thus the spectral radius (and the maximal real positive eigenvalue) of T is equal to

$$r = \omega\lambda_{-m} + \dots + \omega\lambda_{m-1},$$

where $N = 2m$. Rewriting it as a sum of a geometric series with the denominator $e^{2\pi i/L} = \omega^2$, one gets the desired expression for the entropy

$$e^h = r = \omega \frac{e^{2\pi i \cdot m/L} - e^{-2\pi i \cdot m/L}}{\omega^2 - 1} = \frac{\sin \frac{\pi N}{L}}{\sin \frac{\pi}{L}}.$$

The same application of the formula for the Parry measure concludes the proof.

2.3.3 The relation to the dimer and beads models

Let us now approach the same question from a different angle, obtaining the relation to the dimer and beads models.

Freezing the jumps and the beads process

Again, let L, N be fixed. The correspondence that was described in Section 2.1 (see Figure 2.1) allows to transform evolution of maya diagrams to

the dimer covers of the corresponding hexagonal graph. This also applies to maya evolution on the circle, that is transformed to the dimer covers on the graph on the cylinder. However, this map is non-surjective: it becomes bijective if for the maya evolution we authorize (initially forbidden) absence of jumps and simultaneous jumps.

The vertical extension method that we have used in the end of Section 2.1 to handle the simultaneous jumps would not work anymore in the circle case, as the total number of jumps in not anymore fixed. So instead we will use "freezing" techniques, imposing a "tax" on jumping. That is, we again consider a dimer configuration with a high number of levels (of some height M), but this time, associate a (small) weight ε to the "jump" edges, leaving all the others with the weight 1. Then, we take the weight of a dimer configuration to be the product of weights of dimers used, and choose a dimer cover with the probability proportional to its weight.

Consider first the limit where M is chosen to grow as $M \sim \frac{\tau}{\varepsilon}$, where τ is a constant. In this limit, we have the following

Lemma 2.3.1. *Whichever are the boundary (initial and final) conditions, the probability (that is, the proportion of total weight of configurations) of two jumps on the same level converges to zero as $\varepsilon \to 0$.*

Before proving it formally, note that for any n all the configurations with n jumps, all at different levels, have the same probability (as they have the same weight ε^n). In particular, conditioning to a given n gives the choice of moments of jumps that are uniformly chosen among $\binom{M}{n}$. In particular, rescaling the time ε times by denoting $t := \varepsilon k \in [0, \varepsilon M]$ (where k is the vertical coordinate), we see that this conditioning leads in the limit $\varepsilon \to 0$ to the uniform choice of n points on $[0, \tau]$.

We can then consider the bulk limit: make τ go to infinity and shift the origin to $\frac{\tau}{2}$ in the rescaled coordinates. The jump places and (renormalized) moments then provide a cylinder analogue of the bead process, a random subset of $\mathbb{Z}_L \times \mathbb{R}$.

Theorem 2.3.1. *This limit process is given by coupling a maximal entropy measure for the two-sided topological Markov chain and of a Poisson process on $\mathbb{R}$ of constant intensity, providing the jump moments. The intensity of the Poisson process is equal to e^h, where h is the entropy of the Markov chain (given by Theorem 1.1.2).*

Proof of Lemma 2.3.1. Consider the corresponding partition function Z, that is the sum of weights of all the configurations, and its part Z_0 that is given by the sum of weights of configurations with no simultaneous jumps. Let W_n be the number of paths from the initial to the final configuration, consisting of n jumps. It suffices to show that as $\varepsilon \to 0$, both Z and Z_0 converge to the same (positive and finite) limit.

On one hand, we have

$$Z_0 = \sum_n W_n \varepsilon^n \binom{M}{n}. \tag{2.16}$$

On the other hand, when we authorize configurations with simultaneous jumps, we can still enumerate them by a non-decreasing sequence of moments $1 \le k_1 \le \cdots \le k_n \le M$, and the number of such sequences equals $\binom{M+n-1}{n}$. Thus

$$Z \le \sum_n W_n \varepsilon^n \binom{M+n}{n}. \tag{2.17}$$

Note that for any fixed n

$$W_n \varepsilon^n \binom{M}{n} \sim W_n \varepsilon^n \frac{M^n}{n!} = W_n \frac{(\varepsilon M)^n}{n!} \xrightarrow[\varepsilon \to 0]{} W_n \frac{\tau^n}{n!},$$

and the same applies for the terms of the second series. Hence, both series coverge termwise as $\varepsilon \to 0$ to the series

$$\sum_n W_n \frac{\tau^n}{n!},$$

that is convergent (and whose sum is strictly positive). To conclude the proof, it suffices thus to check that their convergence is uniform in ε in some neighbourhood of zero, $(0, \varepsilon_0)$. To do so, we will provide an upper estimate for the terms of these series by a convergent series that does not depend on ε.

Indeed, fix R that is larger than the norm of the transition matrix of our Markov chain, then $W_n < R^n$ for all n. Now, for any $\varepsilon > 0$ if $n \le M$, we have

$$\binom{M+n}{n} \le \binom{2M}{n} < \frac{(2M)^n}{n!},$$

and the corresponding term does not exceed (once $M < \frac{2\tau}{\varepsilon}$)

$$W_n \varepsilon^n \binom{M+n}{n} \le R^n \varepsilon^n \frac{(2M)^n}{n!} < \frac{(4\tau R)^n}{n!};$$

the term in the right hand side provides a convergent series that does not depend on ε. On the other hand, if $M < n$, we have $\binom{M+n}{n} < \binom{2n}{n} < 2^{2n}$, and thus

$$W_n \varepsilon^n \binom{M+n}{n} \leq R^n \varepsilon^n 2^{2n} = (4R\varepsilon)^n < \frac{1}{2^n}$$

once $\varepsilon < \frac{1}{8R}$. Hence, both series Z and Z_0 for all sufficiently small $\varepsilon > 0$ are bounded termwise by the series

$$\sum_n \max(\frac{(4\tau R)^n}{n!}, \frac{1}{2^n}),$$

that is convergent and does not depend on ε. Hence, their convergence is uniform as $\varepsilon \to 0$, and this concludes the proof of the lemma. □

Proof of Theorem 2.3.1. Note first that due to Lemma 2.3.1 the process that we obtain on $[-\frac{\tau}{2}, \frac{\tau}{2}] \times \mathbb{Z}_L$ can be equivalently obtained by passing to the limit only from the configurations with no simultaneous jumps.

Also from Lemma 2.3.1 and from its proof, for any given $\tau > 0$ this limiting process can be described in the following way. First, one randomly chooses a number ξ of jumps, in such a way that the probability of $\xi = n$ is proportional to $W_n \frac{\tau^n}{n!}$. Then, one of W_ξ length ξ paths satisfying the boundary conditions is chosen equiprobably, as well as a set of ξ independently chosen points on $[-\frac{\tau}{2}, \frac{\tau}{2}]$, giving the moments, at which (after putting them in the increasing order) the jumps following the chosen path will occur.

Next, let us describe the "average density" of the jumps: we have the following lemma.

Lemma 2.3.2. *As $\tau \to \infty$, the fraction $\frac{\xi}{\tau}$ between the (random) number of jumps ξ and the total time τ converges in probability to the constant value e^h.*

Proof. Let ρ stay for the spectral radius of the transition matrix of our topological Markov chain; then, $\rho = e^h$. If we had $W_n = \rho^n$, then the distribution of ξ would follow exactly the Poisson law with the parameter $\rho\tau$, and the statement of the lemma would be a mere Law of Large Numbers.

Now, our Markov chain is transitive. If it was also aperiodic, we would have $W_n \sim c\rho^n$ for some constant c. However, it is not; it is easy to check that its minimal period is equal to L, the length of the circle. Thus, for any chosen boundary conditions there exists a residue n_0 such that the number W_n of Markov chain paths of length n behaves as

$$W_n \sim c\rho^n \quad \text{if } n \equiv n_0 \mod L,$$

where c is a constant (depending on the particular choice of the boundary conditions) and $W_n = 0$ otherwise. The conclusion of the lemma then can be deduced from the "pure exponent" case. Indeed, the distribution of ξ for a given τ can be obtained by a series of two operations. First, a Poisson random variable $\pi(\rho\tau)$ is conditioned to be congruent to $n_0 \mod L$. Then, for the obtained probability distribution the probability of each n is multiplied by a bounded factor (corresponding to passing from ρ^n to W_n).

And both these operations do not affect the Law of Large Numbers conclusion. Indeed, the first one selects a part of lower-bounded probability (asymptotically $1/L$-th one, as $\tau \to \infty$), while the second one can change the quotient of probabilities of the events only by a bounded factor (and hence also cannot break the "with probability convergent to 1" statement). Thus, we have the desired Law of Large Numbers: the quotient $\frac{\xi}{\tau}$ converges to ρ in probability as $\tau \to \infty$. □

Now, selecting $n \sim \rho\tau$ uniformly distributed independent points on the interval $[-\frac{\tau}{2}, \frac{\tau}{2}]$ converges as $\tau \to \infty$ to the Poisson process on the real line with the intensity ρ. Thus the same holds if we average on a set of values of n that ξ takes with the probability convergent to 1, on which $\frac{\xi}{\tau} \to \rho$.

Now, for any fixed interval $[a, b]$ on the real line consider the number ξ_1 of the jumps on $[-\frac{\tau}{2}, a]$. Note that in probability ξ_1 tends to infinity, while its residue modulo L is asymptotically uniformly distributed.

For an aperiodic transitive topological Markov chain, the uniform distribution on paths with given boundary conditions in the bulk converges to the maximal entropy measure. Meanwhile, for a period L transitive Markov chain the accumulation points of such uniform distributions are the L components of the maximal entropy measure that are permuted by the dynamics. However, as we take here the "observation window" $[a, b]$ that is separated from the fixed boundary $-\frac{\tau}{2}$ by the random number of steps ξ_1 that has all the residues $\mod L$ asymptotically equiprobable as $\tau \to \infty$, these permuted components are being averaged and one gets exactly the maximal entropy measure. □

Bead process' kernel

We would not go into this alternate approach if it wouldn't lead to some interesting connections. Namely, let us study the random dimer covers that have already appeared in Sec. 2.3.3 via the standard methods, that is, via

the Kasteleyn theorem.

Again, let ε, M be fixed, and we consider a chosen dimer partition of the corresponding graph of height M with the weights ε on the "jump" edges that is chosen randomly in such a way that its probability is proportional to the weight of the configuration (in other words, with respect to the corresponding Gibbs measure).

Let us recall the statement of the Kasteleyn Theorem [28, 29]. Let a planar bipartite graph with a weighted adjacency matrix $W_0 = (\mathbf{w}_{bw})$ be given. Fix additional factors (α_{bw}), such that for any face of the graph, formed by vertices $b_1, w_1, \dots, b_k, w_k$, one has

$$\frac{\alpha_{b_1 w_1}\alpha_{b_2 w_2}\dots\alpha_{b_k w_k}}{\alpha_{b_1 w_2}\alpha_{b_2 w_3}\dots\alpha_{b_k w_1}} = (-1)^{k-1}; \tag{2.18}$$

at least one such choice always exists (it follows from the planarity of the graph). Then for all possible dimer covers $(j, \sigma(j))$ of the graph the products

$$\operatorname{sign}(\sigma)\cdot\prod_j \alpha_{j\sigma(j)}$$

take the same value $\mathbf{a}$. This implies that the determinant of the matrix $W = (w_{bw}\alpha_{bw})$ equals to the product $\mathbf{a}\cdot Z$, where Z is the corresponding statistical sum, as all the dimer covers contribute to the determinant with their weights times $\mathbf{a}$ (and the signs cancel out). Hence the probability of dimers $(b_1, w_1), \dots, (b_k, w_k)$ being chosen for a Gibbs-random configuration is equal to

$$P((b_i, w_i)_{i=1,\dots,k} \text{ chosen}) = \prod_{i=1}^{k}(\alpha_{b_i w_i}\mathbf{w}_{b_i w_i})\cdot\det(K_{w_j b_i})_{i,j=1,\dots,k}, \tag{2.19}$$

where $K = W^{-1}$ is the inverse matrix.

We are going to apply this theorem to our graph, that is bipartite and planar. Indeed, it naturally embeds into a cylinder, which can be sent to the plane using the polar coordinates. Under this embedding, *almost* all the faces of the graph become hexagons. However, there are two exceptions: the inner and the outer faces, that have $2L + 2(L - N) = 4L - 2N$ sides each. The choice of the factors α_{bw} will thus depend on the parity of N.

Namely, for odd N we can take all the α's to be equal to 1: all the faces have number of faces of the form $2(2k + 1)$. However, it turns out that the

following choice will simplify the later computations: we take

$$\alpha_{bw} = \begin{cases} 1, & \text{if } bw \text{ is a jump edge} \\ 1, & \text{if it is a “stone stays” edge} \\ -1, & \text{if it is a “no stone” edge.} \end{cases} \tag{2.20}$$

It is easy to check that this choice satisfies the condition (2.18): the fractions in its left hand side have the same number of (-1)'s in the numerator and denominator. In the same way, for even N we handle the inner and outer faces in the most “rotationally symmetric” way, taking

$$\alpha_{bw} = \begin{cases} \omega = \exp(\pi i/L), & \text{if } bw \text{ is a jump edge} \\ 1, & \text{if it is a “stone stays” edge} \\ -1, & \text{if it is a “no stone” edge.} \end{cases} \tag{2.21}$$

Indeed, for such a choice one gets in the right hand side of (2.18) the fraction $\frac{-\omega}{-\omega} = 1$ for any hexagonal face, and $\omega^L = -1$ for the inner and outer ones, thus satisfying the assumptions of the Kasteleyn theorem.

Now, in our weighted adjacency matrix W_0 there are edges of two different weights: 1 and ε. This (after the application of the Kasteleyn theorem) leads us to the consideration of two *different* possible determinantal-type processes. Namely, we can consider:

- **The presence of stones at given times and positions**; in the limit $\varepsilon \to 0$, their presence is given by the corresponding “stone stays in the place” edges (the probability of a jump at any particular time tends to zero). The product of weights of these edges is equal to 1, and so the corresponding probability tends to the corresponding minor of the limit of the matrix $K = W^{-1}$.

- **The positions and times of the jumps**, in other words, the corresponding bead process. As the jump edges have weight ε, for a k-edges configuration its probability is given by a product

  $$\varepsilon^k \cdot \det(K_{w_j b_i})_{i,j=1,\dots,k}$$

  for odd N (and with an additional ω^k in front for an even N).The factor ε^k corresponds to the density interpretation (we rescale the time by ε), and in the limit $\varepsilon \to 0$ we get a continuous-time determinantal process: the *densities* are determinants of the corresponding minors of the matrix K.

Considering the limit in the second sense, we will see that this jump edges process converges to a circle-based analogue of the beads process studied in [43, 7]. Passing then to the limit $L \to \infty$ allows to recover exactly their beads' process, providing an alternate viewpoint on its correlation kernel (see [7, Eq. (9)]).

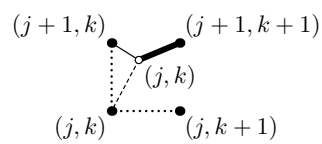

Figure 2.8: "No-stone" edge (dashed line), "stone staying" edge (simple line) and "jumping" edge (bold line), as well as the indices of the corresponding black and white vertices.

To do all of this rigorously, let us first consider the behaviour of such a configuration for a fixed ε. Let M_-, M_+ be given, and $M_- < j \leq M_+$ and $1 \leq k \leq L$ be the time- and circle-wise coordinates respectively. We will use the conventions from Section 2.1: a white vertex with the coordinates (k, j) is joined with the black vertices with the coordinates (k, j), $(k, j+1)$ and $(k+1, j+1)$ (see Fig. 2.8). Let us group the vertices into the (size L) blocks with the same j (time) coordinate. The matrix W then takes the form

$$W(\varepsilon, M_-, M_+) = \begin{pmatrix} -U_1 & B & 0 & \dots & 0 & 0 \\ 0 & -E & B & \dots & 0 & 0 \\ 0 & 0 & -E & \dots & 0 & 0 \\ \dots & \dots & \dots & \dots & \dots & \dots \\ 0 & 0 & 0 & \dots & -E & B \\ 0 & 0 & 0 & \dots & 0 & -U_2^T, \end{pmatrix} \tag{2.22}$$

where $B = E + \varepsilon C$ if N is odd, and $B = E + \omega\varepsilon C$ if N is even, and the matrices U_1 and U_2 of size $L \times (L - N)$ correspond to the initial and final boundary conditions (consisting of ones and zeros only).

Now, let us calculate the inverse matrix $W(\varepsilon, M_-, M_+)^{-1}$: fix some (k, j) and consider the vector $u = u^{(j,k)}$ that is send by $W(\varepsilon, M_-, M_+)$ to the base vector with the only 1 at the moment j of time at the place k. The above

block decomposition allows then to write this equation as

$$\begin{pmatrix} -U_1 & B & 0 & \dots & 0 & 0 \\ 0 & -E & B & \dots & 0 & 0 \\ 0 & 0 & -E & \dots & 0 & 0 \\ \dots & \dots & \dots & \dots & \dots & \dots \\ 0 & 0 & 0 & \dots & -E & B \\ 0 & 0 & 0 & \dots & 0 & -U_2^T \end{pmatrix} \begin{pmatrix} [u_{M_-}] \\ u_{M_-+1} \\ u_{M_-+2} \\ \vdots \\ u_{M_+-1} \\ u_{M_+} \end{pmatrix} = \begin{pmatrix} 0 \\ \dots \\ 0 \\ e_k \\ 0 \\ \dots \\ 0 \end{pmatrix}; \tag{2.23}$$

here $[u_{M_-}], u_{M_-+1}, \dots, u_{M_+}$ are the blocks of u, and in the right hand side the base vector e_k is placed at j-th size L block. We denote the first component $[u_{M_-}]$ (and not by u_{M_-}), because it is of size $L-N$ instead of L, and define $u_{M_-} := U_1([u_{M_-}]) \in \mathbb{R}^L$.

The block lines other than the the last one of the system (2.23) become a recurrent relation

$$\begin{cases} -u_i + Bu_{i+1} = 0, & i \neq j, \quad M_- < i < M_+. \\ -u_j + Bu_{j+1} = e_k. \end{cases} \tag{2.24}$$

The first and the last lines become the "boundary conditions" $u_{M_-} \in V_-$, $u_{M_+} \in V_+$, where $V_- := U_1(\mathbb{R}^{L-N})$ and $V_+ := \ker U_2^T$ are $L-N$ and N-dimensional subspaces respectively. The relation (2.24) implies that

$$u_j = B^{-(j-M_-)} u_{M_-}, \quad Bu_{j+1} = B^{M_+-j} u_{M_+}.$$

Hence we are decomposing the vector e_k as a sum $e_k = -u_- + u_+$, where

$$u_- := u_j \in V_{-,j} := B^{-(j-M_-)} V_-, \quad u_+ := Bu_{j+1} \in V_{+,j} := B^{M_+-j} V_+. \tag{2.25}$$

Now, (i,k')-th element of W^{-1} is the k'-th coordinate of the vector u_i, that is equal to

$$u_i = \begin{cases} B^{j-i} u_-, & i \leq j \\ B^{-(i-j)} u_+, & i > j. \end{cases} \tag{2.26}$$

Note that the matrix $W(\varepsilon, M_-, M_+)$ might be degenerate for small $M := M_+ - M_-$, when there are no possible length M paths joining the given initial and boundary conditions. Actually, the above arguments show that matrix W is invertible if and only if the subspaces $B^M V_-$ and V_+ are transversal (and the corresponding $L \times L$ determinant is easily seen to be equal to $\det W$).

Proposition 2.3.1. *For any ε sufficiently small, as $M_- \to -\infty$, $M_+ \to +\infty$, the elements of the matrix $W(\varepsilon, M_-, M_+)^{-1}$ pointwise converge to those given by $K(j,k;j',k') = K(j'-j,k,k')$, where, considering $K(i,\cdot,\cdot)$ as a $L\times L$ matrix, one has*

$$K(j,\cdot,\cdot) = \begin{cases} -B^{-j}P_-, & j \le 0, \\ B^{-j}P_+, & j > 0. \end{cases}$$

Here P_+ is the projector on the space $\widetilde{V}_+$ spanned by N consecutive Fourier harmonics, from $-m$-th to m-th for odd $N = 2m+1$ and from $-m$-th to $m-1$-th for even $N = 2m$, and $P_- = E - P_+$ is the projector on its orthogonal complement $\widetilde{V}_-$, spanned by the $L-N$ complementary ones.

Proof. Due to the relations (2.25) and (2.26) it suffices to show that the spaces $V_{-,j}$ and $V_{+,j}$ converge in the setting of the proposition respectively to $\widetilde{V}_-$ and $\widetilde{V}_+$. Such a convergence is quite natural to expect, as $\widetilde{V}_+$ is the span of N eigenvectors of B with the largest in absolute value eigenvalues, while $\widetilde{V}_-$ is the span of $L-N$ smallest ones.

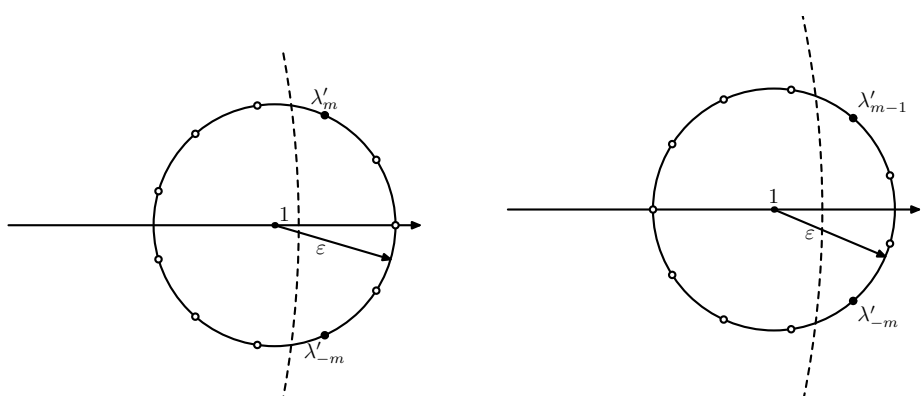

Figure 2.9: Eigenvalues λ'_k, separated into groups of N and $L-N$ by their absolute value for the cases of odd (left) and even (right) N

To show such a convergence formally, we start with the study of $V_{j,+}$, and consider first the case of N odd, $N = 2m+1$. For the action of $B = E+\varepsilon C$ on N-dimensional subspaces of $V = \mathbb{R}^L$, let us pass to the Plucker coordinates, considering the action of $\wedge^N B$ on the space $\wedge^N V$. Take the base of $\wedge^N V$ formed by

$$v_{k_1,\dots,k_N} = e_{k_1} \wedge \cdots \wedge e_{k_N}, \quad k_1 < \cdots < k_N.$$

Then, in the same way as in Section 2.3.2, the action of $\wedge^N B$ in this base is given by a matrix with *non-negative* elements, and there exists a sufficiently large power of $\wedge^N B$ that has all its elements strictly positive. This implies that on the projective space, the $\wedge^N B$-iterations of all the base vectors $v_{k_1,\dots,k_N}$ converge to the direction of the highest absolute value eigenvector of this operator.

At the same time, as B commutes with the rotation C, its eigenvectors (in $\mathbb{C}^L$) are the Fourier harmonics $\sum_k \exp(2\pi ikr/L)e_k, \quad r \in \mathbb{Z}_L$, with the corresponding eigenvalues

$$\lambda'_r = 1 + \varepsilon\zeta_r,$$

where for odd N we denote $\zeta_r := \exp(2\pi ir/L)$ the eigenvalues of the rotation C. The N largest in absolute values are the ones corresponding to $r = -m, \dots, m$, that are the base of $\widetilde{V}_+$, and we have thus obtained the desired convergence of $V_{+,j}$ to $\widetilde{V}_+$.

Now, if N is even, $N = 2m$, again as in Section 2.3.2 we consider the base

$$e'_1 = e_1, \quad e'_2 = \omega e_2, \quad e'_3 = \omega^2 e_3, \quad \dots, \quad e'_L = \omega^{L-1} e_L.$$

Then one has

$$\omega C e'_i = \begin{cases} e'_{i+1}, & i < L \\ -e'_1, & i = L \end{cases}$$

Hence, for $B = E + \varepsilon\omega C$ the operator $\wedge^N B$ again acts on the corresponding base

$$v'_{k_1,\dots,k_N} = e'_{k_1} \wedge \dots \wedge e'_{k_N}, \quad k_1 < \dots < k_N$$

as a matrix with non-negative elements (the signs cancel out if e'_1 occurs out of e'_L), and has a power whose elements are strictly positive.

We thus again get the convergence of directions of $\wedge^N B$-iterations of any of the base vectors under the to the direction of the highest weight eigenvector. The eigenvectors of B are again the Fourier harmonics, with the eigenvalues

$$\lambda'_r = 1 + \varepsilon\zeta_r,$$

where for the even N we denote by $\zeta_r := \exp(2\pi i(r+1/2)/L)$ the eigenvalues of ωC. The $N = 2m$ largest in absolute value are $\lambda'_{-m}, \dots, \lambda'_{m-1}$, and the corresponding eigenvectors (Fourier harmonics) span the space $\widetilde{V}_+$. We have obtained the desired convergence of $V_{+,j}$ to $\widetilde{V}_+$.

Now, in both these cases (N odd or even) the leading eigenvector β of $\wedge^N B$ (that is the Plucker coordinates of $\widetilde{V}_+$) is a vector with all strictly positive coordinates. This implies that the space $\widetilde{V}_+$ is transversal to any of the $N-L$-dimensional coordinate subspaces (spanned by $L-N$ base vectors). Indeed, for any such subspace the wedge product $\beta \wedge e_{k_1} \wedge \cdots \wedge e_{k_{L-N}}$ is equal to $\beta_{k'_1,\ldots,k'_N}\, e_1 \wedge \cdots \wedge e_L$, where $k'_1, \ldots, k'_N$ are the complementary coordinates to $k_1, \ldots, k_{L-N}$, and (as the Plucker coordinate $\beta_{k'_1,\ldots,k'_N}$ is strictly positive) thus is nonzero. This transversality implies that for any such coordinate subspace, in particular, for the space V_-, its B^{-1}-iterations will converge to the space $\widetilde{V}_-$ spanned by the $L-N$ eigenvectors of B with the least norm of the eigenvalues.

□

Remark 2.3.2. As the matrix B commutes with the circle rotation C, and as the Fourier transform diagonalizes it with the eigenvalues λ'_r for the Fourier harmonic $v_r = (e^{-2\pi ikr/L})_{k\in\mathbb{Z}_L}$, we can consider the operator $K(j;\cdot,\cdot)$ as a composition of four operators:

- Fourier transform F;
- Projection that leaves only one of two complementary groups of adjacent Fourier coefficients, of length N (that is, $-m, \ldots, m$ or $-m, \ldots, m-1$ depending on if N is odd or even) for positive j and of length $L-N$ (that is, $m+1, \ldots, L-(m+1)$ or $m, \ldots, L-(m+1)$ depending on if N is odd or even) for negative j;
- Diagonal operator of multiplication by $(\lambda'_r)^{-j}$
- Inverse Fourier transform F^{-1}.

Corollary 2.3.1. *Again, as the matrix B commutes with the circle rotation C, we actually have $K(j;k,k') = K(j,k-k')$, where*

$$K(j,k) = \begin{cases} \frac{1}{L}\sum_{r=-m}^{m}(\lambda'_r)^{-j}e^{-2\pi ikr/L}, & j>0 \\ -\frac{1}{L}\sum_{r=m+1}^{L-m-1}(\lambda'_r)^{-j}e^{-2\pi ikr/L}, & j\le 0 \end{cases} \tag{2.27}$$

for odd $N = 2m+1$ and

$$K(j,k) = \begin{cases} \frac{1}{L}\sum_{r=-m}^{m-1}(\lambda'_r)^{-j}e^{-2\pi ikr/L}, & j>0 \\ -\frac{1}{L}\sum_{r=m}^{L-m-1}(\lambda'_r)^{-j}e^{-2\pi ikr/L}, & j\le 0 \end{cases} \tag{2.28}$$

for even $N = 2m$.

Now, let us pass to the limit as $\varepsilon \to 0$, with the simultaneous time-rescaling by considering $t = \varepsilon j$. Note that even if this order of limits is slightly different from the one in Sec. 2.3.3 (where we passed to the limit first as $\varepsilon \to 0$ on the time intervals $\sim [-\frac{\tau}{2\varepsilon}, \frac{\tau}{2\varepsilon}]$ and then to the limit as $\tau \to \infty$), we still get the same random process as a limit:

Lemma 2.3.3. *Limit of the processes in Proposition 2.3.1 as $\varepsilon \to 0$ coincides with the one described in Theorem 2.3.1.*

Proof. Let τ be fixed. Then, once $M_- < -\frac{\tau}{2\varepsilon}$ and $M_+ > \frac{\tau}{2\varepsilon}$, due to the Gibbs property we can consider the random configuration inside $[-\frac{\tau}{2\varepsilon}, \frac{\tau}{2\varepsilon}] \times \mathbb{Z}_L$ as being sampled in two steps: first the boundary conditions on the levels $\pm\frac{\tau}{2\varepsilon}$, and then the inside part as a Gibbs measure conditional to these boundary conditions. Thus, the restriction of the Gibbs measure on the domain $[-\frac{\tau}{2\varepsilon}, \frac{\tau}{2\varepsilon}]$ can be seen as a mix of the measures discussed in Sec. 2.3.3 (as the boundary conditions are varied).

Now, as $\varepsilon \to 0$, ε-rescaled images of all these measures converge to the same process described in Theorem 2.3.1, and hence the same applies to their average (whichever were the averaging coefficients). □

We can now pass to the limit either in the probabilities of the stones being present, or for the position and moments of their jumps. For the stones, as the probability of their presence is given by an exact determinantal formula for any fixed $\varepsilon > 0$, we have the same kind of formula for their limit:

Theorem 2.3.2. *For the limit process in Theorem 2.3.1, the probability that the* stones *are present at positions $k_1, \dots, k_n$ at times $t_1, \dots, t_m$ is equal to the determinant*

$$\det(\tilde{K}(t_a - t_b, k_a - k_b)_{a,b=1,\dots,n}),$$

where

$$\tilde{K}(t,k) = \begin{cases} \frac{1}{L}\sum_{r=-m}^{m} e^{-t\zeta_r} e^{-2\pi i k r/L}, & t > 0 \\ -\frac{1}{L}\sum_{r=m+1}^{L-m-1} e^{-t\zeta_r} e^{-2\pi i k r/L}, & t \le 0 \end{cases} \tag{2.29}$$

for odd $N = 2m+1$ and

$$\tilde{K}(t,k) = \begin{cases} \frac{1}{L}\sum_{r=-m}^{m-1} e^{-t\zeta_r} e^{-2\pi i k r/L}, & t > 0 \\ -\frac{1}{L}\sum_{r=m}^{L-m-1} e^{-t\zeta_r} e^{-2\pi i k r/L}, & t \le 0 \end{cases} \tag{2.30}$$

for even $N = 2m$.

Corollary 2.3.2. *Take all the t_i equal. Then, what we get is a distribution of probabilities for the configurations of stones at a single moment of time, and Theorem 2.3.2 states that this is a determinantal point process with the kernel given by the projection operator on N adjacent Fourier harmonics. This reproves the statement of Theorem 1.1.2 from the determinantal processes point of view.*

In the same way, consideration of the positions and moments of the jumps gives

Theorem 2.3.3. *For the limit process in Theorem 2.3.1, the common density of the probability for the jumps at $(k_1, t_1), \dots, (k_n, t_n)$ is equal to the determinant*

$$\det(\tilde{K}(t_a - t_b, k_a - k_b - 1)_{a,b=1,\dots,n}) \tag{2.31}$$

for odd N and to the determinant

$$\det(\omega\tilde{K}(t_a - t_b, k_a - k_b - 1)_{a,b=1,\dots,n}) \tag{2.32}$$

for even N.

Note (see Figure 2.8) that the jump edges join a white vertex with the coordinates (j, k) to the black one with the coordinates $(j+1, k+1)$, and this space-shift by 1 leads to the -1 added to the difference of k in (2.31), (2.32).

Next one can remark that the function $\tilde{K}$ given by (2.29) is not perfectly suitable for the determinantal processes study: its asymptotics allows an exponential growth to the past or to the future. However, there is again a freedom in the choice of the gauge (similar to the one that we have already used for the jump edges): we can conjugate the matrix K that we obtain for a finite ε by the diagonal matrix with the elements $(c')^j$, where c' is chosen so that

$$|\lambda'_{m+1}| < c' < |\lambda'_m|. \tag{2.33}$$

This replaces the kernel (2.27) with

$$K_{c'}(j,k) = \begin{cases} \frac{1}{L}\sum_{r=-m}^{m}(\lambda'_r/c')^{-j}e^{-2\pi ikr/L}, & j > 0 \\ -\frac{1}{L}\sum_{r=m+1}^{L-m-1}(\lambda'_r/c')^{-j}e^{-2\pi ikr/L}, & j \le 0, \end{cases} \tag{2.34}$$

that is now exponentially decreasing in both $j \to +\infty$ and in $j \to -\infty$.

Now, as we pass to the limit as $\varepsilon \to 0$, it is natural to take $c' = 1 + \varepsilon c$ (so that its $j = \frac{t}{\varepsilon}$-th power tends to the exponent). The condition (2.33) then becomes

$$\operatorname{Re}\zeta_{m+1} < c < \operatorname{Re}\zeta_m, \tag{2.35}$$

and such a choice of c after passing to the limit leads to the kernel

$$\tilde{K}_c(t,k) = \begin{cases} \frac{1}{L} \sum\limits_{r:\,\operatorname{Re}\zeta_r > c} e^{-t(\zeta_r - c)} e^{-2\pi i k r/L}, & t > 0 \\ -\frac{1}{L} \sum\limits_{r:\,\operatorname{Re}\zeta_r < c} e^{-t(\zeta_r - c)} e^{-2\pi i k r/L}, & t \le 0 \end{cases} \tag{2.36}$$

for the "finite-circle bead process" that exponenitally decreases in both past and future.

A final remark is that passing to the limit as $L \to \infty$ with $N/L \to \rho$ transforms the kernel (2.36) to the one appearing in [7, Eq. (9)] under time renormalization and change of parametrization. Indeed, as $L \to \infty$, the eigenvalues ζ_m, ζ_{m+1} tend to the common limit $g_\infty := e^{\pi i \rho}$, and hence the limit value of c's (from passing to the limit in (2.35)) is

$$c_\infty := \cos \pi\rho.$$

The sums in the kernel (2.36) tend to the integral over the corresponding arcs of the unit circle; the limit kernel thus is

$$\tilde{J}_{beads}(t,k) = \begin{cases} \frac{1}{2\pi} \int_{-\pi\rho}^{\pi\rho} e^{-t(\zeta - c_\infty)} e^{-i\varphi(k-1)}\, d\varphi, & t > 0, \\ -\frac{1}{2\pi} \int_{\pi\rho}^{2\pi - \pi\rho} e^{-t(\zeta - c_\infty)} e^{-i\varphi(k-1)}\, d\varphi, & t \le 0, \end{cases} \tag{2.37}$$

where $\zeta = e^{i\varphi}$. Changing the integration variable to ζ, with $d\varphi = \frac{d\zeta}{i\zeta}$, we get:

$$\tilde{J}_{beads}(t,k) = \begin{cases} \frac{1}{2\pi i} \int_{I_1} e^{-t(\zeta - c_\infty))} \zeta^{-k}\, d\zeta, & t > 0 \\ -\frac{1}{2\pi i} \int_{I_2} e^{-t(\zeta - c_\infty))} \zeta^{-k}\, d\zeta, & t \le 0, \end{cases} \tag{2.38}$$

where $I_1 = \exp(i[-\pi\rho, \pi\rho])$ and $I_2 = \exp(i[\pi\rho, 2\pi - \pi\rho])$ are two complementary arcs of the unit circle joining $\overline{g}_\infty$ and g_∞ (see Fig. 2.10).

Now, let $\rho < 1/2$, and hence $c_\infty > 0$. The function under the integral is holomorphic in $\mathbb{C} \setminus \{0\}$, and hence the integral over the arc I_1 can be replaced with the integral along a straight segment; denoting $\zeta = c_\infty + i\phi\sqrt{1 - c_\infty^2}$ transforms this integral into

$$\sqrt{1 - c_\infty^2} \cdot \int_{[-1,1]} e^{-it\phi\sqrt{1-c_\infty^2}} (c_\infty + i\phi\sqrt{1 - c_\infty^2})^{-k} d\phi.$$

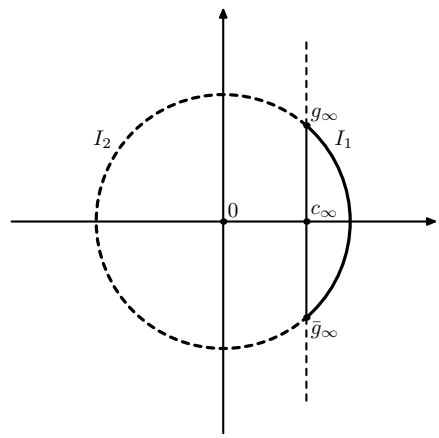

Figure 2.10: Integration paths

In the same way, as the function for $t < 0$ is exponentially decreasing in the left half-plane, the integral over the arc I_2 equals to the integral over $[g_\infty, c_\infty + i\infty] \cup [c_\infty - i\infty, \overline{g}_\infty]$, and thus to

$$-\sqrt{1-c_\infty^2} \cdot \int_{\mathbb{R}\setminus[-1,1]} e^{-it\phi\sqrt{1-c_\infty^2}} (c_\infty + i\phi\sqrt{1-c_\infty^2})^{-k} d\phi.$$

Taking $\gamma := c_\infty$ and rescaling the time $\sqrt{1-c_\infty^2}$ times, we obtain the kernel, appearing in [7, Eq. (9)].

2.4 Young Through The Looking Glass

The study of the Plancherel measures μ_n on the spaces $\mathbb{Y}_n$ in the seminal paper [6], was based on their *poissonization*. Namely, for a fixed $\theta > 0$, the authors consider the mixed sum $\sum_n \frac{e^{-\theta^2}(\theta^2)^n}{n!}\mu_n$ that is a measure on the space of all Young diagrams $\mathbb{Y} = \bigsqcup_n \mathbb{Y}_n$. Then, the authors show that these measures are determinantal ones, with kernels that are explicitly specified.

It is interesting to note, that the perfect matchings encoding allows to explain, *why* these measures are determinantal. The author thanks G. Merzon and V. Kleptsyn for these remarks.

Namely, consider the hexagonal graph corresponding to the encoding of a path in the Young graph, with some "target diagram" λ (see Fig. 2.2).

Denote this graph $\Gamma_{\lambda,M}$, where M is the height of the graph. The target diagram is then specified by upper right "green" edges atop of the last row, being the maya encoding for λ (namely, these edges attachments correspond to the empty holes).

Let us remove these edges, add a mirror image of the same graph, and join it with the initial one by vertical edges at *all* the vertices: see Fig. 2.11, right. Denote this graph by $\widehat{\Gamma}_M$. Then, a perfect matching on the resulting graph is a pair of length M paths in the maya diagram encodings, heading towards the same "target" diagram λ, encoded by the matched pairs that cross the mirror, where on each step each stone either stays or jumps forward. An example of such matching is on Fig. 2.11, right, with the encoded jumps shown on Fig. 2.11, left.

As earlier, let us equip the "jump" edges with a very small weight ε, while taking the height of this graph to be $2M \sim \frac{2}{\varepsilon}\theta$. Then (in the same way as before), as $\varepsilon \to 0$, for a fixed width and growing height graph, the total probability of a simultaneous jump (that is, of existence of a level at which two stones jump simultaneously) tends to 0.

For any given n-cell diagram λ, the perfect matchings in the graph $\Gamma_{\lambda,M}$, that do not encode any simultaneous jumps, are in one-to-one correspondence with a pair of a path to λ in the Young graph (describing the order of the jumps) and of the set of rows when these jumps (in this order) occur. The weight of each such matching is ε^n, there are $\dim\lambda$ different paths towards λ in the Young graph, and hence (as $\varepsilon \to 0$ and accordingly $M \to \infty$) their total weight asymptotically behaves as

$$\binom{M}{n}\varepsilon^n \cdot \dim\lambda \sim \frac{(M\varepsilon)^n}{n!}\dim\lambda \to \frac{\theta^n}{n!}\dim\lambda.$$

The perfect matching in $\widehat{\Gamma}_M$ is a pair of two such matchings with the same target diagram λ, and hence the total weight of matchings corresponding to a given λ asymptotically behaves as

$$\left(\frac{\theta^n}{n!}\dim\lambda\right)^2 = \frac{\theta^{2n}}{n!}\cdot\frac{\dim^2\lambda}{n!} = \frac{(\theta^2)^n}{n!}\cdot\mu_n(\{\lambda\}). \tag{2.39}$$

Thus, normalizing the limiting distribution to the probability one, one will get the poissonization of the Plancherel measures, restricted to the set of diagrams that fit to a given *width*. Finally, as the width tends to the infinity, one gets exactly the poissonization of all the Plancherel measures.

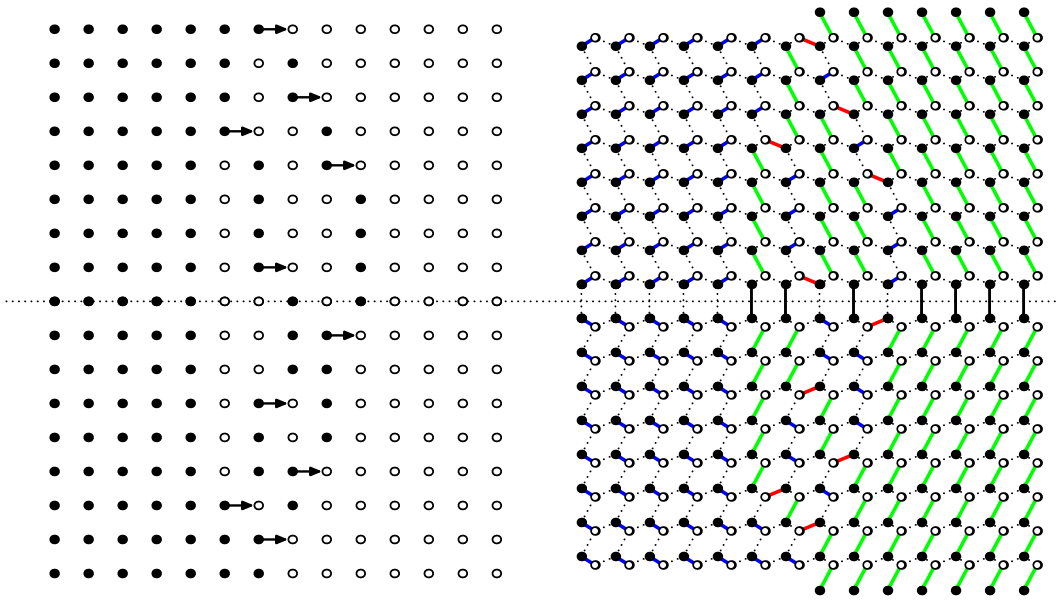

Figure 2.11: Domino tiling for the Poissonization of the Plancherel measure

On the other hand, the normalized probability distribution that comes from a perfect matching on a weighted planar bipartite graph is known to be determinantal (due to Kasteleyn-type arguments). Moreover, as a side remark the same argument explains why the width-restricted (on one or on both sides) poissonizations are also determinantal.

Chapter 3

Random dynamical systems on the real line

3.1 Definitions and notation.

Let $\mathcal{F} = \{f_1, f_2, \dots\}$ be a finite (or infinite) set of "sample" elements of $Homeo^+(\mathbb{R})$ with a probability measure μ on it. Let $\{g_n\}_{n=1}^{\infty}$ be a sequence of i.i.d. random variables, taking values in $\mathcal{F}$ and distributed in accordance with measure μ. In finite (and countable) case it is convenient to have special notations for elementary probabilities; we'll denote these

$$\mathbb{P}(g_n = f_k) = \mu(f_k) := p_k.$$

Consider the probability space $\Omega := (\mathcal{F}^{\mathbb{N}}, \mu^{\otimes \mathbb{N}})$; in these terms, g_n is a nth coordinate of $\omega \in \Omega$. Set

$$F_n = F_{n,\omega} = g_n \circ \cdots \circ g_1,$$

the left random walk on group $G = \langle \mathcal{F} \rangle$. Finally,

$$X_n(x) = F_n(x)$$

is the Markov chain, defined for any $x \in \mathbb{R}$.

All above defines the RDS, to which we would refer as *forward* from now on.

The *inverse* dynamics is defined in the same way for $\hat{\mathcal{F}} = \{f_1^{-1}, f_2^{-1}, \dots\}$, with the corresponding measure $\hat{\mu}$ defined by

$$\hat{\mu}(f_k^{-1}) = \mu(f_k) = p_k. \tag{3.1}$$

It is convenient to add to the considered $\mathcal{F}$ the set of all f_k^{-1} (with $\mu(f_k) = 0$ for any f_k that wasn't there originally) for it to become more symmetric. This allows us to rewrite (3.1) as

$$\hat{\mu}(f) = \mu(f^{-1}) \quad \forall f. \tag{3.2}$$

Intuitively, we can think of the inverse dynamics in three different ways. First is quite direct: instead of each f_k we've taken its inverse f_k^{-1}, thus it is indeed *inverse* dynamics. Second, assuming that the set $\mathcal{F}$ already contains each map together with its inverse, it is not changed by this "inversification", but the probabilities are swapped between each f_i and f_i^{-1} (thus making it the dynamics with the same generating set, but with another, "inverted" measure μ). Thirdly, we may think of the inverse dynamics as of the forward one with inverted time, thus making it a very natural object to investigate. However, one must note that if for a fixed time n the law of F_n for the inverse dynamics coincides with the law of inverse maps of F_n for the forward one, their *evolution* does not (as the order is composition is also inverted by the passing to the inverse).

As noted previously, we do not ask much of any f_k. However, we expect the whole RDS to hold the following property.

Definition 3.1.1. We call the point $x \in \mathbb{R}$ *shiftable*, if for any $a \in \mathbb{R}$ there're exist $k \in \mathbb{N}$ such that probabilities $\mathbb{P}(F_k(x) < x - a)$ and $\mathbb{P}(F_k(x) > x + a)$ are non-zero. Commonly speaking, it means that we can move x arbitrarily far to the left and to the right with non-zero probability in finite amount of time. We say that RDS has the *shiftability* property if any point $x \in \mathbb{R}$ is shiftable.

It is equivalent to the existence of f_{i_1} and f_{i_2} in $\operatorname{supp}\mu$ for any fixed x such that $f_{i_1}(x) < x < f_{i_2}(x)$. In work [10] this is called *unboundedness*.

Now we prove the following auxiliary result:

Lemma 3.1.1. *Let $(\mathcal{F}, \mu)$ be RDS with shiftability property. Then for any $x \in \mathbb{R}$ with probability 1 the limits $\limsup_{n\to\infty} F_n(x)$ and $\liminf_{n\to\infty} F_n(x)$ are infinite.*

Proof. Let us show by contradiction that for every finite interval $I \subset \mathbb{R}$ the probability that the upper limit $\limsup_{n\to\infty} F_n(x)$ takes value in I is equal to 0. Indeed, assume the contrary, that for some $x \in \mathbb{R}$ and $I = (a, b)$ the probability of the event

$$A = \{\omega \in \Omega \mid \limsup F_{n,\omega}(x) \in I\}$$

is strictly positive. Note that $A \subset \bigcup_k A_k$, where

$$A_k = \{\omega \mid \forall n \geq k \quad F_n(x) < b, \quad \text{and } F_n(x) > a \text{ infinitely often.}\}$$

Hence, for some k the event A_k has a positive probability. We fix such k.

Now, the shiftability property implies that there exists a composition $G = f_{i_l} \circ \cdots \circ f_{i_1}$ such that $G(a) > b$. Such a composition of length l has a positive probability p to be applied at every moment, including one of the moments when the image $F_n(x)$ enters I. The arguments below is a way of formalising the following idea. At each moment when $F_n(x) \in I$, the chance to apply G is at least p, and if there is an infinity of such moments, there should be also an infinity of moments when G is applied afterwards, bringing the image $F_{n+l}(x) = G(F_n(x))$ above b.

To proceed formally, consider the conditional probabilities of the event $B = A_k$ with respect to the growing cylinders generated by the first m applied maps $g_1, \ldots, g_m$,

$$\mathbb{P}(B \mid g_1, \ldots, g_m). \tag{3.3}$$

Due to a general statement from the measure theory, the *conditional* probabilities of an event B w.r.t. a growing family of cylinders generating the σ-algebra converge to 0 or to 1 almost surely, and the probability of tending to 1 equals to $\mathbb{P}(B)$. The convergence follows from the martingale convergence theorem (as such conditional probabilities form a martingale), and the values 0 or 1 follow from the fact that every event can be approximated by a cylindrical one up to an arbitrarily small measure. This statement is also an analogue of the statement that almost every point of a measurable set is its Lebesgue density point.

However, such conditional probability can never exceed $(1-p)$. Indeed, for any m, k let N be the first time the iteration $F_n(x)$ visits $(a, +\infty)$ with $n \geq \max(m, k)$. The event *implies* that $N < \infty$, thus

$$\mathbb{P}(B \mid g_1, \ldots, g_m) = \sum_{i \geq \max(m,k)} \mathbb{P}(N = i \mid g_1, \ldots, g_m) \cdot \mathbb{P}(B \mid g_1, \ldots, g_m, N = i). \tag{3.4}$$

But for any N the probability that the next l applied maps correspond to the map G is at least p, and for every such ω for the image $F_{N+l,\omega}(x)$ we have

$$F_{N+l,\omega}(x) = G(F_{N,\omega}(x)) > G(a) > b,$$

and such ω does not belong to B. So all the second factors in the sum (3.4) do not exceed $1-p$, and so does the whole.

Hence, the conditional probability (3.3) converges to zero almost surely, and hence $\mathbb{P}(B) = 0$. This contradiction proves that the probability that the upper limit takes a value in any finite interval vanishes, and thus this limit is almost surely equal to $+\infty$ or $-\infty$.

The second statement of the lemma is proved analogously. □

In the statements of Theorems 1.2.1 and 1.2.2 we assume the set of generating maps $\mathcal{F}$ to be finite. As we will see in Sec. 3.4, this finiteness assumption cannot be dropped completely; however, it can be weakened to the following one (it is easy to see that this is actually the assumption used in their proofs).

Definition 3.1.2. A random dynamical system, generated by a measure μ on $Homeo_+(\mathbb{R})$, has *compact displacement* property, if for any $x \in \mathbb{R}$ its image $\{f(x), f^{-1}(x) | f \in \operatorname{supp} \mu\}$ is contained in some compact interval.

Remark 3.1.1. This property holds automatically if μ is supported on some compact in $Homeo_+(\mathbb{R})$, where the space of homeomorphisms is equipped with the topology of uniform convergence on the compacts of both f and f^{-1}.

The main means to study RDS we're going to use throughout the first half of the Chapter 3, is to look at the behaviour of the points. Therefore we introduce the following functions, which allow us to do it in simpler terms.

Notation 3.1.1. Let us define

$$\phi_+(x) := \mathbb{P}(\lim_{n\to\infty} F_n(x) = +\infty),$$

$$\phi_-(x) := \mathbb{P}(\lim_{n\to\infty} F_n(x) = -\infty),$$

$$\phi_0(x) := 1 - \phi_+(x) - \phi_-(x).$$

The first and the second are the probabilities of the events 'the iterations of x tends to $+\infty$', 'the iterations of x tends to $-\infty$'. The third one is the probability that the images of x do not tend neither to $+\infty$, nor $-\infty$, and due to the Lemma 3.1.1 this is the same as the probability of

$$\limsup_{n\to\infty} F_n(x) = +\infty, \quad \liminf_{n\to\infty} F_n(x) = -\infty$$

(oscillation behaviour). For a finitely generated RDS, this is equivalent to 'there exist an interval that $F_n(x)$ visits inifinitely many times'. In the infinite case it is not true: in Section 3.4 we present a counter-example.

$\hat{\phi}_+, \hat{\phi}_-$ and $\hat{\phi}_0$ are defined in the same manner for $\hat{\mu}$.

Now we can reformulate Theorem 1.2.1 in terms of $\phi_{\pm,0}$.

Theorem 3.1.1. *For a pair of forward and inverse RDS with shiftability one of the following is true (perhaps, after the change of coordinate $x \to -x$ and/or inchanging μ and $\hat{\mu}$):*

1. $\phi_+ \equiv 1$, $\hat{\phi}_- \equiv 1$;
2. $\phi_+ \equiv 1$, $\hat{\phi}_0 \equiv 1$;
3. $\phi_0 \equiv 1$, $\hat{\phi}_0 \equiv 1$;
4. $\phi_0 \equiv 0$, ϕ_+ *and* ϕ_- *are not constant,* $\hat{\phi}_0 \equiv 1$.

Finally, recall the definition of a stationary measure:

Definition 3.1.3. A measure ν on $\mathbb{R}$ is called *stationary* for the RDS $\langle \mathcal{F}, \mu \rangle$ with finite $\mathcal{F}$ if

$$\nu = \sum_{i=1}^{k} p_i (f_i)_* \nu \tag{3.5}$$

where $f_*\nu$ is the push-forward of the measure ν by the map f (that is, $(f_*\mu)(A) = \mu(f^{-1}(A)$ for all Borel sets A).

This definition is naturally generalized for the random dynamics generated by some probability measure μ on $Homeo_+(\mathbb{R})$:

Definition 3.1.4. A measure ν is *stationary* for the corresponding RDS, if

$$\nu = \int (f_*\nu) d\mu(f),$$

or, equivalently, if for any Borel set $A \subset \mathbb{R}$ one has

$$\nu(A) = \int \nu(f^{-1}(A))\, d\mu(f).$$

This definition is also equivalent to the invariance of the measure $\mu^{\mathbb{N}} \times \nu$ for the skew product over the one-sided Bernoulli shift, but we will not use this here.

3.2 Properties of ϕ_+ and ϕ_-

In this section we study properties of functions ϕ_+, ϕ_- and ϕ_0 on their own, without any relation to inverse dynamics. The reasoning holds for both finite and infinite RDS with shiftability property.

First, note that ϕ_+ and ϕ_- are monotonous. Indeed, if for some $\omega \in \Omega$ $F_n(x)$ goes to $+\infty$, then (as all our homeomorphisms preserve orientation) for any $y > x$ and any $n \in \mathbb{N}$ its image $F_n(y) \geq F_n(x)$ and thus also tends to $+\infty$. So ϕ_+ is non-decreasing. Similarly, ϕ_- is non-increasing.

Next proposition states that either every point tends to $+\infty$ (or, similarly, $-\infty$), or the probability to go there vanishes at $-\infty$ (correspondingly, at $+\infty$).

Proposition 3.2.1. *If there exists $\varepsilon > 0$ such that for all $x \in \mathbb{R} : \phi_+(x) \geqslant \varepsilon$, then $\phi_+(x) \equiv 1$.*

Symmetrically, if for some $\varepsilon > 0$ all $x \in \mathbb{R} : \phi_-(x) \geqslant \varepsilon$, then $\phi_-(x) \equiv 1$.

Proof. Consider the event $A \subset \Omega$, stating that the iterations starting from the initial point x do not tend to $+\infty$:

$$A = \{\omega \in \Omega \mid F_{n,\omega}(x) \not\to +\infty, \quad n \to \infty\}.$$

Take the conditional probabilities of this event with respect to the growing cylinders $g_1, \dots, g_m$. On one hand, due to the Markovian property such conditional probability equals to the probability that the iterations of the image point $F_m(x) = g_m \circ \dots \circ g_1(x)$ do not tend to $+\infty$:

$$\mathbb{P}(A \mid g_1, \dots, g_m) = 1 - \phi_+(F_m(x)) \tag{3.6}$$

On the other hand, in the same way as in the proof of Lemma 3.1.1, these probabilities converge to 0 or to 1 almost surely, and the probability of tending to 1 equals to $\mathbb{P}(A)$.

Applying this, we see that the probability $\mathbb{P}(A \mid g_1, \dots, g_m)$ converges almost surely to 0 or to 1. However, it cannot converge to 1, as the right hand side of (3.6) is at most $1 - \varepsilon$ due to the assumption. Hence (again, in the same way as in the proof of Lemma 3.1.1), the limit is almost surely equal to 0, and thus $\mathbb{P}(A) = 0$ due to the martingale property.

□

Until now, we haven't used shiftability in our reasoning. But the following statement shows that it is important: due to it, different points of $\mathbb{R}$ cannot show completely different behavioral patterns – that is, if one can go to any of infinities, so do all of them.

Lemma 3.2.1. *If there exists $x \in \mathbb{R}$ such that $\phi_+(x) > 0$, then for every $y \in \mathbb{R}$ $\phi_+(y) > 0$. Similarly, if there exists $x \in \mathbb{R}$ such that $\phi_-(x) > 0$, then for every $y \in \mathbb{R}$ $\phi_-(y) > 0$.*

Proof. Fix y. Shiftability allows us to move y farther to the right than x with positive probability, say, p. If y is already greater than x, we can skip this step and pose $p = 1$. But any point greater than x goes to infinity with probability at least $\phi_+(x)$, so

$$\phi_+(y) \geq p \cdot \phi_+(x) > 0.$$

□

We then have the following

Proposition 3.2.2. *If there exists x and y such that $\phi_+(x) > 0$ and $\phi_-(y) > 0$, then for every $z \in \mathbb{R}$ $\phi_+(z) + \phi_-(z) = 1$.*

Proof. Applying Lemma 3.2.1, we see that in this case $\phi_+(0), \phi_-(0) > 0$. Note now, that the function $\phi_0(z)$ is thus bounded away from 1. Indeed, due to the monotonicity of $\phi_\pm$ for $z \geq 0$ we have $\phi_+(z) \geq \phi_+(0)$, while for $z \leq 0$ we have $\phi_-(z) \geq \phi_-(0)$, thus

$$\forall z \in \mathbb{R} \quad \phi_+(z) + \phi_-(z) \geq \min(\phi_+(0), \phi_-(0)) =: \varepsilon > 0,$$

and hence

$$\forall z \in \mathbb{R} \quad \phi_0(z) = 1 - \phi_-(z) - \phi_+(z) \leq 1 - \varepsilon. \tag{3.7}$$

As in the proof of Proposition 3.2.1, take any initial point $x \in \mathbb{R}$ and consider the conditional probabilities

$$\mathbb{P}(\lim_{n\to\infty} F_{n,\omega}(x) \neq \pm\infty \mid g_1, \ldots, g_m).$$

On one hand, such a conditional probability is equal to $\phi_0(F_m(x))$ due to the Markovian property. On the other hand, it should (due to the same arguments) converge to 0 or 1, converging to 1 with the probability $\phi_0(x)$. However, due to uniform upper bound (3.7) it cannot converge to 1, hence $\phi_0(x) = 0$.

□

Now we see, that we do not have much freedom with the behavior of the random iterations: at least one of the functions ϕ_+, ϕ_- and ϕ_0 must vanish identically. The next proposition makes this observation even stronger:

Proposition 3.2.3. *Either $\phi_+(z)+\phi_-(z) \equiv 1$, or $\phi_+(z)+\phi_-(z) \equiv 0$. Equivalently, either $\phi_0 \equiv 0$ or $\phi_0 \equiv 1$.*

Proof. Assume that $\phi_+ > 0$. As in the proof of Proposition 3.2.1, take any initial point $x \in \mathbb{R}$ and consider the event $A = \{F_{n,\omega}(x) \to +\infty\}$ and its conditional probabilities w.r.t. $g_1, \dots, g_m$.

Again due to the same measure theory arguments the conditional probability

$$\mathbb{P}(A \mid g_1, \dots, g_m) = \phi_+(F_m(x)) \tag{3.8}$$

converges as $m \to \infty$ almost surely to 0 or to 1, and tends to 1 with the probability equal to $\phi_+(x)$, hence to 0 with the probability $1 - \phi_+(x)$.

Now, due to monotonicity of ϕ_+, if $\phi_+(F_{m,\omega}(x)) \to 0$, then $F_{m,\omega}(x) \to -\infty$. Hence, $\phi_-(x) \geq 1 - \phi_+(x)$, and thus $\phi_+ + \phi_- \equiv 1$. The case $\phi_- > 0$ is treated analogously, and $\phi_+ = \phi_- \equiv 0$ implies $\phi_0 \equiv 1$.

□

3.3 Proof of the Theorem 3.1.1

In the previous section we proved that either one of the functions ϕ_+, ϕ_- and ϕ_0 is identically equal to 1 (immediately forcing two others to vanish), or $\phi_- = 1 - \phi_+$ and both are monotonously approaching 0 and 1, though never reaching. This section is devoted to the duality arguments, relating possible behaviours for μ and $\hat{\mu}$.

We start with the following proposition; it is quite natural to expect, if we think of the inverse dynamics as a dynamics with reverted time.

Proposition 3.3.1. *Suppose $\phi_+ \equiv 1$. Then $\hat{\phi}_+ \equiv 0$. Similarly, if $\phi_- \equiv 1$, then $\hat{\phi}_- \equiv 0$.*

Proof. Let us prove the first statement of the proposition. Fix $x \in \mathbb{R}$. As $\phi_+(x) = 1$,

$$\forall y \in \mathbb{R} \quad \mathbb{P}(F_k(x) > y) \to 1, \qquad \text{as } k \to \infty.$$

Suppose there exists y such that $\hat{\phi}_+(y) = p$. Then

$$\liminf_{n\to\infty} \mathbb{P}(\hat{F}_n(y) > z) \geqslant p.$$

Therefore there exists such $N \in \mathbb{N}$, that

$$\mathbb{P}(x > \hat{F}_n(y)) = \mathbb{P}(F_n(x) > y) > 1 - \frac{p}{2}$$

and $\mathbb{P}(\hat{F}_n(y) > x) > p/2$ simultaneously. This contradiction concludes the proof. $\square$

So, if $\phi_+ \equiv 1$ then either $\hat{\phi}_- \equiv 1$ or $\hat{\phi}_0 \equiv 1$. The first case is illustrated by asymmetrical random walk (sample functions $f_{1,2}(x) = x \pm 1$ with probabilities different from 1/2). The second case is a little trickier, yet still realizable by our means (see Fig.3.1). Put

$$f_1(x) = \begin{cases} x+1, & \text{if } \ x < 0; \\ 2x+1, & \text{if } \ x \geqslant 0; \end{cases} \quad p_1 = \frac{1}{2}.$$

and

$$f_2(x) = x - 1, \ p_2 = \frac{1}{2}.$$

Note that the probability that the iterations $F_{n,\omega}(x)$ starting with $x \geq 0$ tend to $+\infty$ is strictly positive. Namely,

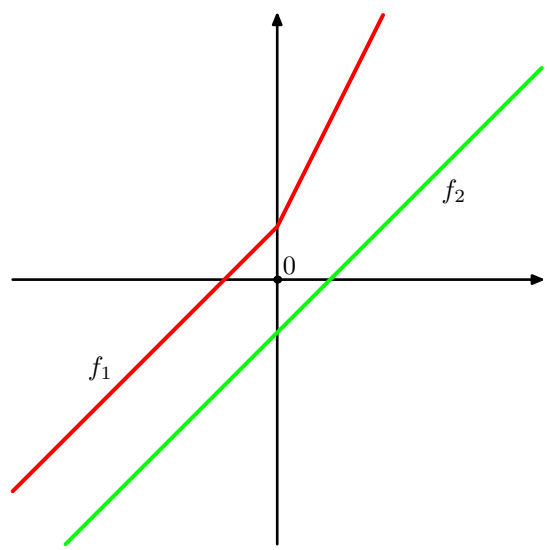

Figure 3.1: Maps f_1 and f_2

Proposition 3.3.2. *For the abovementioned RDS*

$$\phi_+|_{[0,+\infty)} \geq \phi_+(0) > 0.$$

Proof. We will show that for some M large enough, there's a positive probability of $F_{n,\omega}(M)$ tending to infinity without ever reaching 1. The statement of the proposition then follows automatically, as $f_1^M(0) > M$, and the probability of applying f_1 M times is $(1/2)^M > 0$.

On $[1, +\infty)$, we have $f_1(x) \geq \bar{f}_1(x) := x + 2$. Hence, the probability of the event "$\bar{f}_1, f_2$-generated random walk, starting at M, tends to $+\infty$ and always stays in $[1, +\infty)$" is no smaller than the probability of the event "$\bar{f}_1, f_2$-generated random walk, starting at M, tends to $+\infty$ and always stays in $[1, +\infty)$". Now, the latter defines a drifted random walk $G_n(x) = x + \xi_1 + \cdots + \xi_n$, where ξ_j are i.i.d. random variables, taking values -1 and $+2$ with probabilities $1/2$.

Denote by S_n the shifting part of this walk, $S_n := \xi_1 + \cdots + \xi_n$. Then by the Law of Large Numbers, almost surely

$$\lim_{n\to\infty} \frac{S_n}{n} = \mathbb{E}\xi_1 = \frac{1}{2},$$

hence $\lim_{n\to\infty} S_n = +\infty$ and in particular almost surely $\min_n S_n > -\infty$.

In particular, there exists $M > 0$ such that $\min_n S_n > -M + 1$ with positive probability, thus implying the desired

$$\min_n G_n(M) = M + \min_n S_n > 1.$$

□

On $(-\infty, 0]$ our RDS is just a standard "$+1/-1$" random walk, and hence the images of any point $x < 0$ almost surely reach $[0, +\infty)$. Applying the Markov property, we get that $\phi_+|_{(-\infty,0)} \geq \phi_+(0)$, and hence the function ϕ_+ is bounded away from 0. By Proposition 3.2.1, it implies $\phi_+ \equiv 1$.

On the other hand, the trajectories of the inverse RDS almost surely do not tend to infinity. Indeed, on the negative half-line we still have "$+1/-1$" random walk, while $+\infty$ (under a change of coordinates $z = \frac{1}{x}$) becomes a positive Lyapunov exponent point.

Case with $\phi_- \equiv 1$ becomes the one considered above under the change of coordinate $x \to -x$. Similarly, $\hat{\phi}_\pm \equiv 1$ generate the same cases under the interchange of forward and inverse dynamics. All that rests are "almost" symmetrical cases:

1. $\phi_0 \equiv 1$, $\hat{\phi}_0 \equiv 1$;
2. ϕ_+ and ϕ_- are not constant, $\hat{\phi}_0 \equiv 1$;
3. ϕ_+, ϕ_-, $\hat{\phi}_+$ and $\hat{\phi}_-$ are not constant.

Examples for the first two are quite simple to present: classical random walk ($f_{1,2}(x) = x \pm 1$ with probabilities $1/2$) for the former, and the same random walk with additional function $f_3(x) = 2x$ with some positive probability for the latter.

Indeed, as in proposition 3.3.2 we can show that both $\phi_+(0) > 0$ and $\phi_-(0) > 0$, which, due to proposition 3.2.2, yields $\phi_0 \equiv 0$. The $\hat{\phi}_0 \equiv 1$ statement is showed, once again, by a change of coordinates $z = \frac{1}{x}$, as both infinities become negative Lyapunov exponent points.

The third case, as it appears, never realizes.

Proposition 3.3.3. *If ϕ_+ is not constant, then $\hat{\phi}_0 \equiv 1$;*

Proof. In order to prove it, consider the following measure:

$$\nu[x, y] = \phi_+(y) - \phi_+(x). \tag{3.9}$$

It is easy to check straightforwardly that

$$\phi_+(x) = \sum_{i=1}^{k} \phi_+(f_i(x)) \cdot p_i,$$

(where k can be infinite). Thus we conclude that ν is stationary for inverse dynamics. From the definition of ϕ_+ and our assumbtions we conclude that ν is stochastical and non-constant.

Let us take an ergodic component $\tilde{\nu}$ of ν; stochastical ergodicity theorem of Kakutani ([26], [19, Theorem 3.1]) then implies that for almost any starting point t its random orbit is almost surely (asymptotically) distributed with accordance with $\tilde{\nu}$. In particular, it will visit arbitrarily many times a closed interval with any strictly positive measure. Therefore $\hat{\phi}_0(t) = 1$, and then $\hat{\phi}_0 \equiv 1$.

□

Thus we have proved the Theorem 3.1.1.

3.4 Infinite monster

One of the arguments in the finitely generated RDS case was that if a trajectory almost surely does not tend neither to $+\infty$, nor to $-\infty$, then it almost surely endlessly oscillates between the infinities, and thus visits a sufficiently large interval J infinitely often. This section is devoted to construction of a "monstrous" example showing that this is no longer the case for infinitely generated systems.

The idea is quite natural: if we want to make such a system whose orbits avoid any compact interval after some initial amount of time, we need the absolute value of x to tend to ∞ and also allow sufficiently large "jumps", so the orbit could avoid getting "caught" in a finite interval. In order to do so, we consider a sequence of maps, each of which shifts much stronger than the previous one:

$$f_k(x) = x + (-1)^k D_k, \qquad k = 1, 2, \dots, \tag{3.10}$$

where

$$D_k = e^{e^k}, \tag{3.11}$$

taken with sufficiently slowly decreasing probabilities

$$p_k = \frac{1}{k} - \frac{1}{k+1} = \frac{1}{k(k+1)}, \quad k = 1, 2, \dots. \tag{3.12}$$

Theorem 3.4.1. *The trajectories of the RDS, defined by (3.10)–(3.12), almost surely visit any compact interval only finitely many times. The same holds if we replace the maps f_k by any maps*

$$\tilde{f}_k = x + (-1)^k \tilde{D}_k(x) \tag{3.13}$$

such that the difference $\tilde{D}_k(x) - D_k$ is bounded uniformly in k and x.

Proof. Let us call k in $f_k, \tilde{f}_k, D_k$ and $\tilde{D}_k$ its *rank*; let k_n be the (random) sequence of ranks, and let K_n denote the maximal rank appearing up to the n-th iteration:

$$K_n := \max_{j \le n} k_j.$$

From the choice of probabilities p_k we have the following lower estimate for the growth of these maximal ranks:

Lemma 3.4.1. *Almost surely for all n sufficiently large one has $K_n > \sqrt{n}$.*

Proof. The event $\{K_n < \sqrt{n}\}$ coincides with the event $\{k_1 < \sqrt{n}, \dots, k_n < \sqrt{n}\}$, and thus (due to the choice (3.12) of probabilities p_k) has the probability

$$\mathbb{P}(K_n < \sqrt{n}) = (1 - \frac{1}{[\sqrt{n}]})^n < e^{-\sqrt{n}}.$$

The application of Borel–Cantelli Lemma thus concludes the proof. □

Now, once $K_n > \sqrt{n}$ and n is sufficiently large, it is immediate from the definition (3.10) that the highest rank maps (and there is at least one of them) overpower at most $n-1$ lower ranking ones. Namely,

$$f_{k_n} \circ \cdots \circ f_{k_1}(x) = x + \sum_{j=1}^{n} (-1)^{k_j} D_{k_j}.$$

The sum in the right hand side contains at least one (and maybe more) summand equal to $(-1)^{K_n} D_{K_n}$, corresponding to the application of the highest rank map f_{K_n}. Meanwhile, the sum of all the summands corresponding to the lower ranking maps does not exceed in absolute value

$$\sum_{\substack{j \le n, \\ k_j < K_n}} D_{k_j} \le n D_{K_n - 1}.$$

Meanwhile, for all sufficiently large k due to the choice (3.11) of D_k we have

$$D_k > 2k^2 D_{k-1},$$

and as $K_n > [\sqrt{n}]$, this implies

$$D_{K_n} > 2n D_{K_n - 1}.$$

Hence, almost surely for all n sufficiently large we have

$$|x - f_{k_n} \circ \cdots \circ f_{k_1}(x)| > \frac{1}{2} D_{K_n} > \frac{1}{2} D_{[\sqrt{n}]},$$

and this lower bound tends to $+\infty$ as $n \to \infty$.

Finally, assume that the RDS is given by (3.13), and there exists $C > 0$ such that

$$\forall k, \forall x \in \mathbb{R} \quad |\tilde{D}_k(x) - D_k| < C.$$

Then one has

$$|x - \tilde{f}_{k_n} \circ \cdots \circ \tilde{f}_{k_1}(x)| > D_{K_n} - nC - \sum_{\substack{j \le n, \\ k_j < K_n}} D_{k_j} >$$

$$> D_{K_n} - nC - nD_{K_n - 1} > \frac{1}{2} D_{K_n} - nC > \frac{1}{3} D_{K_n} \quad (3.14)$$

once $K_n > [\sqrt{n}]$ and n is sufficiently big, and the right hand side of (3.14) tends to infinity. □

The example above is asymmetric. However, it can be modified to become symmetric. Namely, take the maps

$$f_k^{\pm}(x) = x \pm D_k, \quad n \in \mathbb{N}. \quad (3.15)$$

and associate them with the probabilities

$$p_k^{\pm} = \frac{1}{2} p_k = \frac{1}{2} \cdot \left(\frac{1}{k} - \frac{1}{k+1} \right), \quad k = 1, 2, \ldots, \quad (3.16)$$

where D_k and p_k are given by (3.11) and (3.12) respectively. In particular, one can take $f_k^- = (f_k^+)^{-1}$, thus making the system symmetric.

Theorem 3.4.2. *The trajectories of the RDS, defined by (3.15) and (3.16), almost surely visit any compact interval only finitely many times. The same holds if we replace the maps $f_{\pm k}$ by any maps $\tilde{f}_{\pm k}$ such that the difference $\tilde{f}_{\pm k}(x) - f_{\pm k}(x)$ is bounded uniformly in k and x.*

Proof. Let $k_1, k_2, \ldots$ be i.i.d. random variables with $\mathbb{P}(k_j = k) = p_k$, and $\sigma_1, \sigma_2, \ldots$ i.i.d. random variables taking values in $\{+, -\}$ with

$$\mathbb{P}(\sigma_j = +) = \mathbb{P}(\sigma_j = -) = 1/2.$$

As before, let us call k the *rank* of the maps $f_k^{\pm}$, and let K_n denote the highest rank among the maps chosen on the first n steps,

$$K_n := \max_{j \le n} k_j.$$

The key point is the following lemma.

Lemma 3.4.2. *Almost surely, for all n sufficiently large, there is only one map of the highest rank present in the composition of the first n maps:*

$$\#\{j \le n \mid k_j = K_n\} = 1. \tag{3.17}$$

Proof. Note first that in the same way as in Lemma 3.4.1, we have

$$\mathbb{P}(K_n < n^{2/3}) = (1 - \frac{1}{[n^{2/3}]})^n < e^{-n^{1/3}}.$$

As the series $\sum_n e^{-n^{1/3}}$ converges, almost surely for all n sufficiently large we have $K_n > n^{2/3}$.

Now, consider the events $B_n := \{k_{n+1} = K_n\}$. It suffices to show that almost surely only finitely many of these events take place: once (3.17) holds for a given n, the only way for it to be broken is for $B_{n'}$ to hold for some $n' > n$. Meanwhile, (3.17) holds for an infinite number of values of n, as $K_n \to \infty$.

Now, note, that *conditionally* to $k_1, \dots, k_n$, the probability of the event B_n is equal to p_{K_n}. Hence, the probability of the event B_n is equal to the expectation

$$\mathbb{P}(B_n) = \mathbb{E}p_{K_n} = \sum_k p_k \cdot \mathbb{P}(K_n = k).$$

Let us decompose this sum into two parts: for $K_n < n^{2/3}$ and for $K_n \ge n^{2/3}$:

$$\mathbb{P}(B_n) = \sum_{k<n^{2/3}} p_k \cdot \mathbb{P}(K_n = k) + \sum_{k \ge n^{2/3}} p_k \cdot \mathbb{P}(K_n = k)$$

The former sum in the right hand side does not exceed $\mathbb{P}(K_n < n^{2/3}) < e^{-n^{1/3}}$, while the latter is at most $p_{\lceil n^{2/3} \rceil} < \frac{1}{(n^{2/3})^2} = \frac{1}{n^{4/3}}$. Hence,

$$\mathbb{P}(B_n) < e^{-n^{1/3}} + \frac{1}{n^{4/3}},$$

and the series $\sum_n \mathbb{P}(B_n)$ converges. By Borel–Cantelli Lemma, almost surely only finitely many events B_n take place, and this concludes the proof. □

Now we can conclude in the same way as in the proof of Theorem 3.4.2. Namely, for every n for which (3.17) holds, we have

$$|x - \tilde{f}_{k_n}^{\sigma_n} \circ \dots \circ \tilde{f}_{k_1}^{\sigma_1}(x)| > D_{K_n} - Cn - \sum_{\substack{j \le n, \\ k_j < K_n}} D_{k_j},$$

and (as in (3.14)) the right hand side is at least $\frac{1}{3}D_{K_n}$ once $K_n > \sqrt{n}$ and n is sufficiently big.

□

3.5 Proof of Theorem 1.2.2

Let us first recall that a recurrent RDS on the real line (and, actually, on any other σ-compact metric space) admits a (possibly, Radon) stationary measure. On one hand, this statement is contained in [30, Theorem 5.1], where the function g therein should be taken to be identically equal to 1 on the compact that is almost surely visited infinitely often by orbits starting at any initial point. On the other, we would like to note that it can be seen by adapting an argument from [15, Theorem 5.1].

Proposition 3.5.1. *A recurrent RDS on the $\mathbb{R}$ admits a Radon stationary measure.*

Proof. Let $J \subset \mathbb{R}$ be an interval such that for any initial point x its random images $F_n(x)$ almost surely visit J infinitely often. Take a compactly supported smooth function $\psi : \mathbb{R} \to [0, 1]$, such that $\psi|_J \equiv 1$, and consider a random process of iterations that is stopped on each step at the point x_n with the probability $\psi(x_n)$. That is, *one* iteration of this process starting at some point x_0 is constructed in the following way:

- Take a random image $x_1 = f_{w_1}(x_0)$. With the probability $\psi(x_1)$ the process stops here, and we take x_1 to be the image.
- If the process wasn't stopped on the previous step, take a random image $x_2 = f_{w_2}(x_1)$. With the probability $\psi(x_2)$ the process stops here, and we take x_2 to be the image.
- If the process wasn't stopped on the previous step, take a random image $x_3 = f_{w_3}(x_2)$. With the probability $\psi(x_3)$ the process stops here, and we take x_3 to be the image.
- Etc.

Denote by m_x the distribution of the stopping point for the process starting at the point x; then m_x depends continuously on x. Hence, this process admits, via the usual Kryloff–Bogolyubov procedure, a probability stationary

measure ν_ψ, that is by construction supported on $\operatorname{supp}\psi$. Namely, denote by P_ψ the associated diffusion operator, acting on the space of probability measures on $\operatorname{supp}\psi$,

$$P_\psi \nu := \int_{\mathbb{R}} m_x \, d\nu(x).$$

This action is continuous due to the continuous dependence of m_x on the point x. Then, fix any initial measure ν and consider the sequence of time averages of its images:

$$\bar{\nu}_n := \frac{1}{n} \sum_{j=0}^{n-1} P_\psi^j \nu.$$

Any weak accumulation point of $\bar{\nu}_n$ (that exists due to the compactness of $\operatorname{supp}\psi$) is a P_ψ-invariant measure.

Now, fix a compactly supported function ψ_0, taking values in $[0,1]$, with $\psi_0|_J \equiv 1$. For any $\psi \geq \psi_0$ denote by $\mathcal{M}_\psi$ the space of (non-probability) P_ψ-stationary measures ν, normalized to $\int \psi_0 d\nu = 1$.

Finally, take a *sequence* of functions ψ_k such that $\operatorname{supp}\psi_k \subset \{\psi_{k+1}(x) = 1\}$ and that $\bigcup_k \{\psi_k(x) = 1\} = \mathbb{R}$. From now on, the idea is to "widen" the support of measures ν_ψ to the full real line by considering the measures that are stationary w.r.t. the corresponding P_{ψ_n} and passing to the limit. This can be achieved by several different ways, that we present here to compare (as it seems that such a comparison may also present an interest for the reader).

The most straightforward way is to note that the stationarity relation "inside" the intervals where $P_{\psi_n} \equiv 1$ is exactly the stationarity relation for our dynamical system. Moreover, for any fixed interval J' the measures $\nu(J')$ are uniformly bounded for $\nu \in \mathcal{M}_{\psi_n}$:

Lemma 3.5.1. *For any interval $J' \supset J$ there exists a constant C such that for any ψ satisfying $\psi|_{J'} = 1$ and any $\nu \in \mathcal{M}_\psi$ one has $\nu(J') < C$.*

Proof. Let such (closed) interval J' be fixed. Any its point can be shifted by the RDS to reach J; due to the compactness of J', there exists a uniform constant N such that any point x of J' can be mapped to J in at most N iterations:

$$\forall x \in J' \quad \exists n, g_1, \ldots, g_n \in \mathcal{F} : \quad g_n \circ \cdots \circ g_1(x) \in J.$$

Hence, if for an initial point $x \in J'$ the first n random maps applied are $g_1, \ldots, g_n$, then in at most $n \leq N$ steps of P_ψ-process this point will reach J.

On the other hand, the probability of any composition $g_1 \circ \cdots \circ g_n$ is bounded from below by a constant $(\min_i p_i)^N$. Thus, for any $\nu \in \mathcal{M}_\psi$ one has

$$(N+1)\nu(J) = (\nu + P_\psi \nu + \cdots + P_\psi^N \nu)(J) \geq (\min_i p_i)^N \nu(J').$$

On the other hand,

$$\nu(J) \leq \int \psi_0 d\nu = 1,$$

thus getting a uniform upper bound

$$\nu(J') \leq \frac{N+1}{(\min_i p_i)^N}.$$

□

Now, take a sequence ν_k of P_{ψ_k}-stationary measures. Due to Lemma 3.5.1, for any interval J' the sequence $\nu_k(J')$ is bounded, and hence one can extract a convergent subsequence.

On the other hand, if for some function ψ and the corresponding stationary measure ν_ψ some interval J' is "well inside" the "immediate stopping" $\{\psi = 1\}$ zone, that is, if

$$J' \subset \{x \mid \psi(x) = 1\} \cap \bigcap_{f \in \operatorname{supp} \mu} f^{-1}(\{x \mid \psi(x) = 1\}),$$

then the stationarity of ν_ψ implies that on restriction to J', the measures ν_ψ and $\sum_j p_j (f_j)_* \nu_\psi$ coincide (as the ψ-process makes exactly one step there). Hence, as the zones $\{\psi_k = 1\}$ were chosen to be larger and larger, on any interval J' we have the relation

$$\nu_{\psi_k}|_{J'} = (\sum_j p_j (f_j)_* \nu_{\psi_k})|_{J'}$$

once k is sufficiently large, and passing to the limit, we see that the limit measure ν is a (Radon) stationary measure for our dynamical system.

□

The above argument completes the proof of Proposition 3.5.1. However, it is interesting to note that the measures corresponding to different functions ψ can be related to each other. Namely, first note the following

Lemma 3.5.2. *Let ψ_1, ψ_2 be two continuous compactly supported functions taking values in $[0,1]$, such that* $\operatorname{supp}\psi_1 \subset \{\psi_2 = 1\}$. *Then for any $\nu \in \mathcal{M}_{\psi_2}$ one has $\psi_1\nu \in \mathcal{M}_{\psi_1}$.*

Proof. Consider a one-sided skew product Φ acting on $X := \mathbb{R} \times \mathcal{F}^{\mathbb{N}} \times [0,1]^{\mathbb{N}}$ by the rule

$$\Phi(x, (g_n)_{n=1}^{\infty}, (c_n)_{n=1}^{\infty}) = (g_1(x), (g_{n+1})_{n=1}^{\infty}, (c_{n+1})_{n=1}^{\infty}).$$

Consider also a subset $A_\psi \subset X$,

$$A_\psi := \{(x, (g_n)_{n=1}^{\infty}, (c_n)_{n=1}^{\infty}) \mid c_1 \leq \psi(x)\}.$$

In these terms, one step of the ψ-process, starting at a point x, consists of completing it second and third coordinates, randomly chosen with respect to $\mu^{\mathbb{N}} \times \mathrm{Leb}^{\mathbb{N}}$, and taking a Φ-first return to the set A_ψ. Indeed, the skew product structure corresponds to the μ-random dynamics, while the first return corresponds to the stopping condition. The x-coordinate x' of the resulting first return is distributed w.r.t. m_x, the second is independent from it and is distributed w.r.t. $\mu^{\mathbb{N}}$, and all the components of the third one are distributed w.r.t. the Lebesgue measure, except for c_1 that is conditioned to be on $[0, \psi(x')]$. This implies that the measure ν is stationary for the ψ-stopped process if and only if the measure $\hat{\nu}$ is invariant for this first return map, where the measure $\hat{\nu}$ on X is obtained in the following way: its $(g_n)_{n\geq 1}$- and $(c_n)_{n\geq 2}$-coordinates are independent and distributed with respect to μ and Leb respectively, its x-coordinate is distributed w.r.t. ν, and conditionally to any its value x the c_1-coordinate is distributed uniformly on $[0, \psi(x)]$.

Now, taking a smaller function $\psi_1 \leq \psi_2$ corresponds to the smaller set $A_{\psi_1} \subset A_{\psi_2}$. If a (non-probability) measure $\hat{\nu}_2$ on A_{ψ_2} is invariant for the Φ-first return map on A_{ψ_2}, its restriction to the subset A_{ψ_1} is invariant for the Φ-first return on this subset as well. Now, it is a straightforward check that

$$\hat{\nu}_2|_{A_{\psi_1}} = \hat{\nu}_1,$$

where $\nu_1 = \frac{\psi_1(x)}{\psi_2(x)}\nu_2$ (the factor comes from integration over the c_1-coordinate), thus concluding the proof.

□

This allows to repeat the previous construction in the following way: we have a sequence of maps

$$\cdots \to \mathcal{M}_{\psi_n} \to \cdots \to \mathcal{M}_{\psi_2} \to \mathcal{M}_{\psi_1},$$

where the map from $\mathcal{M}_{\psi_{n+1}}$ to $\mathcal{M}_{\psi_n}$ is given by $\nu \mapsto \psi_n \nu$.

Each set $\mathcal{M}_\psi$ is a compact, thus by standard projective limit construction there exists an agreeing (in the sense of these maps) family $\nu_n \in \mathcal{M}_n$. More precisely, for any fixed k the sequence of images of $\mathcal{M}_n$ inside $\mathcal{M}_k$ (under the corresponding projection) is a decreasing sequence of non-empty compacts, hence providing a non-empty compact intersection $\mathcal{M}'_k$. These new compact sets project to each other surjectively (by construction), and hence any point $\nu_1 \in \mathcal{M}'_1$ can be lifted to such an agreeing chain.

As the measures ν_n agree with each other in the sense of projections, their restrictions on any interval J' stabilize once J' becomes contained in $\{\psi_n = 1\}$, and they are thus of the form $\nu_n = \psi_n \nu$ for some measure ν on the real line. This measure ν is the desired stationary measure (again, as the stationarity condition for our RDS coincides with P_{ψ_n}-stationarity inside the domain $\{\psi_n \equiv 1\}$).

This concludes the second way of proving Proposition 3.5.1.

Finally, we remark that the skew product construction in the proof of Lemma 3.5.2 allows to show that *any* measure $\nu_1 \in \mathcal{M}_{\psi_1}$ is actually of the form $\psi_1 \nu_2$ for some $\nu_2 \in M_{\psi_2}$. Indeed, both dynamics of P_{ψ_1} and P_{ψ_2} are associated to taking the first return to two different sets, A_{ψ_1} and A_{ψ_2}respectively. However, given a (non-probability) invariant measure for the first return map to a smaller set, one can extend it to a (non-probability) invariant measure for the first return map to a larger set (by iterating it until the first return happens in a Kakitani tower-like construction). However, as we do not need this remark for further study, we do not enter into further technical details here.

Remark 3.5.1. The constructed measure is not guaranteed to be fully supported or non-atomic. Actually, taking three maps

$$f_1(x) = x + 1, \quad f_2(x) = x - 1, \quad f_3(x) = x + \frac{1}{10} \sin 2\pi x$$

with equal probabilities, one gets the dynamics for which Radon stationary measures will be supported on $\mathbb{Z}$.

The above argument allows to construct a stationary measure in the case 3 of Theorem 1.2.2. Now, to distinguish this case from the cases 2 and 4, we will need the following two propositions. The first of them handles the case 4:

Proposition 3.5.2. *Assume that the inverse dynamics of RDS is recurrent. Then there exists a finite stationary measure for the inverse dynamics if and only if for the forward dynamics both functions ϕ_+, ϕ_- do not vanish (in other words, that all the points tend to each of $\pm\infty$ with positive probability).*

The second one handles the case 2:

Proposition 3.5.3. *Assume that the inverse dynamics of RDS is recurrent. Then there exists a semi-infinite stationary measure for the inverse dynamics $\hat{\mu}$, such that $\hat{\mu}([x, +\infty) < \infty$, if and only if for the forward dynamics the function $\phi_+ \equiv 1$ (in other words, that all the points tend to $+\infty$).*

Proof of Proposition 3.5.2. The construction is much more straightforward. Namely, if the function $\hat{\phi}_+$ (and hence $\hat{\phi}_-$) is non-constant, then (as was done in Section 3.3) one can take

$$\hat{\nu}((-\infty, x]) = \phi_+(x + 0) \quad \forall x \in \mathbb{R}.$$

In the other direction, assume that there exists a probability stationary measure $\hat{\mu}$ for the inverse dynamics. Then let us consider the function $\varphi(x) := \hat{\mu}((-\infty, x])$. The stationarity relation (3.5) implies that

$$\varphi(x) = \hat{\mu}((-\infty, x]) = \sum p_i (f_i^{-1})_* \varphi((-\infty, x]) = \sum p_i \varphi(f_i(x)),$$

hence the sequence $\varphi(F_n(x))$ forms a martingale. This martingale thus converges almost surely. Moreover, this martingale is bounded, hence the expectation of the limit is equal to its initial value. On the other hand, the only possible limit values are 0 and 1, as both upper and lower limit of the sequence of random iterations can be only $-\infty$ and $+\infty$ (see Lemma 3.1.1). Hence, both probabilities of tending to $-\infty$ and to $+\infty$ are positive, and this concludes the proof. □

Proof of Proposition 3.5.3. Assume first that $\phi_+ \equiv 1$. Then, the random trajectory $F_n(x)$ of every initial point x almost surely tends to $+\infty$, and thus the minimum $\min_n F_n(x)$ is almost surely finite.

Now, for every $y \in \mathbb{R}$ consider the probability

$$\psi_y(x) := \mathbb{P}(\exists n \geq 0 : \ F_n(x) < y) = \mathbb{P}(\min_{n \geq 0} F_n(x) < y).$$

Note that for every $x > y$ it satisfies the full probability relation

$$\psi_y(x) = \sum_i p_i \psi_y(f_i(x)), \tag{3.18}$$

while for $x < y$ it is identically equal to 1.

Consider now the measure $\hat{\nu}_y$, defined by

$$\hat{\nu}_y([x, +\infty)) = \psi_y(x).$$

This measure satisfies the inverse dynamics stationarity relation on the subsets of $(y, +\infty)$.

Now, normalize this measure so that the measure of $[0, +\infty)$ is equal to 1: take

$$\hat{\mu}_y := \frac{1}{\psi_y(0)} \hat{\nu}_y.$$

Note that this family of measures is uniformly bounded on any fixed interval. Indeed, we have

$$\forall x, y, \forall i \quad \psi_y(x) \geq p_i \psi_y(f_i(x)),$$

what implies an upper bound $\psi_y(x') \leq \frac{1}{p_i} \psi_y(f_i^{-1}(x'))$. Due to the shiftability property the point 0 can be moved arbitrarily far to the left: for any x' there exists a composition F such that $F^{-1}(0) < x'$, and thus $\psi_y(x')$ is upper bounded by $\frac{1}{p}$, where p is the probability of its application. This implies a uniform bound for any right ray $[x', +\infty)$.

Now, the relation (3.18) implies that

$$\nu_y|_{(y,+\infty)} = (\sum_i p_i (f_i^{-1})_* \nu_y)|_{(y,+\infty)}. \tag{3.19}$$

As the family of measures ν_y is uniformly bounded on any interval, consider any weak accumulation point $\hat{\mu}$ of $\hat{\mu}_y$ as $y \to -\infty$. Passing to the limit of (3.19), we see that any such limit point will be a stationary measure for the inverse dynamics, by construction finite on $[0, +\infty)$.

In the other direction, if there exists a semi-finite stationary measure $\hat{\mu}$ for the inverse dynamics, let us consider the function $\psi(x) = \hat{\mu}([x, +\infty))$.

This function again leads to a positive martingale $\psi(F_n(x))$, that is now unbounded due to infiniteness of $\hat{\mu}$.

However, a positive martingale still converges almost surely, and now the only its possible limit is 0 (as upper and lower limits of $F_n(x)$ can be only $+\infty$ or $-\infty$, and the function ψ tends to infinity at $-\infty$). Hence, $\psi(F_n(x))$ converges to 0 almost surely, and thus almost surely $F_n(x) \to +\infty$. Thus $\phi_+ \equiv 1$. $\square$

Bibliography

[1] R. M. Adin, Yu. Roichman, Enumeration of Standard Young Tableaux; arXiv:1408.4497

[2] L. Alsedà, M. Misiurewicz, Random interval homeomorphisms, *Publ. Mat.* **58** (2014), 15–36.

[3] A. Backhausz, T. F. Mori, Asymptotic properties of a random graph with duplications; arXiv:1308.1506

[4] A. Berele and A. Regev, Hook Young diagrams with applications to combinatorics and to representations of Lie superalgebras, *Adv. in Math.* **64** (1987), 118–175.

[5] A. Bonifant and J. Milnor, Schwarzian derivatives and cylinder maps, In: Holomorphic Dynamics and Renormalization, Fields Institute communications, v. 53, pp. 1–21. American Mathematical Soc., Providence, RI (2008).

[6] A. Borodin, A. Okounkov and G. Olshanski, Asymptotics of Plancherel measures for symmetric groups, *J. Amer. Math. Soc.* **13** (2000), pp. 481–515.

[7] Cédric Boutillier, The bead model and limit behaviors of dimer models, *Ann. Probab.* **37**:1 (2009), 107–142.

[8] S. Brofferio, D. Buraczewski, On unbounded invariant measures of stochastic dynamical systems, *Ann. Probab.* Volume 43, Number 3 (2015), 1456-1492.

[9] S. Brofferio, D. Buraczewski, E. Damek, On the invariant measure of the random difference equation $X_n = A_n X_{n-1} + B_n$ in the critical

case, *Ann. Inst. H. Poincar Probab. Statist. 48 (2012)*, no. 2, 377–395. doi:10.1214/10-AIHP406.

[10] S. Brofferio, D. Buraczewski, T. Szarek, On uniqueness of invariant measures for random walks on Homeo$^+(\mathbb{R})$. arXiv:2008.01185v1

[11] L. Carlitz and J. Riordan, Two element lattice permutation numbers and their q-generalization, *Duke J. Math.* **31** (1964), pp. 371–388.

[12] C. De Concini, Symplectic standard tableaux, *Adv. in Math.* **34** (1979), 1–27.

[13] W. Czernous, T. Szarek Generic invariant measures for iterated systems of interval homeomorphisms, *Archiv der Mathematik* **114** (2020), pp. 445–455.

[14] K. Czudek, T. Szarek Ergodicity and central limit theorem for random interval homeomorphisms, *Isr. J. Math.* (2020). https://doi.org/10.1007/s11856-020-2046-4

[15] B. Deroin, V. Kleptsyn, A. Navas, K. Parwani, Symmetric random walks on $Homeo^+(\mathbb{R})$, *Annals of Probability Vol. 41*, No. 3B (2013), 2066-2089

[16] J. Dousse, V. Féray, Asymptotics for skew standard Young tableaux via bounds for characters, *Proc. Amer. Math. Soc.* **147** (2019), pp. 4189–4203.

[17] P. Edelman, Tableaux and chains in a new partial order of S_n, *J. Combin. Theory Ser. A* **51** (1989), 181–204.

[18] W. Feit, The degree formula for the skew-representations of the symmetric group, *Proc. Amer. Math. Soc.* **4** (1953), pp. 740–744.

[19] A. Furman, Random walks on groups and random transformations. *Handbook of dynamical systems*, Vol. 1A, pp. 931–1014, North-Holland, Amsterdam, 2002.

[20] M. Gharaei, A. J. Homburg, Random interval diffeomorphisms, *Discrete & Continuous Dynamical Systems* - S, 2017, 10 (2) : 241-272. doi: 10.3934/dcdss.2017012

[21] V. Gorin, Non-intersecting paths and Hahn orthogonal polynomial ensemble, *Functional Analysis and its Applications*, **42**:3 (2008), 180-197.

[22] C. Greene, A. Nijenhuis, H. S. Wilf, Another Probabilistic Method in the Theory of Young Tableaux; *J. Comb. Theory*, Ser. A **37** (1984), 127-135.

[23] Y. Guivarc'h, E. Le Page, Spectral gap properties for linear random walks and Pareto's asymptotics for affine stochastic recursions, *Ann. Inst. H. Poincar Probab. Statist. Volume 52*, Number 2 (2016), 503-574.

[24] Yu. Ilyashenko, V. Kleptsyn, P. Saltykov, Openness of the set of boundary preserving maps of an annulus with intermingled attracting basins, *Journal of Fixed Point Theory and Applications* **3** (2008), pp. 449–463

[25] W. Jockusch, J. Propp, P. Shor, Random Domino Tilings and the Arctic Circle Theorem, arXiv:9801068

[26] S. Kakutani, Random ergodic theorems and Markov processes with a stable distribution. *Proceedings of the Second Berkeley Symposium on Mathematical Statistics and Probability*, 1950, University of California Press, Berkeley and Los Angeles (1951), pp. 247261.

[27] I. Kan, Open sets of diffeomorphisms having two attractors, each with an everywhere dense basin, *Bull. Am. Math. Soc.*, **31** (1994), pp.68–74

[28] P. W. Kasteleyn, Dimer statistics and phase transitions. J. Mathematical Phys., **4** (1963), 287–293.

[29] P. W. Kasteleyn, Graph theory and crystal physics. In Graph Theory and Theoretical Physics, pages 43–110. Academic Press, London, 1967.

[30] M. Lin, Conservative markov processes on a topological space, *Israel J. Math.* **8** (1970), pp. 165–186.

[31] B. F. Logan, L. A. Shepp, A variational problem for random Young tableaux. *Adv. Math.* **26** (1977), pp. 206–222.

[32] A. H. Morales, I. Pak, G. Panova, Hook formulas for skew shapes I. q-analogues and bijections, *J. Combin. Theory*, Ser. A **154** (2018), 350–405.

[33] A. H. Morales, I. Pak, G. Panova, Hook formulas for skew shapes II. Combinatorial proofs and enumerative applications, *SIAM Jour. Discrete Math.* **31** (2017), 1953–1989.

[34] A. H. Morales, I. Pak, G. Panova, Hook formulas for skew shapes III. Multivariate and product formulas; arXiv:1707.00931.

[35] A. H. Morales, I. Pak, G. Panova, Asymptotics of the number of standard Young tableaux of skew shape, *Eur. J. Combin* **70** (2018), 26–49.

[36] A. H. Morales, I. Pak, M. Tassy, Asymptotics for the number of standard tableaux of skew shape and for weighted lozenge tilings; arXiv:1805.00992

[37] H. Naruse and S. Okada, Skew hook formula for d-complete posets; arXiv:1802.09748

[38] W. Parry, Intrinsic Markov chains. *Trans. Amer. Math. Soc.* **112** (1964) pp. 55–66.

[39] B. Pittel, D. Romik, Limit shapes for random square Young tableaux, *Adv. in Appl. Math.* **38**:2 (2007), pp. 164–209

[40] M. Pollicott, R. Sharp, S. Tuncel, P. Walters, The mathematical research of William Parry FRS, *Ergodic Theory and Dynamical Systems*, **28**:2 (2008), pp. 321–337.

[41] W. Jockusch, J. Propp, P. Shor, Random Domino Tilings and the Arctic Circle Theorem; arXiv:math/9801068

[42] P. Sniady, Asymptotics of characters of symmetric groups, genus expansion and free probability, *Discrete Math.* **306**:7 (2006), 624–665

[43] W. Sun, Dimer model, bead model and standard Young tableaux: finite cases and limit shapes; arXiv:1804.03414

[44] T. Szarek, A. Zdunik, Attractors and invatiant measures for random interval homeomorphisms, unpublished manuscript.

[45] A. Vershik, The limit form of convex integral polygons and related problems; *Funktsional. Anal. i Prilozhen.* **28**:1 (1994), 16–25, 95.

[46] A. M. Vershik and S. V. Kerov, Asymptotics of the Plancherel measure of the symmetric group and the limiting form of Young tableaux, *Doklady AN SSSR* **233**:6 (1977), pp. 1024–1027; English translation: *Soviet Mathematics Doklady* **18** (1977), pp. 527–531.

[47] A. M. Vershik and S. V. Kerov, Asymptotic behavior of the largest and the typical dimensions of irreducible representations of the symmetric group, *Funct. Anal. Appl.*, **19**:1 (1985), pp. 21–31.

UNIVERSITÉ DE RENNES 1

Titre : Dynamique aléatoire dans des tableaux de Young et sur la droite réelle

Mots clés : Dynamique aléatoire, tableaux de Young, TASEP, mesure stationnaire

Résumé : Cette thèse concerne l'étude de dynamique aléatoire dans deux situations différentes : celle des tableaux de Young aléatoires et celle de la dynamique sur la droite réelle.

La première partie est consacrée à l'étude de tableaux de Young aléatoires et de leur comportement limite. Il s'avère que la description locale d'un tableau de Young aléatoire de grande taille donnée est reliée à un nouveau processus, une modification de TASEP (Totally Asymmetric Simple Exclusion Process). Je détermine l'entropie topologique et la mesure d'entropie maximale de cette modification, qui se révèle être déterminantale. J'utilise cette description pour écrire le principe variationnel des tableaux de Young aléatoires, ainsi que pour retrouver les noyaux de processus de perles et pour donner une explication de l'apparition du processus de sinus sur le bord des diagrammes de Young aléatoires.

La deuxième partie est consacrée à l'étude de systèmes dynamiques aléatoires sur la droite réelle. J'étudie la dualité entre le comportement dynamique des systèmes formés par une famille d'applications et par celui de leurs inverses. Il s'avère que sous des hypothèses assez faibles, il n'y a que quatre comportement possibles pour les couples formés par ces systèmes et leur inverse, ces comportements se décrivent selon l'existence d'une mesure stationnaire finie, infinie ou semi-infinie, et selon les propriétés de recurrence et de convergence des points vers l'infini.

Title: Random dynamics in Young diagrams and on the real line

Keywords: Random dynamics, Young diagrams, TASEP, stationary measure

Abstract: This thesis is devoted to the study of random dynamics in two different situations, for the random Young tableaux and on the real line.

The first part is devoted to the study of random Young tableaux and to the question of their limit behaviour. It turns out that the local description of a random Young tableau of a large given shape is related to a new process, a modification of the TASEP (Totally Asymmetric Simple Exclusion Process). For this modification, I find its topological entropy as well as the measure of maximal entropy, that turns out to be determinantal. I use this description to write down the variational principle for the random Young tableaux, as well as to re-obtain the kernel for the beads processus and to give an explanation for the appearance of the sine-process on the border of random Young diagrams.

The second part is devoted to the study of dynamical systems on the real line. I study the duality of behaviour between such systems and the systems formed by the inverse maps. It turns out that under sufficiently weak assumptions, any system (together with the system of inverses) falls in one of the four classes of possible behaviour (concerning the existence of a finite, infinite or semi-infinite measure, as well as its recurrence or orbits converging to the infinity).